

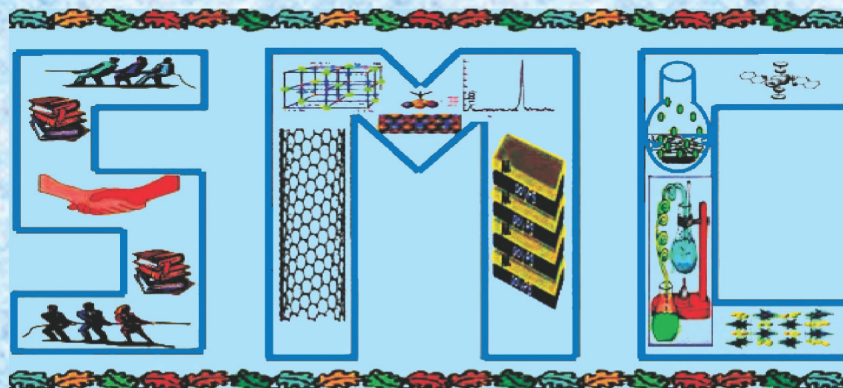
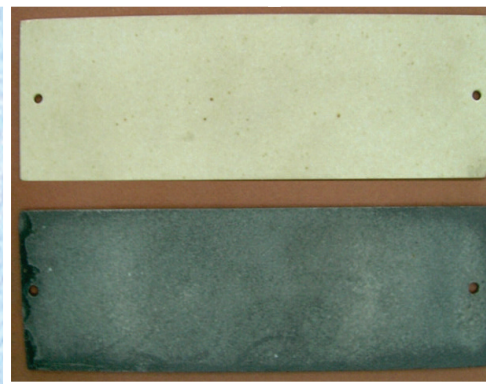
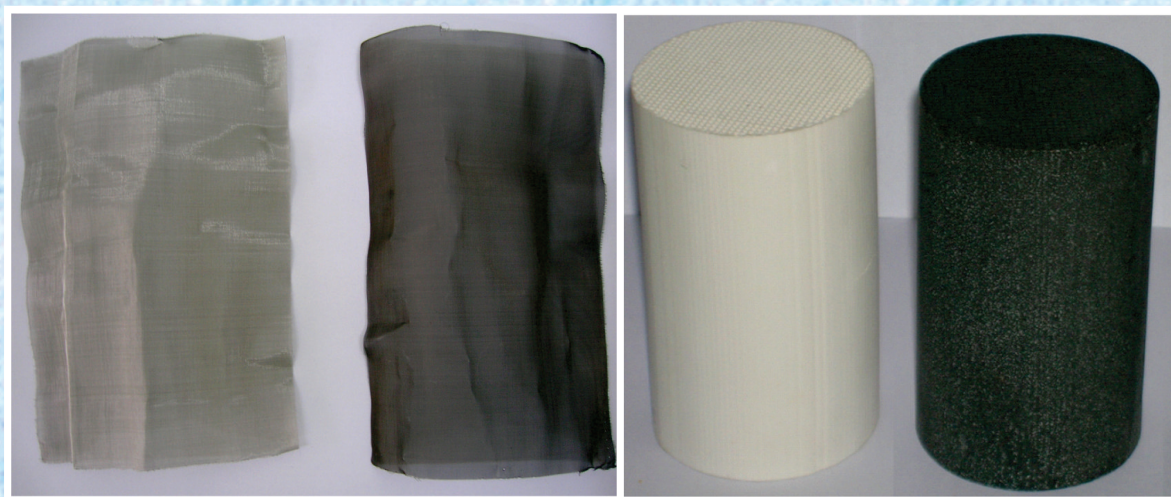
SMC Bulletin

A Publication of the Society for Materials Chemistry

Volume 4

No. 3

December 2013



SOCIETY FOR MATERIALS CHEMISTRY

Society for Materials Chemistry

Society for Materials Chemistry was mooted in 2007 with following aims and objectives:

- (a) to help the advancement, dissemination and application of the knowledge in the field of materials chemistry,
- (b) to promote active interaction among all material scientists, bodies, institutions and industries interested in achieving the advancement, dissemination and application of the knowledge of materials chemistry,
- (c) to disseminate information in the field of materials chemistry by publication of bulletins, reports, newsletters, journals.
- (d) to provide a common platform to young researchers and active scientists by arranging seminars, lectures, workshops, conferences on current research topics in the area of materials chemistry,
- (e) to provide financial and other assistance to needy deserving researchers for participation to present their work in symposia, conference, etc.
- (f) to provide an incentive by way of cash awards to researchers for best thesis, best paper published in journal/national/international conferences for the advancement of materials chemistry,
- (g) to undertake and execute all other acts as mentioned in the constitution of SMC.

Executive Committee

President

Dr. S. K. Sarkar
Bhabha Atomic Research Centre
Trombay, Mumbai, 400 085
sarkarsk@barc.gov.in

Vice-Presidents

Dr. V. K. Jain
Bhabha Atomic Research Centre
Trombay, Mumbai, 400 085
jainvk@barc.gov.in

Prof. Sandeep Verma

Indian Institute of Technology
Kanpur
sverma@iitk.ac.in

Secretary

Dr. P. A. Hassan
Bhabha Atomic Research Centre
Trombay, Mumbai, 400 085
hassan@barc.gov.in

Treasurer

Dr. Sandeep Nigam
Bhabha Atomic Research Centre
Trombay, Mumbai, 400 085
snigam@barc.gov.in

Members

Dr. K. Ananthasivan
Indira Gandhi Centre for Atomic Research
Kalpakkam, 603102

Dr. (Smt.) A. Banerjee
Bhabha Atomic Research Centre
Trombay, Mumbai-400085

Dr. K. Bhattacharya
Bhabha Atomic Research Centre
Trombay, Mumbai-400085

Dr. D. Das
Bhabha Atomic Research Centre
Trombay, Mumbai-400085

Dr. G. K. Dey
Bhabha Atomic Research Centre
Trombay, Mumbai-400085

Dr. P. Sujata Devi
CSIR Central Glass & Ceramic Research
Institute, Kolkata-700032

Dr. C. P. Kaushik
Bhabha Atomic Research Centre
Trombay, Mumbai-400085

Dr. T. Mukherjee
Bhabha Atomic Research Centre
Trombay, Mumbai-400085

Dr. M. C. Rath
Bhabha Atomic Research Centre
Trombay, Mumbai-400085

Dr. (Smt.) S. S. Rayalu

CSIR National Environmental
Engineering Research Institute, Nagapur

Prof. S. D. Samant

Institute of Chemical Technology
Mumbai

Dr. A. K. Tyagi

Bhabha Atomic Research Centre
Trombay, Mumbai-400085

Dr. R. K. Vatsa

Bhabha Atomic Research Centre
Trombay, Mumbai-400085

Co-opted Members

Prof. A. Ajayaghosh
CSIR – National Institute for
Interdisciplinary Science and Technology
Thiruvananthapuram
ajayaghosh@niist.res.in

Prof. A. K. Ganguli

Director, Institute for Nanoscience and
Technology
ashok@chemistry.iitd.ernet.in

Prof. S. Ram

Indian Institute of Technology - Kharagpur
sram @ matsc.iitkgp.ernet.in

Dr. A. K. Tripathi

Bhabha Atomic Research Centre
Trombay, Mumbai-400085
catal@barc.gov.in

Contact address

Society for Materials Chemistry

C/o Chemistry Division

Bhabha Atomic Research Centre, Trombay, Mumbai, 400 085, India

Tel: +91-22-25592001, E-mail: socmatchem@gmail.com

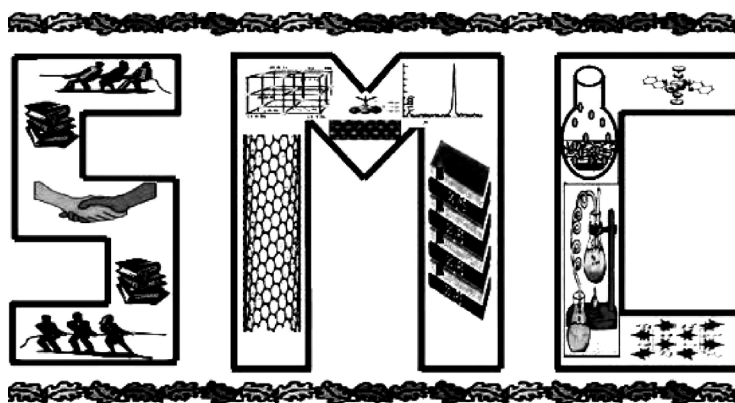
SMC Bulletin

A Publication of the Society for Materials Chemistry

Volume 4

No. 3

December 2013



SOCIETY FOR MATERIALS CHEMISTRY

SMC Bulletin

Vol. 4

No. 3

December 2013

Guest Editors

Dr. Salil Varma
Chemistry Division
Bhabha Atomic Research Centre
Trombay, Mumbai, 400 085
e-mail: svarma@barc.gov.in

Dr. Arvind Kumar Tripathi
Chemistry Division
Bhabha Atomic Research Centre
Trombay, Mumbai, 400 085
e-mail: catal@barc.gov.in

Editorial Board

Dr. Arvind Kumar Tripathi
Chemistry Division
Bhabha Atomic Research Centre
Trombay, Mumbai, 400 085
e-mail: catal@barc.gov.in

Dr. Shyamala Bharadwaj
Chemistry Division
Bhabha Atomic Research Centre
Trombay, Mumbai, 400 085
e-mail: shyamala@barc.gov.in

Dr. Manidipa Basu
Chemistry Division
Bhabha Atomic Research Centre
Trombay, Mumbai, 400 085
e-mail: deepa@barc.gov.in

Dr. Aparna Banerjee
Product Development Division
Bhabha Atomic Research Centre
Trombay, Mumbai, 400 085
e-mail: aparnab@barc.gov.in

Dr. Sandeep Nigam
Chemistry Division
Bhabha Atomic Research Centre
Trombay, Mumbai, 400 085
e-mail: snigam@barc.gov.in

Published by

Society for Materials Chemistry
C/o. Chemistry Division
Bhabha Atomic Research Centre, Trombay, Mumbai, 400 085
E-mail: socmatchem@gmail.com,
Tel: +91-22-25592001

Please note that the authors of the paper are alone responsible for the technical contents of papers and references cited therein

Front cover shows various catalysts developed for mitigation of hydrogen; noble metal on SS wire gauze; noble metal on cordierite honeycomb and Noble metal on cordierite plate.

Guest Editorial



Salil Varma



Arvind Kumar Tripathi

It has given us immense pleasure to be associated with the special thematic issue of SMC bulletin on catalytic materials. Catalytic reactions play all important roles in our life. Most biological reactions that build the human body and control the functioning of the brain and other vital organs, photosynthesis, and majority of chemical processes that are utilized in chemical technology are all catalytically driven. Utility of such processes in the industry range right from oil refining by cracking of crude petroleum for the production of chemicals by hydrogenation, dehydrogenation, partial oxidation and organic molecular rearrangement to ammonia synthesis and fermentation at baker's shop. All these reactions occur repeatedly by a sequence of elementary steps that include adsorption, surface and lattice diffusion, chemical rearrangement of the adsorbed reaction intermediates and desorption of the products.

Keeping in terms with the current development of materials for their application in the field of catalysis, this issue covers topics ranging from development of materials of varied morphologies and physico-chemical properties and their application as catalysts in usage varying from environmental remediation, electro-catalysis, fine chemical synthesis, hydrogen generation, nuclear reactor safety and various other processes of relevance to Department of Atomic Energy. The role of computational chemistry in designing of catalysis materials has also been included in this issue. The editors thank the authors from different organisations for their valuable contributions to scientifically enrich this special issue.

The next issue of the bulletin is proposed to be on the theme of "Carbon based Materials". Readers are encouraged to send their feedbacks which will enable us to improve the SMC bulletin.



From the desks of the President and Secretary



Dr. Sisir K Sarkar
President



Dr. P. A. Hassan
Secretary

Dear Fellow Members and Readers,

Greetings from the Executive Council of Society for Materials Chemistry (SMC).

Since its inception, SMC has been actively involved in bringing out theme-based bulletin issues which serve as a platform to highlight the advances made in the field of materials chemistry and also encourage young researchers / academicians to join our fast growing society already having more than 700 life members. During the past few months, our efforts have been focused on the preparation for organising the 2nd National Workshop on Materials Chemistry – Catalytic Materials (NWMC-2013 : CAT-MAT) to be held at Anushaktinagar during November 22-23, 2013. This event is fully supported by DAE-BRNS and is being jointly organized by SMC and Chemistry Division, BARC. It is really a pleasure to bring this special issue on “Catalytic Materials” which is being published on the eve of NWMC-2013. We would like to put on record our sincere thanks to the Guest Editors Dr. Salil Varma and Dr. A. K. Tripathi who have taken keen initiative to bring out this issue on Catalytic Materials.

Catalytic materials play an important role in enabling development of advanced technologies for the sustainable growth of society and economy. Designing new catalytic materials with specific properties has been of great interest to material chemists. This issue comprises eight contributed articles spanning over the entire spectrum of catalyst materials ranging from design, development; synthesis and applications. There is no doubt that this field will continue to develop strongly, with contributions from researchers in chemistry, physics, chemical engineering and material science. It is also hoped that our readers will enjoy the mix of topics presented here and perhaps find the inspiration to push this field a step further toward greater success in both knowledge development and commercialization. We would like to acknowledge the individual and collective contributions of the authors and editors of this issue. They represent an admirable group of busy but unselfish professionals volunteering their limited time tending to the scientific “commons” on which we all depend

Finally, we wish to express our gratitude to all members of SMC for their continued support and cooperation in the growth of the society.



CONTENTS

	Feature articles	Page No.
1.	Designing of Nanoarchitectures for Photo and Electrocatalytic Applications <i>Aparna Ganguly, Oruganti Anjaneyulu, Debashree Das and Ashok K Ganguli</i>	1
2.	Photocatalytic Activity of Cellulose Acetate-tin (IV) Molybdate Nanocomposite in Solar Light <i>B.S. Rathore, Gaurav Sharma and Deepak Pathania</i>	11
3.	N-Heterocyclic Carbene (NHC) in Organometallic Catalysis -Contributions from IIT Kanpur <i>Sayantani Saha and Jitendra K. Bera</i>	17
4.	Anisotropic Effect of Hematite Nanostructure and its Modification for Photocatalytic Application <i>Gajendra Kumar Pradhan and Kulamani Parida</i>	23
5.	Effect of Different Phases of Mg-Al Hydrotalcites, Formed by Calcination, on the Knoevenagel Reaction of Benzaldehydes and Malononitrile. <i>Rohit Gupta, Siddheshwar Kshirsagar, Savita Ladage and Shrinivas D. Samant</i>	29
6.	Novel Supported ionic liquid catalysed synthesis of tetraarylporphyrins <i>Deepali A. Kotadia and Saurabh S. Soni</i>	35
7.	Heterogeneous Photocatalysis: Novel Approach for Carbon-Carbon Bond Forming Reactions <i>Sudhir S. Arbuj, Bina N. Wani and Uttam P. Mulik</i>	40
8.	Modeling of materials for H-Economy using DFT: Implications toward nanocatalysis <i>Chiranjib Majumder, Seemita Banerjee and Sandeep Nigam</i>	47
9.	Development of Catalysts for Various Applications Related to DAE Programs <i>Shyamala R. Bharadwaj</i>	53

Designing of Nanoarchitectures for Photo and Electrocatalytic Applications

Aparna Ganguly^a, Oruganti Anjaneyulu^b, Debashree Das^b and Ashok K Ganguli^{a, b, c, *}

^aNanoscale Research Facility, Indian Institute of Technology, Delhi, New Delhi 110016

^bDepartment of Chemistry, Indian Institute of Technology, New Delhi- 110016

^cInstitute of Nano Science & Technology, Mohali, Punjab 160062.

E-mail: ashokganguliitd@gmail.com

Abstract

Designing of environmentally benign, effective and low-cost materials for the production of clean energy carrier i.e. hydrogen has been of immense interest. Direct approaches for degradation of organic pollutants and water splitting process include semiconductor particles as photocatalyst. This article discusses and highlights the development of catalysts and also discusses the various aspects that affects electro and photo catalysis. We will be discussing in detail the wet chemical synthesis that allow to tune the size, morphology and band gap of the anisotropic nanostructures including (type -II) core-shell architectures. We also highlight the importance of alloy nanoparticles, metal oxides and metal nanoparticles designed for electrocatalytic studies (hydrogen and oxygen evolution) along with the various parameters which collectively leads to enhancement of the efficiency of the catalysts.

1. Introduction

21st century has witnessed revolutionary growth in technological and industrial sectors. This rapid change has led to depletion of natural sources like fossil fuels as well as environmental problems associated with hazardous wastes, contaminated ground water and toxic air contaminants. The major challenge of today's materials chemist is to find remediation for all these problems. Catalysis (Photo and Electro) is one of the best approaches towards a solution for energy conversion and the destruction (or) transformation of hazardous chemical wastes [1]. Photocatalysis is a chemical process catalyzed by semiconductor solids that can absorb visible and UV light, remains chemically and biologically inert and photo stable, is inexpensive and nontoxic [2]. Major breakthrough for photoelectrolysis came in 1972 when Fujishima and Honda discovered electrochemical photolysis of water on titanium dioxide [3]. Watanabe and coworkers evaluated the photocatalytic ability, photoinduced hydrophilicity of various metal oxides to decompose organic compounds. Based on their study, metal oxides were classified into four categories based on their behavior over the two photochemical reactions: (1) active in both photocatalytic oxidation and photoinduced hydrophilicity (TiO_2 , SnO_2 , ZnO); (2) only active in photo catalytic oxidation (SrTiO_3); (3) only active in photo induced hydrophilicity (WO_3 , V_2O_5); (4) and inactive over both processes (CeO_2 , CuO , MoO_3 , Fe_2O_3 , Cr_2O_3 , In_2O_3) [4]. Among the photocatalysts studied, TiO_2 is the only material used at industrial scale due to its photoactivity, higher stability and lower cost [4] and is one of the most explored photo catalytic materials. Among the three phases known (rutile, anatase and brookite) anatase

is mostly used in photocatalytic applications owing to its inherent superior properties [5, 6]. Effect of substitution of p block elements (B, C, N, F, S, P, and I) either at Ti^{4+} and O^{2-} lattice site provides favorable surface-electronic structure, modulates the band gap energy for visible light response and facilitates efficient charge carrier transfer process [7-10]. Bamwenda et al reported the effect of Au or Pt deposited on TiO_2 for the H_2 generation. The rate of H_2 production is quite high for the Pt deposited TiO_2 as compared to the Au deposited ones because of the effective trapping and pooling of photogenerated electrons as Pt sites have higher ability for the reduction [11]. There are several other reports where Pt/ TiO_2 has been used for hydrogen production from methanol [12], photoinduced reforming of organic compounds at room temperature with simultaneous production of H_2 [13], Pt and Au/ TiO_2 photocatalysts for methanol reforming [14] etc. The incorporation of TiO_2 nanoparticles with graphene or graphene oxide (GO) nano sheets not only increase the surface area of the nanohybrid materials but also expanded the light absorption range and enabled fast charge transportation, which enhanced capacity of rapidly adsorbing and photo degradation of organic dyes [15].

To explain the photocatalysis by ZnO, Morrison and Freund [16] utilized two new electrical measuring techniques: "current doubling" for detection of hole and free-radical based reactions and the "capacity method" for the detection of electron based reactions. These techniques in conjunction with standard chemical methods were used to analyze the detailed reactions during ZnO photocatalysis. Hydrogenated ZnO nanorod arrays were known to show exceptional hydrogen production ability

compared to ZnO powders. The superior photocatalytic performance is because of the increased carrier density, improved charge transport and large active surface area [17]. Wang et al demonstrated a novel and simple approach to fabricate a 2D shell ZnO array structure to enhance the interaction between incident light and the material [18]. The enhancement remarkably increased the two-photon excitation efficiency of the material and, utilizing the two-photon induced electron-hole pairs in ZnO, they realized photocatalysis under monochromatic visible light for the first time.

Xiao reported the synthesis of three-dimensional arrayed ZnO/TNTs (TiO₂ nanotubes) heterostructure which exhibits superior photocatalytic activities compared to its counterparts of pure ZnO, TNTs. This can be attributed to the excellent photostability, large exposed surface area of TNTs to surrounding medium, interface between ZnO and TNTs greatly promotes efficient separation of photogenerated electron-hole charge carriers [19].

Liu et al [20] reported an ecofriendly method for the synthesis of highly effective ZnO/g-C₃N₄ photocatalysts. Their study on photocatalytic mechanism revealed that the electrons injected directly from the conduction band of g-C₃N₄ to that of ZnO, results in the production of •O²⁻ and •OH radicals in the conduction band of ZnO. Simultaneously, the rich holes in the valence band of g-C₃N₄ oxidized Rhodamine B directly to promote the photocatalytic degradation reaction. Balachandran and Swaminathan reported [21] the hetero junction Bi₂S₃-ZnO photocatalyst which exhibits higher photocatalytic activity for the degradation of Acid Black 1 in the UV region as well as in the visible region because of the low recombination rates of photoinduced electron-hole pairs.

Luo et al [22] reported novel hierarchical RGO-ZnO composites exhibiting enhanced photocurrent and photocatalytic performance because of the large surface area of hierarchical structured ZnO hollow spheres as well as excellent electron transport and reduced electron-hole pair recombination resulting from the graphene. Pawar et al [23] recently reported the incorporation of RGO into the CdS and ZnO structures, the photo-degradation performance toward methyleneblue (MB) degradation under visible light illumination was significantly improved compared with that of just CdS and ZnO. This composite degraded MB within 40 min. Photoluminescence quenching, increased optical absorbance, and high specific surface area (23.08 m²g⁻¹) also contributed to the high degradation efficiency. The developed RGO-CdS-ZnO composites have a potential application in water purification devices.

Apart from TiO₂ and ZnO, there are several other well studied semiconductor materials which include, binary oxides [24-27]: WO₃ [28, 29], V₂O₅ [30, 31], Iron oxides [32,33], Bi₂O₃ [34,35], NiO [36,37], Nb₂O₅ [38,39], Ta₂O₅ [40], ZrO₂ [41,42], CeO₂ [43,44], Ga₂O₃ [45,46]. Binary sulfides: CdS [47], Sb₂S₃ [48] & ternary oxides: BiVO₄ [49], Bi₂WO₆ [50,51], Bi₂MoO₆ [52,53] and oxyhalides like BiOX (X = F, Cl, Br and I [54-55]).

Another important process which has gained importance over the past decade is electrocatalysis where decomposition of water produces hydrogen and oxygen at the cathodic and anodic electrodes respectively [56]. Electrocatalysis is enhancement of electrode kinetics by a material by minimizing the over potential. A key process in an electrocatalytic reaction is the adsorptive interaction of the reactants with surface sites of the catalyst in the presence of the electric field. This interaction is strongly dependent on the surface properties of the catalyst. To maximize this interaction for developing an efficient electrode material i.e. high surface area, enhanced electrical conductivity, high surface concentrations of corner and edge atoms, low coordination numbers of surface atoms and unique electronic properties (quantum size effects), long term stability and low cost forms the essential requirements. These are best met by nanoparticles of transition metal oxides [57]. Considerable progress has been made in development of oxygen evolving anodes with low over potential like noble metals as Pt, Pd, alloys as Pt₃Co, [58] oxides like RuO₂, IrO₂, MnO₂, PtO₂ and OsO₂ [57,59,60] etc. Among the binary oxides of Ru, Pt and Ir, RuO₂ is cheaper as well as it shows low overvoltage [61] but these electrodes have less stability and are easy to corrode during prolonged oxygen evolution [62]. Ternary oxides with perovskite structures like LaNiO₃, LaCoO₃, SrFeO₃ etc. and with spinel like Co₃O₄, MCo₂O₄ (M= Ni, Mn, Cr) have been found to be stable anodic electrodes [63]. Core-shell structured Pt-Co nanoparticles exhibit high Pt mass activity for the ORR making them promising candidates for next generation proton exchange membrane fuel cells [64]. Abe and coworkers demonstrated a co-reduction strategy for the preparation of Pt₃Ti in the form of nanoparticles. They have shown that both atomically disordered and ordered Pt₃Ti nanoparticles have a higher electrocatalytic performance than conventional electrocatalysts in terms of their low onset potentials for fuel oxidation and low affinity toward CO adsorption. In particular, atomically ordered Pt₃Ti nanoparticles demonstrate a promising performance as anode catalysts for direct fuel cells. The high electrocatalytic performance of atomically ordered Pt₃Ti nanoparticles shows that Pt-based intermetallic compounds containing early *d*-metal elements, Zr, Hf, V, Nb, or Ta, are worthy of further study [65].

In this review, we have tried to emphasize on the both the catalytic processes (electro & photo) catalyzed by metal, metal oxides, alloy nanostructures synthesized using wet chemical methods. We have also investigated the various factors that collectively affect the catalytic process and enhance the efficiency.

2. Methodology

Three major routes have been explored for designing the nanostructures viz, reverse micellar route, surface functionalization and hydrothermal process.

Surfactant aggregates specially “reverse micelles” have been extensively used for synthesis purposes [66]. Reverse micelles contain aqueous core which acts as a microreactor. The presence of surfactant helps in controlling the growth of the particles. Scheme I shows a typical reaction between two reactants within reverse micelles. Various types of surfactants i.e. cationic and non-ionic surfactants have been used for the formulation of microemulsions. The product obtained post reaction was washed well with solvent in order to remove the surfactant and dried at room temperature (Fig. 1).

Hydrothermal (solvothermal) method is a low temperature, wet chemical route for synthesis of highly crystalline products (advantageous to increase the photocatalytic efficiency of the material). Homogeneous and less aggregated products can be obtained using this method. Reaction occurs at elevated temperature and pressure. The morphology and size of the products can be controlled by adjusting the hydrothermal reaction conditions. The sample obtained after hydrothermal treatment is subjected to calcination at different temperatures. With the help of hydrothermal treatment incorporation of various alkali metal ions as well as transition metal ions into titanate nanotubes has been achieved by ion exchange process in alkaline condition.

For the synthesis of core-shell nanorods, the well-known surface-functionalized method has been employed using citric acid as a surface-functionalized agent. By varying the concentration of the citric acid, core shell nanorods with varying diameter and different shell thickness were optimized. In the case of ZnO/CdS core-shell nanorods, the reaction of carboxylic acids with ZnO is a well-known reaction in surface science. Carboxyl groups are easily self-assembled on the surface of the ZnO, because of their strong adsorption energy via their carboxylate function to the Zn centers. This surface functionalization helps largely to form uniform coating on the ZnO core layer by the segregation of the coagulated ZnO nanorods probably by electrostatic interactions.

3. Results & discussion

3.1 Photocatalysis

A detailed study has been carried out for the synthesis and photocatalytic behavior of TiO₂ nanospindles [67]. Reverse micellar route has been explored to design the synthesis of nanospindles of titanium dioxide & have studied in detail the various factors that collectively decides the efficiency of the photocatalyst. The use of w/o micro emulsion offers a unique micro environment in which mono dispersed nanoparticles of TiO₂ with a narrow size distribution could be achieved. These anisotropic TiO₂ nanostructures (spindles) have diameter of 6 nm and length of 30 nm (Fig. 2a) with high degree of thermostability and are observed to be monodispersed with high surface area (~ 200 m²/g). TiO₂ nanospindles showed nearly twice the photocatalytic efficiency of Degussa P25 TiO₂ and was observed to be stable even after three cycles (Fig. 2b).

In addition, nanotubes derived from titanium dioxide are considered to be a promising alternative and exhibits a wide variety of applications including photovoltaic (solar energy conversion), photocatalytic, semiconductor, catalytic support, and gas sensing properties, especially when prepared as a nanomaterial [68-70]. A systematic study has been carried out to explore the various properties of TiO₂-based nanotubes doped with nickel ions [71]. The stability of the samples, changes in shape and morphology, change in textural properties (surface area), phase change, photocatalytic activity, and hydrogen absorption capacity as a function of calcination temperature have been investigated. Where, titanate nanotubes containing 2.5 wt% Ni were synthesized from TiO₂ sol using hydrothermal treatment under alkali condition followed by a simple ion-exchange process. The study revealed that the titanate phase containing Ni ions was converted to the anatase phase after certain heat treatments but, at the same time, the tubular morphology was partially lost. Investigation of photocatalytic properties demonstrated that the as-prepared Ni-titanate nanotubes were observed to be photocatalytically inactive, but when heated at temperatures below 500 °C their activity was significantly enhanced with the change in phase. The calcined nanotube samples carrying nickel ion showed better photocatalytic activity than calcined nanotube samples containing protons (Table 1). Photocatalytic efficiency can also be improved by designing one dimensional core/shell nanorod with type-II band alignment. The presence of a shell made of semiconductor material with relatively wider band gap can effectively protect the core from photo corrosion especially in the case when the shell is not excited by incident light. The internal field within the core material

is thought to influence band bending at the core/shell interface and promote the separation of photogenerated charge carriers [72]. The micron-sized core is necessary to provide the appropriate length scale for band bending and light absorption [73, 74].

ZnO nanostructures that provide an ideal geometrical structure for effective carrier transport and therefore reduces the charge recombination and increases the efficiency of ZnO photocatalyst. The ability to form uniform CdS shell layers on one-dimensional nanostructures (ZnO nanorod arrays) with control of the shell thickness is a key step toward the high-efficiency photocatalysts. This facilitates the effective injection of photogenerated electrons from CdS into ZnO and reduces the rate of recombination between electron-hole pairs. In type-I core/shell heterostructures, both the electrons and the holes are confined in the core compared to type-II structures, the electrons and holes are separated between the core and the shell, giving rise to a significant increase in the exciton

lifetime, which is advantageous for applications in both solar cells and photocatalysis [75]. Core/shell nanorod arrays of ZnO/CdS have been synthesized with varying shell thickness by the surface functionalization method using citric acid as a surface functionalizing agent [76]. Figure 3a indicates the bare ZnO nanorods whereas Fig. 3b shows the ZnO/CdS core/shell structures.

The inset shows optical absorbance spectra of the uncoated ZnO nanorods, and ZnO/CdS core shell nanorod arrays with varying shell thickness. Core/shell nanorod with variable shell thickness (10–30 nm) are obtained by varying the concentration of surface functionalizing agent. The role of shell thickness dependent on photocatalytic properties have been investigated in detail and Table 2 tabulates the absorbance band, PL band, current, and photocatalytic efficiency of ZnO and ZnO/CdS Core/Shell Nanorod Arrays with varying shell thickness. ZnO based nanostructures sensitized with inorganic semiconductor nanocrystals such as CdS, In₂S₃, CdSe, PbS, InP, Ag₂S and

Table 1. Effect of heat treatment on the crystallite size (anatase phase), BET surface area and percent photonic efficiency for the Ni-TNT samples.

Sample	Calcination temperature	Anatase crystallite size (nm)	BET surface area (m ² /g)	Photonic efficiency (mole S ⁻¹ × m ⁻³)
Ni-TNT	Room temp.	*	306.76	**
	300 °C	3.721	279.30	0.2058
	400 °C	9.887	203.21	0.5763
	500 °C	17.67	114.27	0.4417
	600 °C	24.5	78.764	0.2584
	700 °C	38.3	37.422	0.1049
	800 °C	Rutile	20.097	0.0605
	900 °C	Rutile	03.420	0.0032

*Anatase is absent in the phase, ** Photonic efficiency is nearly zero.

Table 2. Absorbance Band, PL Band, Current, and Photocatalytic Efficiency of ZnO and ZnO/CdS Core/Shell Nanorod Arrays with Varying Shell Thickness

Sample	Shell Thickness (nm)	Absorbance Band (nm)	PL Band (nm)	Current (A)	Photocatalytic Efficiency (%)
ZnO	-	372	380	9.22 × 10 ⁻⁷	70.0
ZnO/CdS1	10	425	460	8.09 × 10 ⁻⁶	85.0
ZnO/CdS2	15	442	473	1.62 × 10 ⁻⁵	91.5
ZnO/CdS3	30	465	490	1.75 × 10 ⁻⁵	98.0

Bi_2S_3 can generate multiple electron-hole pairs per photon and consequently enhance the photocatalytic efficiency [77]. For an efficient electron transfer between the sensitizer (here In_2S_3) and photocatalyst (ZnO), the energy level of the conduction band of the photocatalyst must be lower than that of the sensitizers. These results demonstrate that the core/shell nanorod arrays provide a facile and compatible frame for potential applications in nanorod-based solar cells and as efficient photocatalysts.

3.2 Electrocatalysis

Very fine and uniform nanoparticles of copper has been obtained by the thermal decomposition of copper oxalate nanorods in an argon atmosphere [78]. The precursor nanorods were obtained using a microemulsion method and has been extensively characterized using X-ray diffraction, scanning electron microscopy, transmission electron microscopy (TEM) and X-ray photoelectron spectroscopy (XPS). The initial precursor of copper oxalate crystallizes in

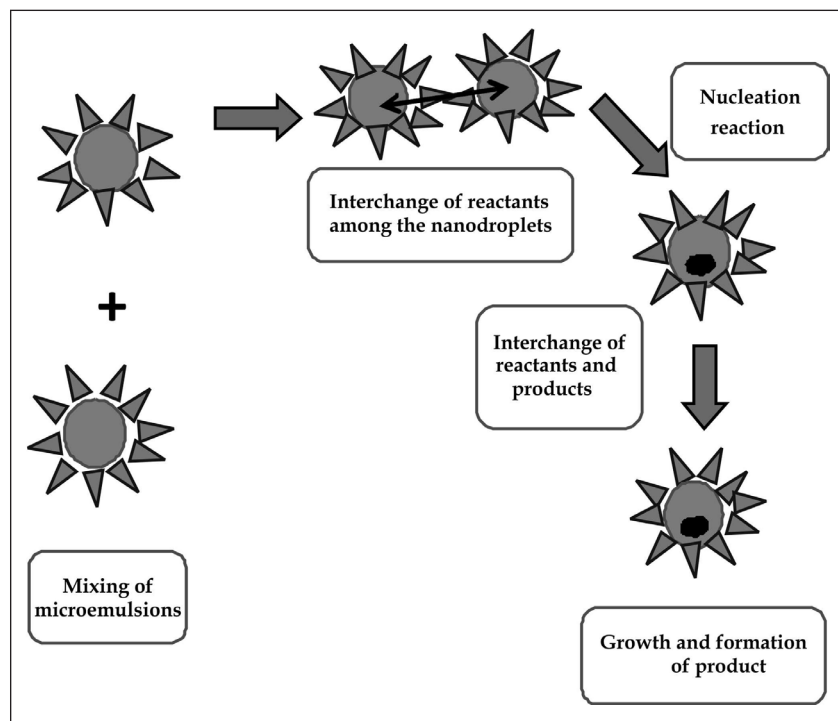


Figure 1: Mechanism of the formation of nanoparticles in microemulsions.

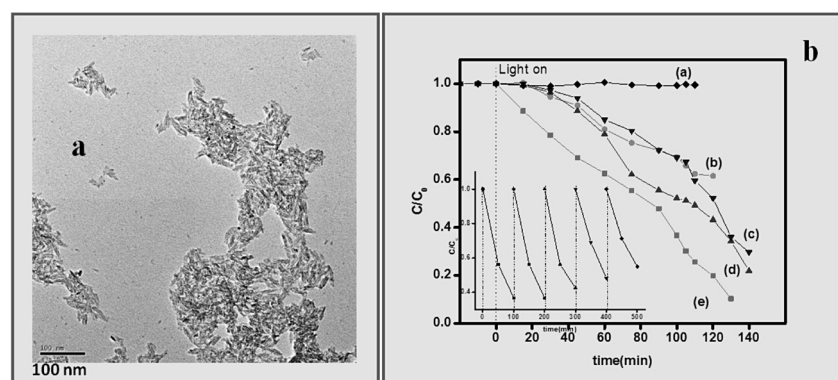
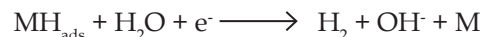


Figure 2(a): TEM micrographs of TiO_2 nanospindles synthesized using reverse micellar method (inset: TEM image of a single TiO_2 nanospindle) : (b) Photocatalytic degradation of Rhodamine B at 546 nm as a function of irradiation time performed on TiO_2 nanospindles (a) blank experiment (absence of catalyst) (b) at pH = 4 (c) Commercial TiO_2 (Degussa P25) (d) at pH = 8.5 (e) at pH = 8.5 with O_2 purging. (inset: Cycling studies of photodecomposition of TiO_2 nanospindles under UV light and photograph showing the degradation of rhodamine B using TiO_2 nanospindles in 2h) [adapted from ref: 67].

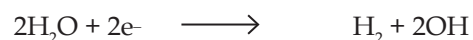
the orthorhombic system (JCPDS- 210297). On heating the precursor at 325 °C in argon, monophasic copper nanoparticles with a face centered cubic ($Fm\bar{3}m$) crystal system was obtained. The crystallite size of the particles was calculated to be 7 nm using Scherrer's formula. The average diameter of the spherical nanoparticles was found to be 4–6 (± 0.2) nm and are highly crystalline. The electrochemical properties of the Cu nanoparticles were evaluated using cyclic voltammetry. The concept of electroactive surface area (ESA) [79-81] is very significant for calculating the current density. ESA was determined electrochemically by applying the following formula [82].

$$ESA = Q_{H} / \{Q_{ref} (\text{Cu loading})\}$$

QH is calculated by extrapolating the curve obtained from cyclic voltammetry. The Q_{ref} for copper is 420 $\mu\text{C cm}^2$ [83,84]. The electroactive surface areas of Cu nanoparticles on the glassy carbon electrode and on the Pt electrode were found to be 0.052 $\text{cm}^2 \text{mg}^{-1}$ and 0.119 $\text{cm}^2 \text{mg}^{-1}$ respectively. Copper nanoparticles were used as electrocatalysts for hydrogen evolution reaction by applying a negative potential from -1.5 to 0 V for both the working electrodes (glassy carbon as well as platinum) in 0.5 M KOH solution. Fig. 4 shows the HER study of copper nanoparticles on (a) glassy carbon and (b) platinum electrodes. The hydrogen generation is according to the equations given below:



where M = electrocatalyst



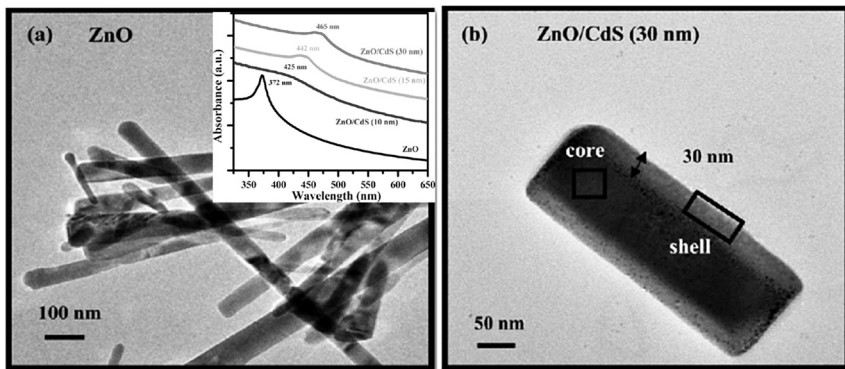


Figure 3: TEM images of (a) ZnO nanorods , inset shows optical absorbance spectra of the uncoated ZnO nanorods, and ZnO/CdS coreshell nanorod arrays with varying shell thickness and (b) ZnO/CdS [adapted from ref: 76].

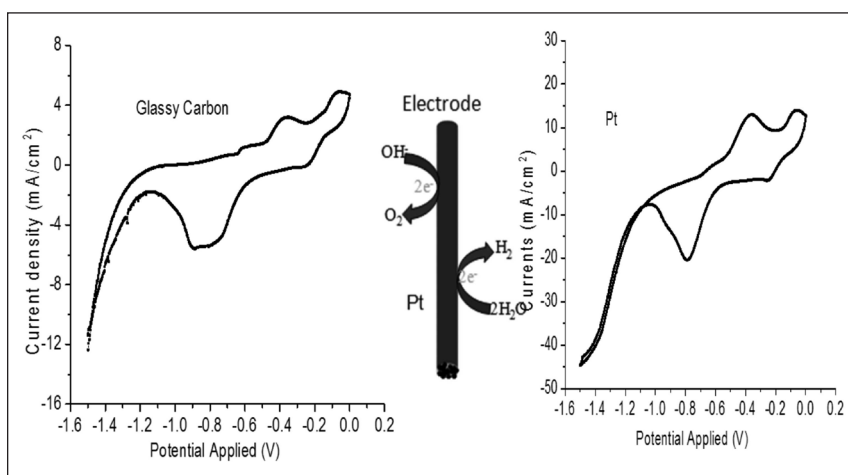


Figure 4: HER study of copper nanoparticles on (a) glassy carbon and (b) platinum electrodes [adapted from ref: 78]. Schematic representation depicting the electrode process.

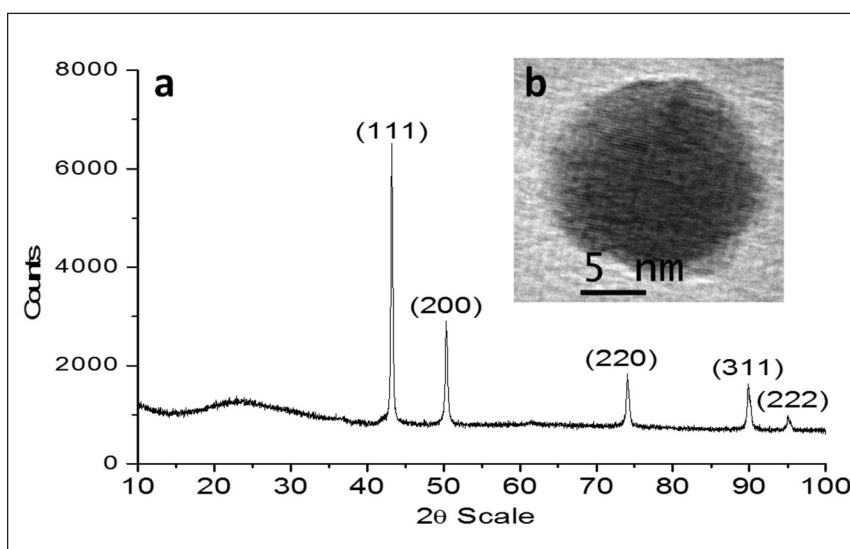
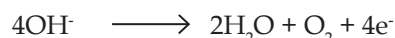


Figure 5: Powder x-ray diffraction pattern of copper nanoparticles (after HER over glassy carbon electrode) and (b) TEM micrograph of copper nanoparticles after HER over glassy carbon electrode [adapted from ref: 78].

For the glassy carbon electrode, two redox peaks were observed at -0.61 V and -0.36 V. These peaks are observed due to the oxidation of Cu to Cu⁺ and to Cu²⁺. The maximum current density was found to be 12 (0.2) mA cm⁻² at an applied potential of -1.50 V which is the current density for HER. Also in the case of platinum as the working electrode, two redox peaks were observed at potentials : -0.62 V and -0.37 V due to the oxidation of Cu nanoparticles. The maximum current density was 46 (± 0.6) mA cm⁻² at 1.50 V. The current density depends critically on the surface area and morphology. The copper nanoparticles obtained by us show excellent stability for 50 cycles (recorded continuously). Stability is also confirmed by the monophasic nature of copper nanoparticles shown by x-ray diffraction pattern (Fig. 5a) after the hydrogen evolution reaction. The particles remained stable spherical in nature as they were before electrocatalysis, with average diameters of 15–20 (±1) nm (Fig. 5b). Oxygen evolution reaction was also studied for these copper nanoparticles using cyclic voltammetry. The electrode containing copper nanoparticles as electrocatalysts showed an increase in oxidation current at 0.52 V potential for both the working electrodes (glassy carbon and Pt). The following reaction occurs at the electrode surface



The peak current is proportional to the amount of oxygen generated during the electrochemical reaction. The maximum current density at 0.8 V potential is 1.6 (±0.01) mAcm⁻² and 15 (±0.3) mAcm⁻² using the glassy carbon and platinum electrode respectively.

Wet chemical methods were also employed for the synthesis of core shell and composites of copper - cobalt. The hydroxide precursor was amorphous and on heating under hydrogen conditions results in the formation of Cu-Co core-shell and composite type nanoparticles. With the help of XPS studies, it was concluded that the shell consists of Cu-Co alloy, whereas

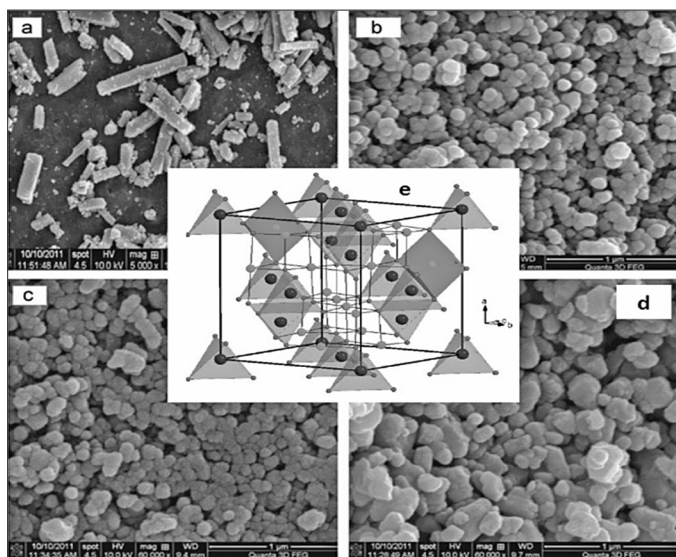


Figure 6: FESEM micrographs for Mg_2MnO_4 obtained from oxalate precursor by heating at (a) 500° C (b) 600° C (c) 700° C (d) 800° C (e) structure of cubic spinel structure [adapted from ref: 87].

the core comprises of Cu-Co composite particles and we estimate the shell thickness to be ~15 nm, which matches closely with TEM studies. Note that surface energies of cobalt, copper and copper-cobalt alloy are 2.709, 1.934, and 0.75 J m⁻², respectively [85]. On the basis of the surface energies, we may conclude that copper cobalt alloy would prefer to be on the surface as is observed. By decreasing the concentration of the reducing agent from 20 M to 1M during the synthesis leads to the formation of a composite phase containing Cu and Co (no core-shell structures). PXRD patterns clearly show the formation of biphasic mixture of copper and cobalt that could be indexed on the basis of face centered cubic cell reported for copper (JCPDS # 851326) and cobalt (JCPDS # 150806).

Four irreversible peaks were observed for both the core shell & composite nanostructures. The peaks may be understood as due to formation of four couples (in basic medium): Cu/Cu⁺ and Cu⁺/Cu²⁺ for copper and Co/Co²⁺ and Co²⁺/Co³⁺. At a potential of -1.2 V, Cu-Co nanocomposite based cell leads to higher current density than core-shell nanostructures. However, at about -1.5 V these two materials have almost the same hydrogen evolution efficiency. The nanocomposite may therefore be slightly better for HER activity at lower potentials than 1.4 V. The current density (~15 mA/cm²) for nanocrystalline Cu-Co particles was found to be much higher (5 times) than the current generated (~3 mA/cm²) for bulk Cu-Co alloy [86].

Apart from metal & alloy nanoparticles, microemulsions have also been used for the synthesis of oxide nanoparticles.

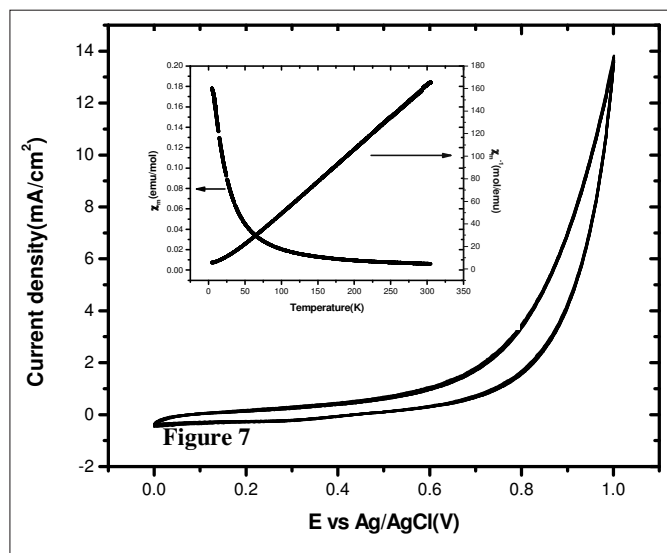


Figure 7: Cyclic voltammogram (30 cycles) of Mg_2MnO_4 obtained at 500° C shows the maximum current density at 14 mA/cm² with onset potential at 0.65V. Inset shows the χ_m vs. T plot for the magnetic oxide [adapted from ref: 87].

Mixed metal oxalates of magnesium & manganese have been obtained using microemulsions made up of cationic surfactants [87]. The oxalate precursor was calcined at higher temperature to obtain the oxide. On increasing the calcination temperature of the oxalate precursor from 600°C to 800°C, particle size increased from 25 to 50 nm at 600°C, to 60–90 nm at 700°C and 100–120 nm at 800°C as confirmed from FESEM (Fig. 6). Electrochemical studies (oxygen evolution reaction) have been carried out by loading the catalyst nanoparticles (at 500°C) on a glassy carbon electrode acting as a working electrode. Oxygen evolution reaction is an anodic process which is enhanced with catalyst's surface properties like high surface to volume ratio [88]. These nanostructures show an increased current at 0.65V versus an Ag/AgCl reference electrode. Mg_2MnO_4 shows better electrocatalytic efficiency (current density of 14 mA/cm², onset potential: 0.65V) towards oxygen evolution reaction compared to other ternary manganites like $MgMnO_3$ (current density: 0.06 mA/cm², onset potential: 1.9V [89]) and $ZnMnO_3$ (current density: 4–5 mA/cm², onset potential: 1V [90]). The cyclic voltammogram for 30 consecutive cycles show negligible variation in activity which indicates its stability in alkaline medium. The stability of the electrode is an important role for electrocatalytic applications [91]. Mg_2MnO_4 nanorods exhibit Curie-Weiss behavior (50–300K) with a Weiss constant of 14K (Fig. 7). The magnetic moment of this compound was observed to be 3.91 μB which matches with the theoretical magnetic moment of 3.87 μB thereby confirming the presence of tetravalent manganese.

4. Conclusions

The current research work is focused on electro and photocatalysts which have applications in energy and environmental issues. Highly active photocatalysts (TiO_2 , ZnO/CdS and $\text{ZnO}/\text{In}_2\text{S}_3$) have been synthesized by microemulsion, surface functionalized and hydrothermal route, along with copper, copper-cobalt alloy and mixed metal oxides of magnesium & manganese as electrocatalysts. The various synthetic parameters like alkali concentration, reaction temperature and reaction time play important role in the formation of these nanoparticles. The high photocatalytic activity is attributed due to small size, large surface area, crystalline and anisotropic nature of the material. The electrocatalytic properties of the nanosized metal and alloy nanoparticles are found to be better than observed for the bulk counterpart. Wet chemical routes discussed in this review prove to be a useful method for the synthesis of various types of oxide nanomaterials.





Acknowledgements

The authors acknowledge Nanoscale Research Facility, funded by DeiTy for the facilities & Dept. of Science & Technology for funding. AG & DD thanks NRF, DeiTy for financial assistance.

References

- M. R. Hoffmann, S. T. Martin, W. Choi and D. W. Bahnemannt, *Chem. Rev.*, 95 (1995) 69.
- A. Kubacka, M. Fernandez-García and G. Colon, *Chem. Rev.*, 112 (2012) 1555.
- A. Fujishima and K. Honda, *Nature*, 238 (1972) 37.
- M. Miyauchi, A. Nakajima, T. Watanabe and K. Hashimoto, *Chem. Mater.*, 14 (2002) 2812.
- K. Hashimoto, H. Irie and A. Fujishima, *Jpn. J. Appl. Phys.*, 44 (2005) 8269.
- O. Carp, C. L. Huisman and A. Reller, *Prog. Solid State Chem.*, 32 (2004) 33.
- M. A. Fox and M. T. Dulay, *Chem. Rev.*, 93 (1993) 341.
- L. Gomathi Devi and R. Kavitha, *Appl. Catal., B: Environmental*, 140–141 (2013) 559.
- T. Sreethawong, S. Laehsatee and S. Chavadej, *Int. J. Hydrogen Energy*, 33 (2008) 5947.
- Q. Xiang, J. Yu, W. Wang and M. Jaroniec, *Chem. Commun.*, 47 (2011) 6906.
- G.R. Bamwenda, S. Tsubota, T. Nakamura and M. Haruta, *J. Photochem. Photobiol. A* 89 (1995) 177. T. Chen, Z. Feng, G. Wu, J. Shi, G. Ma, P. Ying, and C. Li, *J. Phys. Chem. C*, 111, (2007) 8005.
- A. Patsoura, D. I. Kondarides and X. E. Verykios, *Catal. Today*, 124 (2007) 94.
- A. Naldoni, M. D. Arienzo, M. Altomare, M. Marelli, R. Scotti, F. Morazzoni, E. Sellia, and V. D. Santo, *Appl. Catal. B: Environmental* 130–131 (2013) 239.
- Z. Zhang, F. Xiao, Y. Guo, S. Wang and Y. Liu, *ACS Appl. Mater. Interfaces*, 5 (2013) 2227.
- P. Wang, J. Wang, T. Ming, X. Wang, H. Yu, J. Yu, Y. Wang and M. Lei, *ACS Appl. Mater. Interfaces*, 5 (2013) 2924.
- S. R. Morrison and T. Freund, *J. Chem. Phys.*, 47 (1967) 1543.
- X. Lu, G. Wang, S. Xie, J. Shi, W. Li, Y. Tong and Y. Li, *Chem. Commun.*, 48 (2012) 7717.
- F. Wang, D. Zhao, Z. Xu, Z. Zheng, L. Zhang and D. Shen, *J. Mater. Chem. A*, 1 (2013) 9132.
- F.-X. Xiao, *ACS Appl. Mater. Interfaces* 4 (2012) 7055.
- W. Liu, M. Wang, C. Xu, S. Chen and X. Fu, *J. Mol. Catal. A: Chemical* 368–369 (2013) 9.
- S. Balachandran and M. Swaminathan, *Dalton Trans.*, 42 (2013) 5338.
- Q. P. Luo, X. Y. Yu, B. X. Lei, H. Y. Chen, D. B. Kuang, and C.-Y. Su, *J. Phys. Chem., C*, 116 (2012) 8111.
- R. C. Pawar and C. S. Lee, *Appl. Catal., B: Environmental* 144 (2014) 57.
- X. Wang, Z. Wu, Y. Wang, W. Wang, X. Wang, Y. Bu and J. Zhao, *J. Hazard. Mater.* 262 (2013) 16.
- B. Li, T. Liu, Y. Wang and Z. Wang, *J. Colloid Interface Sci.*, 377 (2012) 114.
- M. Hara, T. Kondo, M. Komoda, S. Ikeda, K. Shinohara, A. Tanaka, J.N. Kondo and K. Domen, *Chem. Commun.*, (1998) 357.
- Y. Zhang, B. Deng, T. Zhang, D. Gao and A.-W. Xu, *J. Phys. Chem. C*, 114 (2010) 5073.
- K. Hayat, M.A. Gondal, M.M. Khaled, Z.H. Yamani and S. Ahmed, *J. Hazard. Mater.* 186 (2011) 1226.
- H. Kim, K. Senthil and K. Yong, *Mater. Chem. Phys.*, 120 (2010) 452.
- M. Shahid, D. S. Rhen, I. Shakir, S. P. Patole, J. B. Yoo, S.-J. Yang and D. J. Kang, *Mater. Lett.*, 64 (2010) 2458.
- B. Li, Y. Xu, G. Rong, M. Jing and Y. Xie, *Nanotechnology* 17 (2006) 2560.
- Y. Wang, C. S. Liu, F. B. Li, C. P. Liu and J. B. Liang, *J. Hazard. Mater.* 162 (2009) 716.
- X. Xie, H. Yang, F. Zhang, L. Li, J. Ma, H. Jiao, J. Zhang, *J. Alloys Compd.* 477 (2009) 90.
- J. Eberl and H. Kisch, *Photochem. Photobiol. Sci.* 11 (2008) 1400.
- L. Zhang, W. Wang, J. Yang, Z. Chen, W. Zhang, L. Zhou and S. Liu, *Appl. Catal. A: Gen.* 308 (2006) 105.
- X. Song and L. Gao, *J. Phys. Chem. C*, 112 (2008) 15299.
- K. Hayat, M. A. Gondal, M. M. Khaled and S. Ahmed, *J. Mol. Catal. A: Chem.*, 336 (2011) 64.
- H. Kominami, K. Oki, M. Kohno, S.-I. Onoue, Y. Kera and B. Ohtani, *J. Mater. Chem.*, 11 (2001) 604.
- A. G. S. Prado, L. B. Bolzon, C. P. Pedroso, A. O. Moura, and L. L. Costa, *Appl. Catal. B: Environ.*, 82 (2008) 219.
- Y. Zhu, F. Yu, Y. Man, Q. Tian, Y. He and N. Wu, *J. Solid*

- State Chem., 178 (2005) 224.
41. C. Karunakaran and S. Senthilvelan, *J. Mol. Catal. A: Chem.*, 233 (2005) 1.
 42. A. A. Ashkarran, S. A. A. Afshar, S. M. Aghigh and M. Kavianipour, *Polyhedron*, 29 (2010) 1370.
 43. P. Ji, J. Zhang, F. Chen, M. Anpo, *Appl. Catal. B: Environ.* 85 (2009) 148.
 44. P. Ji, J. Zhang, F. Chen and M. Anpo, *J. Phys. Chem. C*, 112 (2008) 17809.
 45. Y. Hou, L. Wu, X. Wang, Z. Ding, Z. Li and X. Fu, *J. Catal.*, 250 (2007) 12.
 46. B. Zhao and P. Zhang, *Catal. Commun.*, 10 (2009) 1184.
 47. Y. Yang, N. Ren, Y. Zhang and Y. Tang, *J. Photochem. Photobiol. A: Chem.*, 201 (2009) 111.
 48. M. Sun, D. Li, W. Li, Y. Chen, Z. Chen, Y. He and X. Fu, *J. Phys. Chem. C*, 112 (2008) 18076.
 49. A. Kudo, K. Omori and H. Kato, *J. Am. Chem. Soc.*, 121 (1999) 11459; S. Tokunaga, H. Kato, A. Kudo, *Chem. Mater.* 13 (2001) 4624–4628.
 50. Z. Zhang, W. Wang, M. Shang and W. Yin, *J. Hazard. Mater.* 177 (2010) 1013;.
 51. F. Amano, A. Yamakata, K. Nogami, M. Osawa and B. Ohtani, *J. Am. Chem. Soc.*, 130 (2008) 17650.
 52. L. Zhang, T. Xu, X. Zhao and Y. Zhu, *Appl. Catal. B: Environ.*, 98 (2010) 138.
 53. L. Xie, J. Ma and G. Xu, *Mater. Chem. Phys.*, 110 (2008) 197.
 54. Z. Ai, W. Ho, S. Lee and L. Zhang, *Environ. Sci. Technol.*, 43 (2009) 4143.
 55. M. Shang, W. Wang and L. Zhang, *J. Hazard. Mater.*, 167 (2009) 803.
 56. H. C. Chien, W. Y. Cheng, Y. H. Wang, T. Y. Wei and S. Y. Lu, *J. Mater. Chem.*, 21 (2011) 18180.
 57. S. Trasatti, *Electrochim. Acta*, 29 (1984) 1503.
 58. J. M. Sedlak, R. J. Lawrance and J. F. Enos, *Int. J. Hydrogen Energy*, 6 (1981) 159.
 59. M. Subhramannia, B. K. Balan, B. R. Sathe, I. S. Mulla and V. K. Pillai, *J. Phys. Chem. C*, 111 (2007), 16593.
 60. O. Roetschi and P. Delahay, *J. Chem. Phys.*, 23 (1955) 556.
 61. S. Trasatti and G. Buzzanca, *J. Electroanal. Chem.*, 29 (1971) 100.
 62. H. Zheng, J. Huang, W. Wang and C. Ma, *Electrochem. Commun.*, 7 (2005) 1045.
 63. P. Rasiyah and A. C. C. Tseung, *J. Electrochem. Soc.*, 130 (1983) 2384.
 64. D. Wang, H. L. Xin, R. Hovden, H. Wang, Y. Yu, D. A. Muller, F. J. DiSalvo and H. D. Abruña, *Nature Mater.*, 12 (2013) 81.
 65. H. Abe, F. Matsumoto, L. R. Alden, S. C. Warren, H. D. Abruña, and F. J. DiSalvo, *J. Am. Chem. Soc.*, 130 (2008) 5452.
 66. A. K. Ganguli, A. Ganguly and S. Vaidya, *Chem. Soc. Rev.*, 39 (2010) 474.
 67. D. Das, A. Shivhare, S. Saha and A. K. Ganguli, *Mater. Res. Bull.*, 47 (2012) 3780.
 68. P. Wang, S. M. Zakeeruddin, J. E. Moser, M. K. Nazeeruddin, T. Sekiguchi and M. Gratzel, *Nature Mater.*, 2 (2003) 402.
 69. Z. R. Tian, W. Tong, J. Y. Yong, N. G. Duan, V. V. Krishnan and S. L. Sui, *Science*, 276 (1997) 926.
 70. Y. K. Zhou, L. Cao, F. B. Zhang, B. L. He and H. L. Li, *J. Electrochem. Soc.*, 150 (2003), A1246.
 71. M. Qamar, S. J. Kim and A. K. Ganguli, *Nanotechnology*, 20 (2009) 455703.
 72. L. Li, X. Liu, Y. Zhang, P. A. Salvador and G. S. Rohrer, *Int. J. Hydrogen Energy*, 38 (2013) 6948.
 73. E. K. Akdogan, C. J. Rawn, W. D. Porter, E. A. Payzant and A. Safari, *J. Appl. Phys.*, 97 (2005) 084305.
 74. M. Yashima, T. Hoshina, D. Ishimura, S. Kobayashi, W. Nakamura and T. Tsurumi, *J. Appl. Phys.*, 98 (2005) 014313.
 75. K. Sungjee, B. Fisher, H.-J. Eisler and M. G. Bawendi, *J. Am. Chem. Soc.*, 125 (2003) 11466.
 76. S. Khanchandani, S. Kundu, A. Patra, and A. K. Ganguli, *J. Phys. Chem. C*, 116 (2012) 23653.
 77. S. Khanchandani, S. Kundu, A. Patra, and A. K. Ganguli, *J. Phys. Chem. C*, 117 (2013) 5558.
 78. Bharat Kumar, S. Saha, M. Basu and A. K. Ganguli, *J. Mater. Chem. A*, 1 (2013) 4728.
 79. S. Trasatti and O. A. Petrii, *J. Electroanal. Chem.*, 327 (1992) 353.
 80. M. Subhramannia, K. Ramaiyan and V. K. Pillai, *Langmuir*, 24 (2008) 3576.
 81. R. S. Dey and C. R. Raj, *J. Phys. Chem. C*, 114 (2010) 21427.
 82. Z. Hamoudi, M. A. E. Khakani and M. Mohamedi, *Int. J. Electrochem. Sci.*, 7 (2012) 1666.
 83. C. L. Green and A. Kucernak, *J. Phys. Chem. B*, 106 (2002) 1036.
 84. S. A. S. Machado, A. A. Tanaka and E. R. Gonzalez, *Electrochim. Acta*, 36 (1991) 1325.
 85. J. Ahmed, A. Ganguly, S. Saha, G. Gupta, P. Trinh, A. M. Mugweru, S. E. Lofland, K. V. Ramanujachary and A. K. Ganguli, *J. Phys. Chem. C*, 115 (2011) 14526.
 86. L. Brossard and B. Marouis, *Int. J. Hydro. Energy*, 19 (1994) 231.
 87. N. Garg, Menaka, K. V. Ramanujachary, S. E. Lofland and A. K. Ganguli *J. Solid State Chem.*, 197 (2013) 392.
 88. M. Subhramannia and V. K. Pillai, *J. Mater. Chem.*, 18 (2008) 5858.
 89. P. Saha, M. K. Datta, A. Manivannan and P. N. Kumta, *ECSMeet. Abstr.*, 5 (2012) 353.
 90. K. Izumiya, E. Akiyama, H. Habazaki, A. Kawashima, K. Asami and K. Hashimoto, *J. Appl. Electrochem.*, 27 (1997) 1362.
 91. H. Zheng, J. Huang, W. Wang and C. Ma., *Electrochem. Commun.*, 7 (2005) 1045.

	<p>Dr Aparna Ganguly obtained her BSc (Hons) in chemistry from Sri Venkateshwara College, University of Delhi in 2002. Later she obtained her MSc in chemistry from University of Delhi with specialisation in physical chemistry in 2004 and Ph D. in Material Chemistry from Jamia Millia Islamia on synthesis of functionalized nanostructures. After working at Central University of Rajasthan, she is currently working as a project scientist at Nanoscale Research Facility .IIT Delhi. Her research interest lies in the synthesis & properties of novel materials especially functionalized porous oxides.</p>
	<p>Dr. Oruganti Anjaneyulu completed(2002) B.Sc from Andhra Loyola College, Vijayawada and MSc (Chemistry) from Karnatak University Dharwad(2004). He has completed(2012) PhD in Inorganic chemistry from University of Hyderabad. Since Dec. 2012, working as research associate with Prof. Ashok K Ganguli at IIT Delhi on graphene-bismuth composites towards photocatalytic applications.</p>
	<p>Ms Debashree Das obtained her BSc (Hons) in Chemistry from Banaras Hindu University, in 2003. Later she obtained her MSc in chemistry from Indian Institute of Technology Roorkee, in 2005. Her PhD thesis is focussed on photocatalytic studies of Ti, Nb and Ta based oxides. Currently she is working as a Project associate, under the supervision of Prof. A. K. Ganguli, at Nano Research facility, IIT Delhi.</p>
	<p>Dr A.K. Ganguli is currently the Director of Institute of Nano Science & Technology, Mohali and a Professor of Chemistry at IIT Delhi. His key interests are in microemulsions mediated design of nanomaterials, photo- and electrocatalysis and superconducting materials. He has published more than 200 papers in international journals. Dr Ganguli has been awarded with various prestigious fellowships & awards including the Materials Research Society award in 2006 and the Chemical Research Society of India Medal in 2007 and the CRSI-CNR Rao Medal (2013). He is a fellow of the Indian Academy of Sciences and the National Academy of Sciences, India.</p>

Photocatalytic Activity of Cellulose Acetate-tin (IV) Molybdate Nanocomposite in Solar Light

B.S. Rathore, Gaurav Sharma and Deepak Pathania*

Department of Chemistry, Shoolini University, Solan, Himachal Pradesh (India) -173212

E-mail:dpathania74@gmail.com

Abstract

Cellulose acetate tin (IV) molybdate nanocomposite (CA/TMNC) has been synthesized by simple and efficient sol gel process. The nanocomposite was characterized using Fourier transform infrared spectroscopy (FTIR), transmission electron microscopy (TEM) and X-ray diffraction (XRD). The CA/TMNC was explored for its photocatalytic activity for the degradation of methylene blue dye from aqueous solution. The photocatalytic degradation of methylene blue dye was studied for 120 min with irradiation at 660 nm wavelength. The dye degradation of 82% was recorded within 60 min of irradiation time. The photodegradation of MB dye using nanocomposite was fitted well in pseudo-first-order kinetics.

Keywords: Photocatalysis, Nanocomposite, Methylene blue.

1. Introduction

Due to fast industrialization, natural water has been polluted continuously by the release of effluents. Various industries such as textile, paper, paints etc have been discharging heavy metals and chemicals continuously into water bodies. Such polluted water containing toxic and carcinogenic substances may cause adverse effect to the human health and creating immense threat to ecological system, if not treated properly before release into environment [1-3]. Due to the colorful nature of dyes they can be easily visualized. Dyes are synthetic origin and have complex aromatic molecular structure which makes them more stable and difficult to biodegrade. The dyes can decompose into carcinogenic aromatic amines under aerobic conditions which can cause serious health problems like allergy, dermatitis, skin irritation, cancer etc to animals and human beings. So the attempt has been made by researchers for the treatment of wastewater containing dyes at source before being discharged into water bodies.

A large number of conventional methods such as chemical precipitation, ion exchange, electro dialysis, ultra filtration, membrane separation, photodegradation, electrochemical oxidation etc. have been have been explored for the removal of organic pollutants [4-10]. However, conventional methods have not economically and environmentally feasible for the removal of the dyes and metal ions from polluted water. Adsorption is one of the most effective techniques among the methods reported for the degradation of pollutants due to its economically viable, technically feasible and environmentally acceptable [11-15].

Recently, organic- inorganic hybrid nanocomposite materials have received much attention because of high performance due to different integrated combinations [16]. Organic materials have many limitations such as decreased mechanical strength and less removal capacity at high temperature [17]. The inorganic materials have some limitations besides the advantages like good selectivity for metal ions, stability at high temperature and radiation fields [18]. Therefore, to overcome these limitations, organic-inorganic nanocomposite material has been introduced which were significantly used in environmental applications [19-26].

Now a day, a significant attention has been drawn for the synthesis of cellulose based nanocomposite material due to its superior properties such as low cost, high-volume application, easy processability, renewable nature and possibility of recycling [24].

Thus the present work deals with the synthesis of cellulose acetate-tin (IV) molybdate nanocomposite (CA/TPNC) ion exchanger by simple sol-gel method. The photocatalytic activity of CA/TPNC material was explored for the degradation of methylene blue (MB) dye. The synthesized composite material was characterized by transmission electron microscopy (TEM), Fourier transform infrared (FTIR) and X-ray diffractometer. The photocatalytic degradation of MB was determined using ultraviolet visible spectroscopy.

2. Experimental

2.1 Reagents and instruments

All reagents used in this were of analytical grade. The main reagents used were tin (IV) chloride, sodium

dihydrogen phosphate (LobaChemia Pvt. Ltd., Mumbai, India), Formic acid (E Merck Ltd., India), cellulose acetate (CDH Pvt. Ltd., New Delhi, India). Double distilled water was used for dilution and preparation of required solution for synthesis. Absorbance of samples was recorded using UV-Visible spectrophotometer (Shimadzu UV-1601, Japan). A digital pH meter (Elico LI-10, India), FTIR spectrophotometer (Perkin Spectrum-400), X-ray diffractometer (X'pert Pro Analytical, Switzerland), Transmission electron microscopy (Hitachi, H7500, Germany), Muffle furnace (MSW-275, India) and water bath incubator shaker were used.

2.2 Preparation of cellulose acetate-tin(IV) molybdate nanocomposite (CA/TMNC)

Cellulose acetate-tin (IV) molybdate phosphate nanocomposite (CA/TMNC) material was synthesis using simple sol gel method as mentioned earlier [27,28]. In this process, firstly 0.1 M solution of tin (IV) chloride was mixed with 0.1M solution of molybdate phosphate in 1:1 ratio by volume with constant stirring for 1h at room temperature. The pH of the solution was adjusted to 0-1 with the help of 1M HNO₃. The precipitates of tin (IV) molybdate were formed. Further, the gel of cellulose acetate (CA) was prepared in concentrated formic acid. The gel was added to the precipitates of tin (IV) molybdate solution and mixed thoroughly with constant stirring for 5h. The resulting mixture was kept for 24h at room temperature for digestion with random shaking. The supernatant liquid was removed and precipitates were filtered under suction. The precipitates were washed with distilled water

to remove the excess acid. The precipitates of CA/TMNC were dried at 50°C temperature for 12 h.

2.3 Photocatalytic activity of CA/TMNC

The photocatalytic reaction was performed by the slurry type batch reactor method [29]. A double walled Pyrex vessel was used for experiment and temperature of the vessel was maintained to 30±0.3°C. For adsorption studies, a suspension consisting of catalyst (CA/TMNC) and dye solution was stirred and kept in dark to attain the equilibrium. Whereas, in case of photocatalytic experiment the suspension prepared from composite ion exchanger and dye was five minutes and exposed to natural solar light. At particular time intervals the solution was taken (3mL) and centrifuged to eliminate the composite ion exchanger particles. The concentration of dyes was detected using UV-Vis spectrophotometer at 662 nm wavelength. The degradation efficiency of dye was calculated as follow:

$$\% \text{ Degradation} = \frac{C_e - C_t}{C_e} \times 100$$

Where C₀ and C_t are the initial and instant concentration of methylene blue dye.

2.4 FTIR studies

The FTIR analysis 10 mg of CA/TMNC was mixed with 100 mg of KBr and grounded to a very fine powder. A transparent was formed by applying pressure. The FTIR spectrum was recorded between 400 and 4000 cm⁻¹.

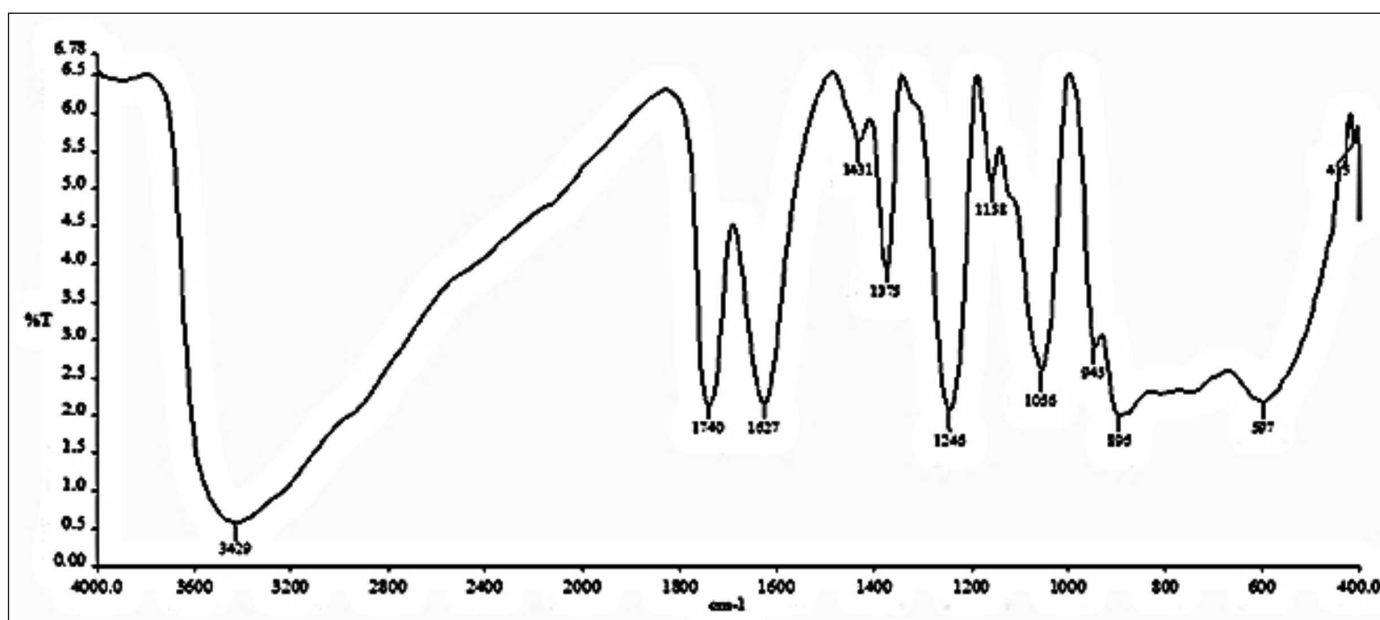


Fig. 1. FTIR spectrum of CA/TMNC.

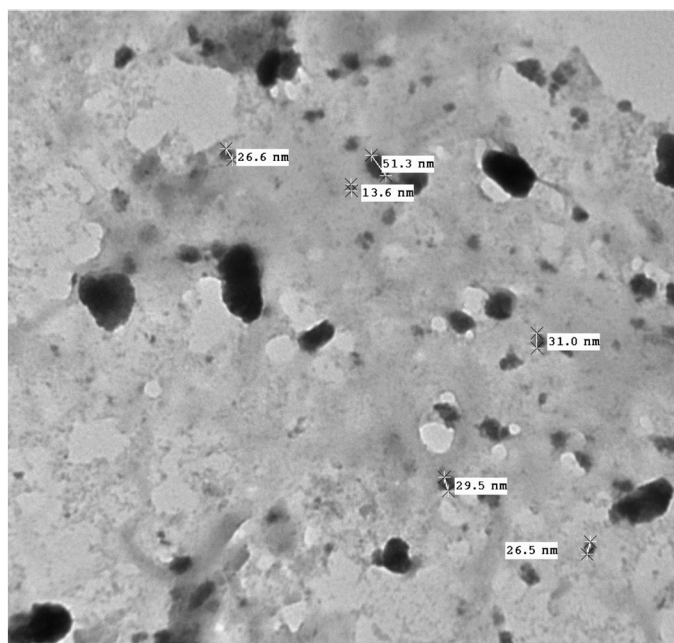


Fig. 2. TEM photographs of CA/TMNC.

Transmission electron microscopy (TEM) studies

Transmission electron microphotograph of CA/TMNC was recorded using Hitachi transmission electron microscope.

2.5 X-ray analysis

The X-ray diffraction pattern of the CA/TMNC was recorded by X-ray diffractometer using CuK α radiation ($\lambda = 1.5418\text{\AA}$).

3. Results and discussion

The FTIR spectrum of CA/TMNC was shown in Fig. 1. The broad peak at 3429 cm^{-1} may be attributed due to the O-H stretching vibration [30]. The peaks in the regions 597 cm^{-1} may be assigned to metal oxide groups. Absorption band at 1740 cm^{-1} corresponds to carbonyl of ester group in cellulose acetate. The peak at 1627 cm^{-1} was due to free water molecule (water of crystallization) and strongly bonded -OH group in the matrix. A sharp peak at 1375 cm^{-1} indicates deformation vibration of hydroxyl groups [31].

The absorption band at 1246 cm^{-1} may be due to the vibration associated in the skeletal ring of sugar monomers. The presence of characteristics peaks of CA and TM in the spectra clearly indicated the formation of CA/TM nanocomposite.

TEM image of CA/TMNC was shown in Fig. 2. The TEM results indicated homogeneous distribution of CA and TM particles in the composite. The darker portion represents CA wrapped TM while white portion corresponds to polymeric CA backbone. The average particles of 29 nm were observed from the TEM images.

The XRD pattern of CA/TMNC was shown in Fig. 3. The result shows weak intensity peak thereby suggested the amorphous nature of the nanocomposite.

3.1 Photocatalytic activity of CA/TM Nanocomposites

The photodegradation of methylene blue using CA/TMNC, tin molybdate (TM) and cellulose acetate (CA)

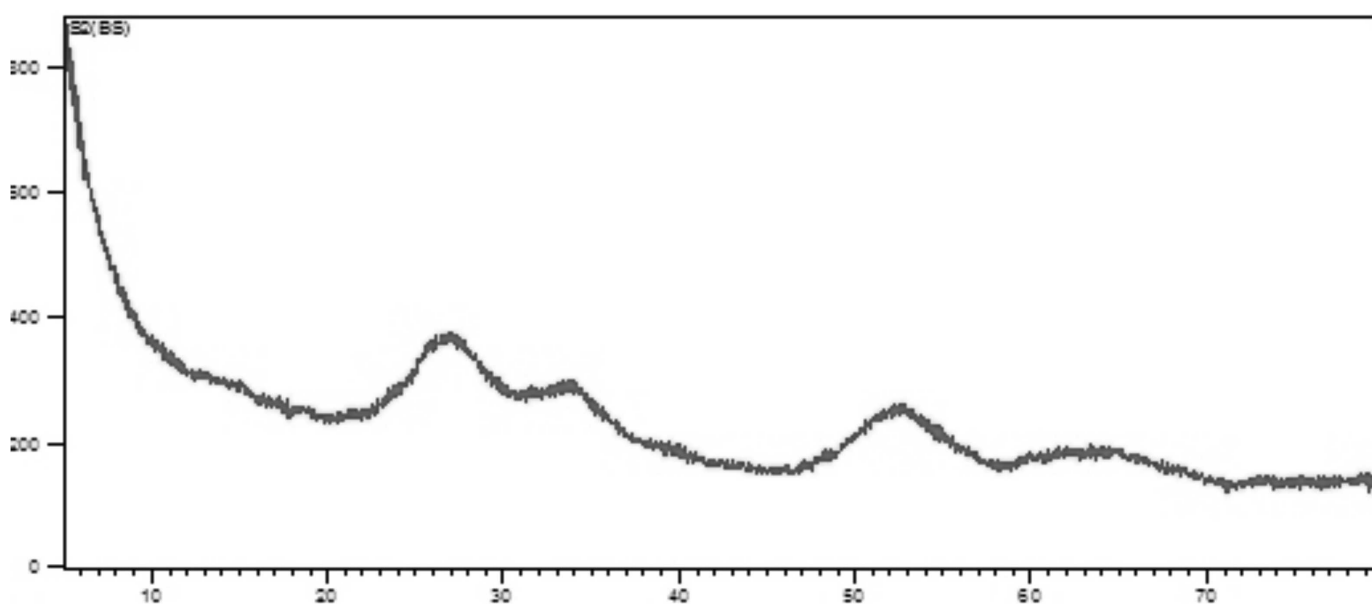


Fig. 3. X-rays diffraction pattern of CA/TMNC

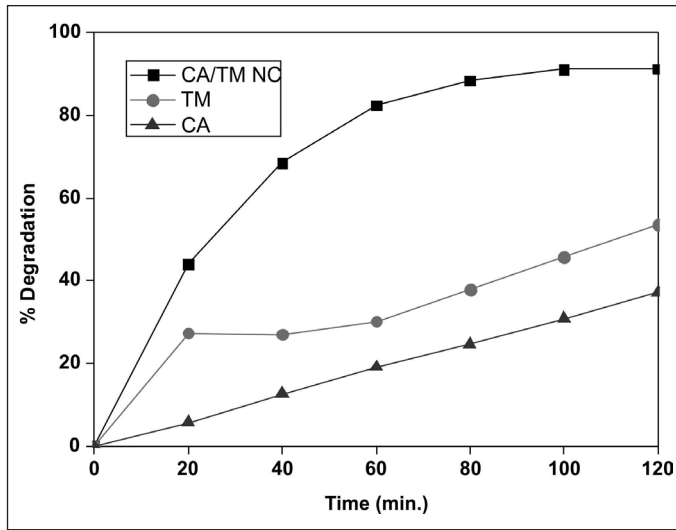


Fig. 4 Photodegradation of Methylene Blue onto CA/TMNC, TM and CA

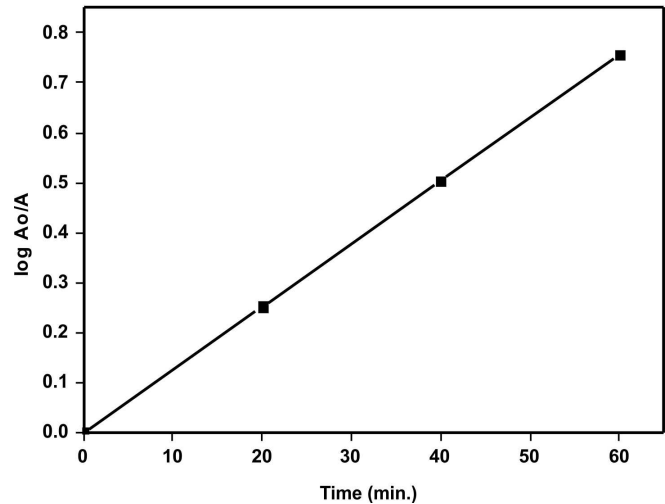


Fig. 6 Photocatalytic degradation kinetics of methylene blue dye

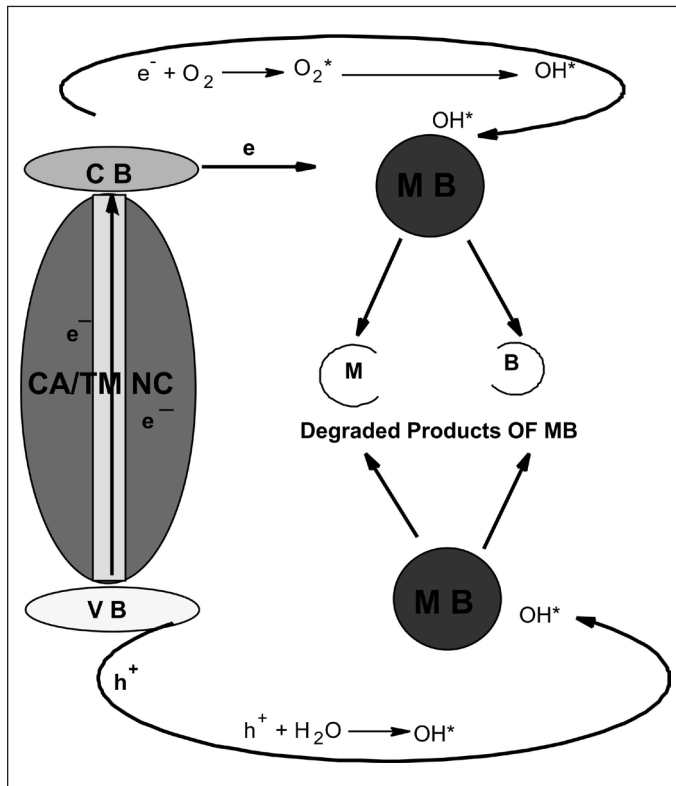
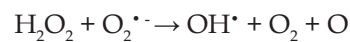
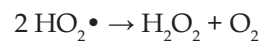
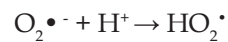
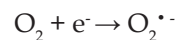
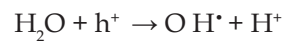
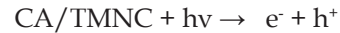


Fig. 5 Scheme for photodegradation on MB using CA/TMNC

were investigated in presences of solar light. The results of the photodegradation of MB were shown in Figure 4. The decrease in the dye absorbance with time indicated that the dye was degraded in aqueous solution using nanocomposite. The maximum degradation of dye was recorded for CA/TMNC compared to TM and CA in presence of solar light. It has been observed that about 91% of dye was degraded in 120 minutes compared to 53 and 37% for TM and CA, respectively.

In the typical photodegradation reaction, the CA/TMNC was irradiated with solar light produced electron-hole pair ($h\nu + e^-/e^-CB$). The conduction band electrons were transferred to catalyst surface. The conduction band electrons reduced the O_2 and forms hydroxyl radicals. The highly oxidizing OH^\cdot radicals caused the degradation of MB dye.



The excited electron from the photocatalyst conduction band enters into the molecular structure of MB and disrupts its conjugated system. The hole at the valence band generates OH^\cdot via reaction with water or OH^- . The OH^\cdot was used for oxidation of organic compound as shown in Figure 5.

The rate of photocatalytic degradation of methylene blue dye was determined using pseudo-first order kinetic model [25]:

$$r = -\frac{dC}{dt} = k_{app} C$$

On integrating the above equation, we get

$$\ln C_0/C_t = K_{app} t$$




where k_{app} is the apparent rate constant, C_0 is the concentrations of dye before illumination and C_t is the concentration of dye at time t . The plot of $\ln C_0/C_t$ vs irradiation time showed a linear correlation which demonstrated that the photodegradation of MB dye using CA/TM NC followed the pseudo-first-order kinetics (Figure 6) [25]. The correlation coefficient value R^2 was observed to 0.999 indicated the feasibility of the reaction. The value of rate constant k (0.01259 min^{-1}) was calculated from the slope of the plot.

4. Conclusion

The synthesized cellulose acetate-tin (IV) molybdate nanocomposite was successfully explored for the photochemical degradation of methylene blue. The TEM micrographs reveals that the particle size of CA/TMNC was between 15 and 55 nm. FTIR studies also confirmed the formation of composite material. 91% of MB dye was degraded within 120 minutes of solar light exposure. The kinetic studies of photodegradation indicated that CA/TMNC obey the pseudo-first-order kinetic model with R^2 of 0.999.

References

- V. K. Gupta, P. J. M. Carrott, M. M. L. R. Carrott and Suhas, *Environmental Science and Technology*, 39 (2009) 783.
- Z. M. Siddiqi and D. Pathania, *Indian Journal of Environmental Protection*, 22 (2002) 201.
- V. K. Gupta, A. Rastogi and A. Nayak, *Journal of Colloid and Interface Science*, 342 (2010) 533.
- K. G. Bhattacharyya and A. Sharma, *Dyes and Pigments*, 65 (2005) 51.
- V. K. Gupta, A. Mittal, V. Gajbe and J. Mittal, *Industrial & Engineering Chemistry Research*, 45 (2006) 1446.
- V. K. Gupta, A. Mittal, L. Kurup and J. Mittal, *Journal of Colloid and Interface Science*, 304 (2006) 52.
- V. K. Gupta and I. Ali, *Journal of Environmental Science and Technology*, 42 (2008) 766.
- D. Pathania, R. K. Rana and D. Singh, *International Journal of Theoretical and Applied Science*, 1 (2009) 25.
- D. Pathania and R. Sharma, *Advanced Materials Letters*, 3 (2012) 136.
- D. Pathania and S. Sharma, *Tenside Surfactants Detergents*, 4 (2012) 306.
- V. K. Gupta, I. Ali and V. K. Saini, *Water Research*, 41(15) (2007) 3307.
- V. K. Gupta, R. Jain and S. Varshney, *Journal of Colloid and Interface Science*, 312 (2007) 292.
- V. K. Gupta, S. Agarwal and T. A. Saleh, *Water Research*, 45 (2011) 2207.
- V. K. Gupta, A. Mittal, A. Malviya and J. Mittal, *Journal of Colloid and Interface Science*, 335 (2009) 24.
- A. Mittal, J. Mittal, A. Malviya and V. K. Gupta, *Journal of Colloid and Interface Science*, 344 (2010) 497.
- A. Clearfield, *Solv. Extn. Ion Exch.* 18 (2000) 655.
- S. A. Nabi, and A. H. Shalla, *Journal of Hazardous materials*, 163 (2009) 657.
- C. B. Amphlett, *Inorganic Ion Exchangers*, Elsevier, Amsterdam, 1964.
- O. Arrad and Y. Sasson, *J. Organ. Chem.* 54 (1989) 4993.
- A. A. Khan and A. A. Alam, *React. Func. Polym.* 55 (2003) 277.
- K. G. Varshney, N. Tayal, A. A. Khan and R. Niwas, *Colloid Surf. A : Physicochem. Eng. Asp.* 181 (2010) 123.
- A. P. Gupta, H. Agarwal and S. Ikram, *J. Indian chem. Soc.* 80 (2003) 57.
- B. Zhang & D. M. Poojary, A. Clearfield, G. Peng, *Chem. Mater.* 8 (1996) 1333.
- I. Ali, *Chemical Reviews*, 112 (2012) 5073.
- V. K. Gupta, S. Agarwal, D. Pathania, N. C. Kothiyal, G. Sharma, *Carbohydr. Poly.* 96 (2013) 277.
- V. K. Gupta, D. Pathania, P. Singh, B. S. Rathore, P. Chauhan, *Carbohydr. Poly.* 95 (2013) 434.
- K. G. Varshney, P. Gupta and N. Tayal, *Colloid Surf. B* 28 (2003) 11.
- W. A. Siddiqui, S. A. Khan, and Inamuddin. *Colloids and Surf. A* 295 (2007). 193.
- V. K. Gupta, D. Pathania, S. Agarwal and P. Singh, *Journal of Hazardous Materials*, 243 (2012) 179.
- W. A. Siddiqui, S. A. Khan and Inamuddin, *Colloids and Surfaces A: Physicochemical Engineering Aspects*, 295 (2007) 193.
- Inamuddin, S. A. Khan, W. A. Siddiqui and A. A. Khan, *Talanta*, 71 (2007) 841.

	<p>Gaurav Sharma is pursuing his Ph.D research under the supervision of Dr. Deepak Pathania at Shoolini University, Solan, HP. He is working as Assistant Professor, School of Chemistry, Shoolini University, Solan, Himachal Pradesh. He had obtained his M.Sc from Barkatullah Vishwavidyalaya, Bhopal, MP and M.Phil degree from Shoolini University, Solan, HP. He had published about 07 papers in journals of repute. His area of research includes analytical chemistry, nanocomposites, bimetallic nanoparticles, nanocomposite ion exchangers, environmental chemistry, water purification and drug delivery etc.</p>
	<p>Bhim Singh Rathore is pursuing his Ph.D research under the supervision of Dr. Deepak Pathania at Shoolini University, Solan, HP. He is working as Associate Professor, Department of Chemistry, Government PG College, Solan, Himachal Pradesh. He is also Press Secretary, Him Science Congress Association, Himachal Pradesh. He had obtained his M.Sc and M.Phil degree from Himachal Pradesh University, Shimla. He had published about 10 papers in journals of repute. His area of research includes polymer based composites, nanocomposite ion exchangers, environmental chemistry, photocatalysis etc.</p>
	<p>Deepak Pathania is Associate Professor, Department of Chemistry, Shoolini University Solan, Himachal Pradesh, India. He is also serving as founder President, Him Science Congress Association, Himachal Pradesh. He started his teaching career in 2001 from NIT, Jalandhar, Punjab. He has served as Head Department of Applied Sciences and Humanities in 2008. He is members of different professional scientific societies. He had guided 4 Ph.D and 8 M.Phil students for their degree. Presently he is guiding 4 Ph.D and 2 M. Phil students. He had authorized six books in different areas of interest from believed publishers. He had about 80 publications to his credit. His area of research includes polymer based composites, nanocomposite ion exchangers, graft copolymerization, fiber reinforced composite, environmental chemistry, photocatalysis etc.</p>

N-Heterocyclic Carbene (NHC) in Organometallic Catalysis – Contributions from IIT Kanpur

Sayantani Saha and Jitendra K. Bera*

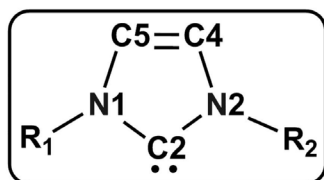
Department of Chemistry and Center for Environment Science and Engineering
Indian Institute of Technology Kanpur, Kanpur 208016 India
e-mail: jbera@iitk.ac.in

Abstract

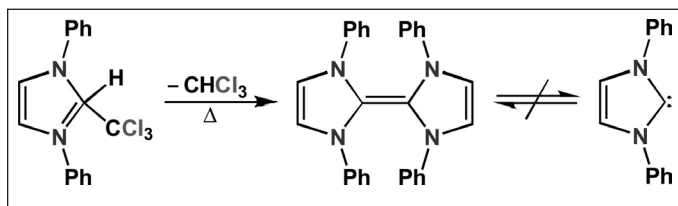
The prospect of metal–N-heterocyclic carbene complexes (NHC) is evaluated as catalysts for a wide variety of organic transformation reactions. Multifaceted coordination of naphthyridine functionalized NHC is demonstrated in this work. A diruthenium(I) based catalyst incorporating NHC is synthesized that catalyzes carbene transfer reactions. Bifunctional Rh(I) based catalyst hydrates organic nitrile to corresponding amide efficiently. Bulky substituents at nitrogen atoms of a bis-NHC ligand afforded a mixed C-2/C-4 bound Ru(II) complex that catalyzes carboxylic addition to terminal alkynes.

1. Introduction

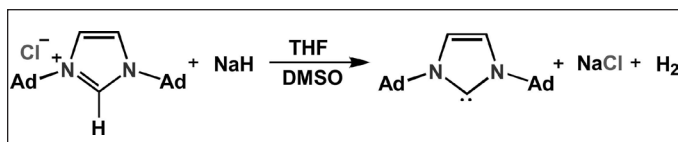
N-heterocyclic carbene (NHC) ligands (Scheme 1) are an emerging class of ligands in the area of organic and organometallic catalysis.[1] Wanzlick first reported thermal α -elimination of chloroform from corresponding imidazole adduct (1960) but the free carbene could not be isolated. (Scheme 2).[2] Thirty years later, Arduengo isolated 1,3-diadamantylimidazole-2-ylidene, the first stable NHC, obtained by the deprotonation of the corresponding imidazolium salt (Scheme 3).[3] Subsequently, several air-stable NHCs are reported and a few of them are even commercially available in free state.[4]



Scheme 1. N-heterocyclic carbene (NHC).

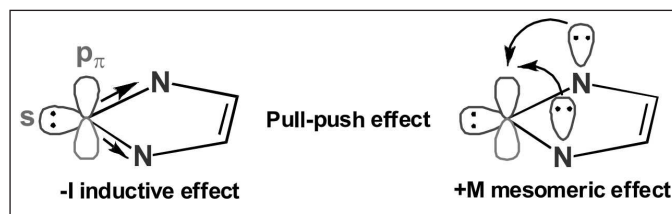


Scheme 2. Dimerization of imidazole-based carbenes.



Scheme 3. Synthesis of 1,3-diadamantylimidazole-2-ylidene

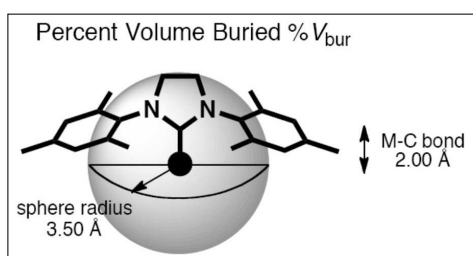
NHC is a neutral compound that contains a divalent carbon atom with six electrons in its valence shell. The stability of NHC depends on its steric-electronic factors. The unusual stability of NHC can be explained by a push-pull effect (Scheme 4).[5] The nitrogens withdraw electron density inductively to stabilize σ orbital on carbon. Further stabilization is attained by π donation from nitrogen atom into vacant p_{π} orbital of the carbene carbon. Combination of these two effects increases the σ - p_{π} gap and favors the singlet state. On the other hand NHCs have inherent tendency to dimerize. Incorporation of bulky wingtip group prevents dimerization and hence increases the stability of NHCs.



Scheme 4. Electronic stabilization of NHCs.

Remarkable amount of experimental and computational investigations are carried out to understand the nature of metal–NHC bonding.[6] NHCs are considered a good σ -donor through the $C(\sigma) \rightarrow M(d_z^2)$ orbital. Both filled and empty π and π^* orbitals on NHC ring can contribute to metal–NHC bond. The $d \rightarrow \pi^*$ back-donation is observed for electron rich metal atoms.[7] The concept of π -donation from NHC to transition metal has taken shape in recent years for electron poor metal atoms. The MO analysis of electron deficient 14e complex $[Ir(I^tBu)_2]PF_6$ ($I^tBu = N,N$ -di(*tert*-butyl)imidazol-2-ylidene) reveals the existence of $NHC \rightarrow M \pi$ -donation which is attributed to its unusual stability.[8]

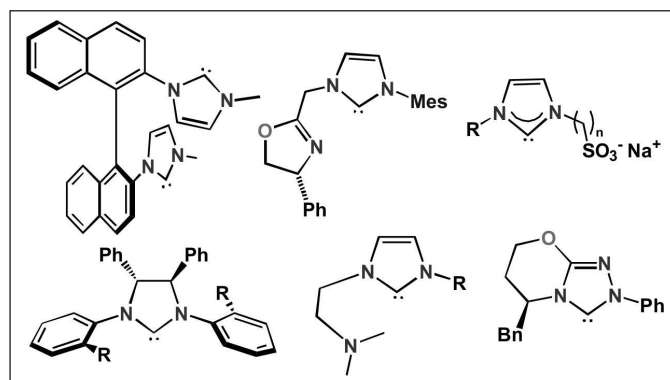
Studies have shown that the bond dissociation energy (BDE) in metal-NHC complex is clearly dependent on the steric properties of the NHC ligands. Several methods have been undertaken in order to quantify steric parameters, which in conjunction with electronic parameters characterize a ligand. To quantify the steric factor, Nolan and Cavallo proposed a model which is known as 'percent buried volume' ($\% V_{bur}$). It is defined as the percent of total volume of a sphere occupied by a ligand, while the sphere has a defined radius with the metal atom present at the center of the sphere (Scheme 5).[9] A comparative study for $[Cp^*Ru(L)Cl]$ complexes reveals that the $\% V_{bur}$ show linear correlation with the corresponding BDE, which suggests that the BDEs can essentially be controlled by the steric requirements of the NHC ligands.[10]



Scheme 5. Model for steric parameter determination of NHCs.

Appropriately designed NHCs are superior σ -electron donor than the most basic phosphine ligands.[11] Trialkyl phosphines, which are vulnerable to moisture, oxygen and readily undergo oxidative degradation during catalysis, are largely being replaced by NHCs.[12] The pioneering work by Herrmann on the application of NHC-metal complexes initiated a surge in activity toward the applications of metal-NHC complexes in organometallic catalysis.[13] Trialkyl phosphine containing organometallic catalysts are being upgraded to their NHC analogues. A few notable examples are the modification of Grubbs' catalyst, Wilkinson's catalyst and Crabtree's catalyst.[14]

One drawback of NHC ligands is that they are particularly susceptible to reductive elimination. Systematic studies on the decomposition pathways have revealed that one effective way to resist the decomposition via reductive elimination is to use relatively inflexible chelating NHC ligands. Accordingly, a large numbers of functionalized NHCs have been introduced in the literature. Furthermore, introduction of functional groups bring about several unique properties like hemilability, chirality and ligand topology into the ligand. Electronic properties of NHCs can also be precisely tuned by functionalization. Attachment of functional groups to nitrogen atoms makes them ideally suited for the synthesis of the donor-functionalized NHC ligands. A list of functionalized NHC ligands are provided in Scheme 6.

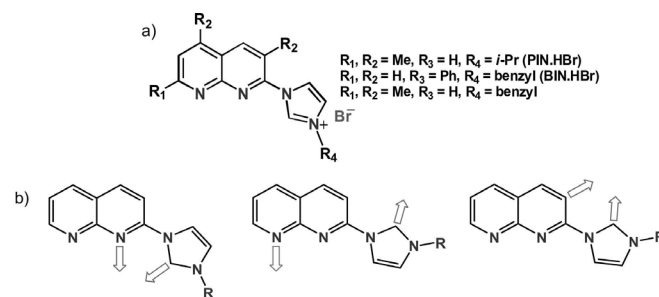


Scheme 6. Some functionalized NHCs.

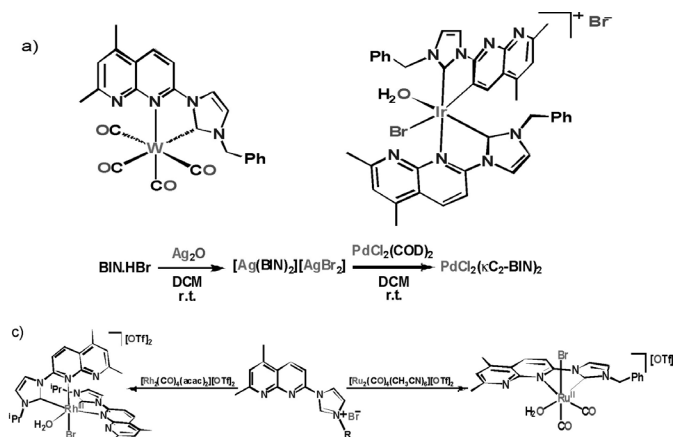
2. Functionalized NHC in Organometallic Catalysis

Multifaceted Coordination of Naphthyridine-functionalized NHC

A set of naphthyridine-functionalized ligands was synthesized that exhibit diverse coordination modes (Scheme 7a and b). By using different metal-based precursors, a host of metal-NHC compounds have been synthesized. The synthetic process primarily involves the generation of free NHC by application of base (t BuOK) and subsequent coordination with the metal based precursors (W, Ir, Rh) (Scheme 8a). Alternatively, Ag-



Scheme 7. Naphthyridine-functionalized NHC ligands and their diverse coordination modes.



Scheme 8. a) Metal-NHC complexes, b) Trans-metalation route to Pd-NHC complex, c) Reactivity of metal-metal bonded compounds with NHC precursor ligands.

NHC salt is prepared at first by treating imidazolium salt with Ag_2O and subsequent trans-metalation reaction with metal halides affords metal-NHC complex (Pd) (Scheme 8b).[15] We have also developed an oxidative route to metal-NHC complexes by treating NHC precursors with metal-metal bonded complexes $\text{Ru}_2(\text{CO})(\text{CH}_3\text{CN})_6(\text{BF}_4)_2$ or $\text{Rh}_2(\text{acac})_2(\text{CO})_4(\text{OTf})_2$.[16](Scheme 8c)

Bimetallic Catalysis

Site-directed anchoring of naphthyridine-functionalized N-heterocyclic carbene (NHC) was achieved on a metal-metal singly-bonded diruthenium(I) platform. The PIN. HBr afforded an unsupported compound $\text{Ru}_2(\text{CO})_4(\kappa^2\text{C}_2\text{N}_1\text{-PIN})_2\text{Br}_2$ whereas judicious alteration in the NHC ligand resulted in the bridged compound $\text{Ru}_2(\text{CO})_4(\text{CH}_3\text{COO})(\mu^2\text{-}\kappa^2\text{C}_2\text{N}_1\text{-BIN})\text{Br}$ (**2**) (Fig. 1). X-ray analysis reveals the chelate binding of PIN on each ruthenium at equatorial sites for **1**, and the bridge-chelate binding of BIN spanning the diruthenium core for **2**. The catalytic utilities of the BAr^{F} (tetrakis(3,5-bis(trifluoromethyl)phenyl)borate) salts of these compounds are evaluated towards carbene transfer reactions from ethyl diazoacetate (EDA) including aldehyde olefination, cyclopropanation and X-H ($\text{X}=\text{O}, \text{N}$) insertions (Scheme 9).[17]

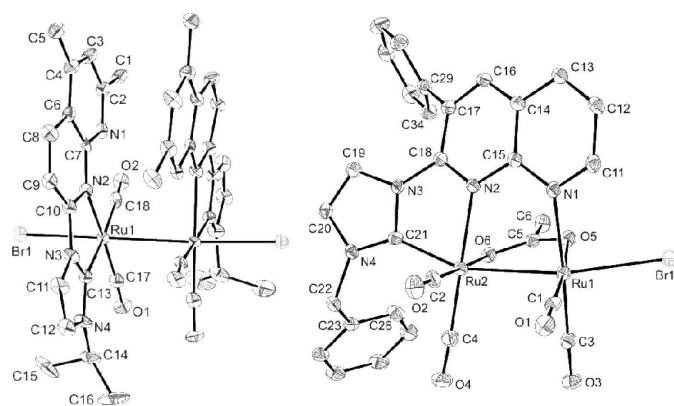
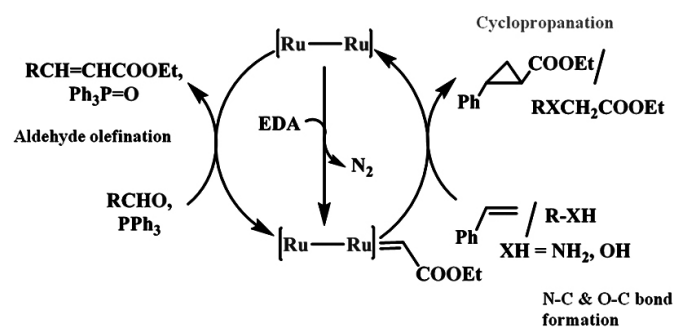


Fig. 1. Structure of diruthenium(I) compounds **1** and **2**.



Scheme 9. Carbene-transfer catalysis by the diruthenium(I) complex.

The commonality in this set of transformations is the intermediacy of a diruthenium(I) species $[\text{Ru}^{\text{I}}\text{-}$

$\text{Ru}^{\text{I}}=\text{CH}(\text{COOEt})]$. Initially, EDA reacts with the diruthenium catalyst and forms dimetal-carbenoid intermediate with the extrusion of N_2 . For the aldehyde olefination reaction, the incipient carbene is transferred to the phosphine resulting in the phosphorane $\text{Ph}_3\text{P}=\text{CHCOOEt}$. In a controlled experiment, the phosphorane was identified by ^{31}P NMR spectroscopy in absence of aldehyde. The ylide then reacts with aldehyde to produce the new olefin and phosphine oxide. The phosphine oxide was identified in the GC-MS. Involvement of the Wittig type reaction explains higher reactivity of the electron deficient aldehydes which make the carbonyl carbon more electronegative facilitating the nucleophilic attack of the ylide carbon to aldehyde. It should be pointed out that the diruthenium complex catalyses the formation of the ylide and not the subsequent Wittig reaction. For cyclopropanation, N-C and O-C bond formation reactions, the respective substrate alkene, amine and alcohol directly attack the metal-carbene intermediate and generate the products.

In addition, we have employed an anionic N-heterocyclic carbene (NHC) ligand ferrocenoyl(1-mesityl-imidazol-2-ylidene-3-yl)amide to synthesize a binuclear Ag(I) complex **3** (Figure 2). X-ray structure reveals a $[\text{Ag}\cdots\text{Ag}]$ core spanned by two ligands, each bridging two metals through carbene carbon and amido nitrogen. This neutral complex **3** is highly soluble in a variety of organic solvents and is thermally stable. Complex **3** efficiently catalyses aniline-mediated synthesis of substituted quinolines from 2-aminobenzaldehyde and terminal alkynes.[18]

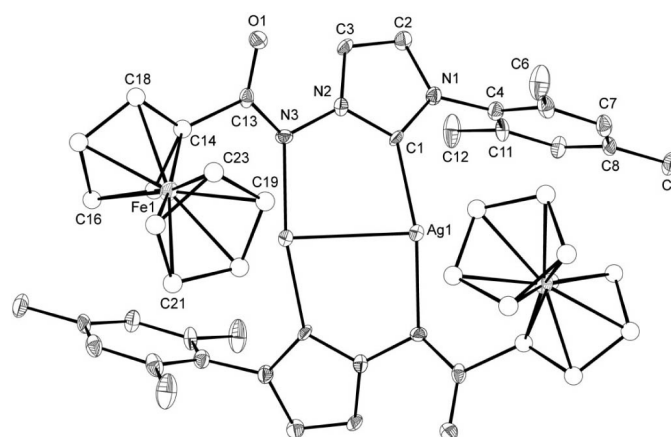


Fig. 2. Structure of disilver(I) compound **3**.

Bifunctional Catalysis

Hydration of organic nitriles is a significant process for the preparation of organoamides which have vast industrial and pharmacological applications. For example, organic amides are frequently used in the synthesis of lubricants, detergent additives, drug stabilizers, etc. One of the most

noteworthy industrially important amides is acrylamide which mostly is used to synthesize polyacrylamides. Compound **4** (Fig. 3) is shown to be an excellent catalyst for the hydration of a wide variety of organonitriles at ambient temperature, providing the corresponding organoamides (Scheme 10). In general, smaller substrates gave higher yields compared with sterically bulky nitriles. A turnover frequency of 20 000 h⁻¹ was achieved for the acrylonitrile. A similar Rh(I) catalyst without the naphthyridine appendage

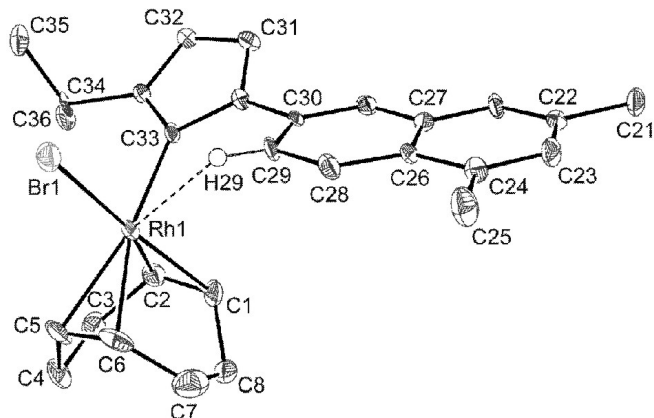
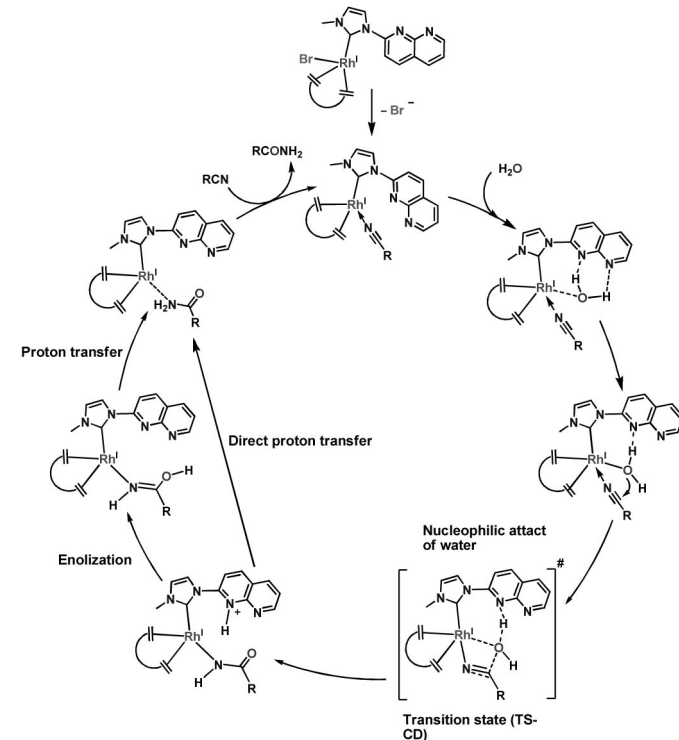


Figure 3. Structure of rhodium(I) complex 4.



Scheme 10. Hydration of nitrile to amide catalyzed by 4.

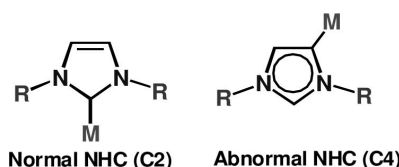


Scheme 11. Bifunctional mechanism for the hydration of organonitrile catalyzed by 4.

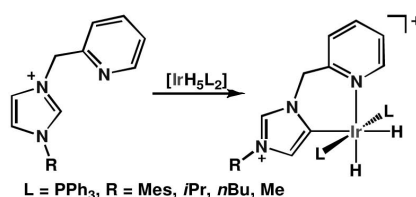
turned out to be inactive. DFT studies are undertaken to gain insight on the hydration mechanism. DFT calculations reveal multicomponent cooperativity involving proton movement from the water to the naphthyridine nitrogen and a complementary interaction between the hydroxide and the nitrile carbon (Scheme 11). Bifunctional water activation and cooperative proton migration during the catalytic cycle open up new possibilities for organometallic catalysis.[19]

C4-Bound N-Heterocyclic Carbene

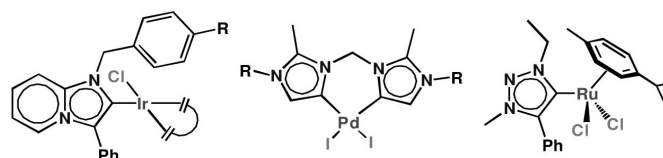
Normally NHC coordinates through the C2 center, although C4/C5 coordination also occurs under certain conditions (Scheme 12).[20] Crabtree reported the first synthesis of an Ir-NHC complex where NHC coordinates through the C4/C5 carbon atom (Scheme 13).[21] This type of NHC coordination is defined as 'abnormal' carbenes (aNHC). Blocking C2 position of heterocycle is a logical way to access C4/C5 position. A few illustrative examples of metal-a NHC complexes are shown where C2 position is blocked (Scheme 14).[22] Following the same principle, Albrecht synthesized several methylene-bridged bis-carbene complexes where both NHC fragments bind in abnormal fashion. Counter anion is reported to influence the C2/C4 NHC binding.[23] The identification of bases used for deprotonation also plays a role in determining modes of carbene bindings.[24] Steric congestion imposed by bulky groups at wingtip imidazole nitrogens favors the abnormal binding even when C2 is free.



Scheme 12. Different NHC coordination modes.



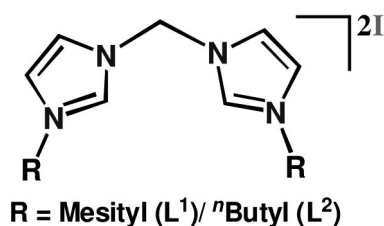
Scheme 13. Synthesis of first abnormal carbene.



Scheme 14. C2-bound abnormal NHC metal complexes.

Abnormal carbene complexes do not easily convert into normal carbenes. Studies show that abnormal NHC is better σ -electron donor than its normal counterpart. Because of that, aNHC is reported to exhibit superior catalytic activity, and promote certain reactions that are not accessible by C2-bound metal-NHC compounds. Toward this direction, we synthesized methylene-spaced bis-carbene ligands with different wingtip groups (Scheme 15). For mesityl group, we isolated a mixed normal/abnormal NHC compound (Compound 5) whereas ⁿBu wingtip groups afforded normal NHC complex 6. Interestingly, in case of the latter, the metal Ru is oxidized due to highly basic nature of the NHC ligand. X-ray structure and NMR spectroscopy for 5 unambiguously confirm that one of the ligands binds Ru through the usual imidazole C₂ carbon atoms whereas the second ligand adopts a mixed normal and abnormal coordination to the same metal center. But in compound 6 both ligands exhibit normal coordination modes. Increasing the size of N-substituents of NHC-CH₂-NHC ligand from n-butyl to mesityl groups shifts ligand coordination from an all-normal to a mixed normal/abnormal binding to the same metal.

We then examined the catalytic utility of both compounds for carboxylic acid addition to terminal alkynes for the synthesis of enol esters (Scheme 16). Both compounds afford anti-Markovnikov (AM) products with Z-selectivity. In general, compound 5 was found to be more reactive in terms of yield and selectivity. Due to the abnormal binding mode of the ligand compound 5 exhibit different structural and electronic characteristics



Scheme 15. Bis-carbene ligand precursors.

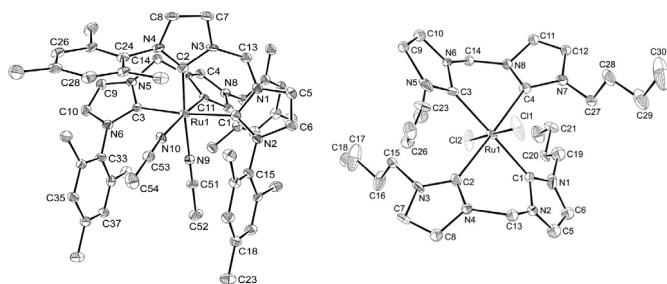
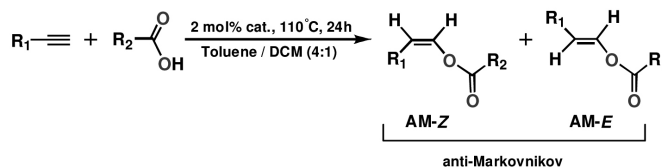


Figure 4. X-ray structures of bis-NHC metal complexes 5 and 6.



Scheme 16. Carboxylic acid addition reaction to terminal alkynes.

which are further reflected in their contrasting catalytic responses.[25]

Conclusion

This mini-review describes an account of our activity on the design and development of organometallic catalysts containing functionalized N-heterocyclic carbene ligands. Gaining inspiration from design strategies of natural metalloenzyme active sites, several catalysts are developed based on dimetal constructs. We have demonstrated that installation of naphthyridine-functionalized NHC ligand on a [Ru^I-Ru^I] core boost the efficiency of carbene transfer catalysis. New anionic carbene is designed for supporting a [Ag^I...Ag^I] core. A bifunctional ligand is fabricated that anchors to metal through NHC unit and utilizes the naphthyridine unit to activate water and subsequently hydrates nitrile to amide. By incorporating bulky group at imidazolium nitrogen, Ru complex with mixed C₂/C₄-bound bis-NHC complex is synthesized which show superior activity towards carboxylic addition reaction to terminal alkynes. Recent efforts are directed to develop new bifunctional NHC ligands and apply their metal complexes in the conversion of cheap and abundant small molecules to value added chemicals.

Acknowledgement

J.K.B. thanks DST for the Swarnajayanti fellowship and S. S. thanks CSIR, India, for a research fellowship.

References

- (a) *N-Heterocyclic Carbenes in Transition Metal Catalysis*; Glorius, F., Ed.; Springer: Berlin, 2007; Topics in Organometallic Chemistry Vol. 21. (b) Herrmann, W. A. *Angew. Chem., Int. Ed.* **2002**, *41*, 1290. (c) Enders, D.; Niemeier, O.; Henseler, A. *Chem. Rev.* **2007**, *107*, 5606. (d) Benhamou, L.; Chardon, E.; Lavigne, G.; BelleminLaponnaz, S.; César, V. *Chem. Rev.* **2011**, *111*, 2705. (e) Kumar, A.; Ghosh, P.; *Eur. J. Inorg. Chem.* **2012**, 3955.
- Wanzlick, H. W. *Angew. Chem. Int. Ed.* **1962**, *1*, 75.
- Arduengo, A. J.; Harlow, R. L.; Kline, M. J. *Am. Chem. Soc.* **1991**, *113*, 361.
- Enders, D.; Breuer, K.; Raabe, G.; Runsink, J.; Teles, J. H.; Melder, J. P.; Ebel, K.; Brode, S. *Angew. Chem. Int. Ed.* **1995**, *34*, 1021.
- Paulung, L. *Chem. Commun.* **1980**, 688.
- (a) Jacobsen, H.; Correa, A.; Poater, A.; Costabile, C.; Cavallo,

- L. *Coord. Chem. Rev.* **2009**, 253, 687. (b) Cavallo, L.; Correa, A.; Costabile, C.; Jacobsen, H. J. *Organomet. Chem.* **2005**, 690, 5407. (c) Díez-González, S.; Nolan, S. P. *Coord. Chem. Rev.* **2007**, 251, 874.
7. (a) Hu, X. L.; Tang, Y. J.; Gantzel, P.; Meyer, K. *Organometallics* **2003**, 22, 612. (b) Garrison, J. C.; Simons, R. S.; Kofron, W. G.; Tessier, C. A.; Youngs, W. J. *Chem. Commun.* **2001**, 1780. (c) Tulloch, A. A. D.; Danopoulos, A. A.; Kleinhenz, S.; Light, M. E.; Hursthouse, M. B.; Eastham, G. *Organometallics* **2001**, 20, 2027. (d) Sanderson, M. D.; Kamplain, J. W.; Bielawski, C. W. *J. Am. Chem. Soc.* **2006**, 128, 16514.
 8. Scott, N. M.; Dorta, R.; Stevens, E. D.; Correa, A.; Cavallo, L.; Nolan, S. P. *J. Am. Chem. Soc.* **2005**, 127, 3516.
 9. (a) Clavier, H.; Nolan, S. P.; *Chem. Commun.* **2010**, 46, 841. (b) Hillier, A. C.; Sommer, W. J.; Yong, B. S.; Petersen, J. L.; Cavallo, L.; Nolan, S. P. *Organometallics* **2003**, 22, 4322. (c) Poater, A.; Cosenza, B.; Correa, A.; Giudice, S.; Ragone, F.; Scarano, V.; Cavallo, L. *Eur. J. Inorg. Chem.* **2009**, 1759.
 10. (a) Dorta, R.; Stevens, E. D.; Scott, N. M.; Costabile, C.; Cavallo, L.; Hoff, C. D.; Nolan, S. P. *J. Am. Chem. Soc.* **2005**, 127, 2485. (b) Singh, S.; Kumar, S. S.; Jancik, V.; Roesky, H. W.; Schmidt, H.-G.; Noltemeyer, M.; *Eur. J. Inorg. Chem.* **2005**, 3057.
 11. (a) Tolman, C. A.; *Chem. Rev.* **1977**, 77, 313. (b) Kühl, O.; *Coord. Chem. Rev.* **2005**, 249, 693.
 12. (a) Huang, J.; Stevens, E. D.; Nolan, S. P.; Petersen, J. L. *J. Am. Chem. Soc.* **1999**, 121, 2674.
 13. Herrmann, W. A.; Elison, M.; Fischer, J.; Köcher, C.; Artus, G. R. *J. Angew. Chem., Int. Ed.* **1995**, 34, 2371.
 14. (a) Schrock, R. R.; Murdzek, J. S.; Bazan, G. C.; Robbins, J.; Dimare, M.; Oregan, M. *J. Am. Chem. Soc.* **1999**, 121, 2674. (b) Weskamp, T.; Schattenmann, W. C.; Spiegler, M.; Herrmann, W. A. *Angew. Chem., Int. Ed.* **1998**, 37, 2490. (c) Ackermann, L.; Fürstner, A.; Weskamp, T.; Kohl, F. J.; Herrmann, W. A. *Tetrahedron Lett.* **1999**, 40, 4787. (d) Weskamp, T.; Kohl, F. J.; Herrmann, W. A. *J. Organomet. Chem.* **1999**, 582, 362.
 15. Sinha, A.; Rahaman, S. M. W.; Sarkar, M.; Saha, B.; Daw, P.; Bera, J. K. *Inorg. Chem.* **2009**, 48, 11114.
 16. (a) Sinha, A.; Daw, P.; Rahaman, S. M. W.; Saha, B.; Bera, J. K. *J. Organomet. Chem.* **2011**, 696, 1248. (b) Sinha, A.; Sarbajna, A.; Dinda, S.; Bera, J. K. *J. Chem. Sci.* **2011**, 123, 799.
 17. Saha, B.; Ghatak, T.; Sinha, A.; Rahaman, S. M. W.; Bera, J. K. *Organometallics* **2011**, 30, 2051.
 18. Sarbajna, A.; Sadhukhan, N.; Saha, S.; Bera, J. K. *Indian J. Chem. A.* **2013**, 52A, 1072.
 19. Daw, P.; Sinha, A.; Rahaman, S. M. W.; Dinda, S.; Bera, J. K. *Organometallics* **2012**, 31, 3790.
 20. (a) Schuster, O.; Yang, L.; Raubenheimer, H. G.; Albrecht, M. *Chem. Rev.* **2009**, 109, 3445. (b) Arnold, P. L.; Pearson, S. *Coord. Chem. Rev.* **2007**, 251, 596. (c) Sau, S. C.; Santra, S.; Sen, T. K.; Mandal, S. K.; Koley, D. *Chem. Commun.* **2012**, 48, 555.
 21. Gründemann, S.; Kovacevic, A.; Albrecht, M.; Faller, J. W.; Crabtree, R. H. *J. Am. Chem. Soc.* **2002**, 124, 10473.
 22. (a) Bacciu, D.; Cavell, K. J.; Fallis, I. A.; Ooi, Li. *Angew. Chem., Int. Ed.* **2005**, 44, 5282. (b) Alcarazo, M.; Roseblade, S. J.; Cowley, A. R.; Fernández, R.; Brown, J. M.; Lassaletta, J. M. *J. Am. Chem. Soc.* **2005**, 127, 3290.
 23. Kovacevic, A.; Gründemann, S.; Miecznikowski, J. R.; Clot, E.; Eisenstein, O.; Crabtree, R. H. *Chem. Commun.* **2002**, 2580.
 24. Gründemann, S.; Kovacevic, A.; Albrecht, M.; Faller, J. W.; Crabtree, R. H. *Chem. Commun.* **2001**, 2274.
 25. Saha, S.; Ghatak, T.; Saha, B.; Doucet, H.; Bera, J. K. *Organometallics* **2012**, 31, 5500.



S. Saha studied B.Sc at University of Calcutta (2005-08) and M. Sc. at IIT Delhi (2008-10). She is currently pursuing Ph. D. at Department of Chemistry, IIT Kanpur, under the supervision of Prof. J. K. Bera. Her research area includes synthesis and catalytic evaluation of binuclear complexes.



J. K. Bera received his M. Sc. from the University of Kalyani in 1993 and his Ph. D. from the Indian Institute of Science in 1999. After a couple of postdoctoral stints at Purdue University and at Texas A&M University, he joined the faculty at IIT Kanpur in 2003 where he is presently a Professor. He is the recipient of the Ramanna fellowship and the Swarnajayanti fellowship from DST, India, and has received the CRSI bronze medal for the year 2011. Bera's research interests span synthetic, structural and mechanistic organometallic chemistry. Recent efforts are directed toward bifunctional activation of small and abundant molecules and their catalytic transformations to useful and value-added chemicals.

Anisotropic Effect of Hematite Nanostructure and its Modification for Photocatalytic Application

Gajendra Kumar Pradhan and Kulamani Parida*
 CMC Department, CSIR-IMMT, Bhubaneswar-751013
 Email: paridakulamani@yahoo.com

Abstract

We have successfully synthesized α -Fe₂O₃ with different shapes via hydrothermal precipitation technique, in presence of (NH₄)₂HPO₄ as the structure directing agent to find out the effect of anisotropy on the photocatalytic activity. To further enhance the activity, one-dimensional α -Fe₂O₃ nanorod and graphene nanocomposites were also fabricated by simple hydrothermal technique. The obtained products were characterized by X-ray diffraction (XRD), transmission electron microscopy (TEM), selected area electron diffraction (SAED), scanning electron microscopy (SEM), diffused reflectance spectroscopy (DRUV-vis) and fourier transform infrared spectroscopy (FTIR). The phase and crystallinity were confirmed from the XRD study. Electron microscopy study clearly indicates the formation of different morphologies of nanocrystals. The α -Fe₂O₃ nanostructures and α -Fe₂O₃ nanorod/RGO composite were used as model systems for studying the shape dependent photocatalytic degradation of phenol. Among all nanostructure materials, α -Fe₂O₃/RGO composite showed 70% efficiency towards degradation of phenol under visible light illumination. The high activity of α -Fe₂O₃ nanorod/RGO composite has been discussed in terms of 1D architecture, crystallite size and morphological ordering.

1. Introduction

Design and development of one-dimensional (1D) iron oxide nanostructures are still challenging and important aspects of research in nanoscience and nano-technology due to their unique size and shape-dependent properties. Iron oxide with morphological variation such as nanospheres, nanorods, nanowires, nanotubes, nanonecklaces, nanorices, airplanes, tetrapods, peanuts, nanoflower and nanospindles have been studied by various research groups [1-2]. Fabrication of α -Fe₂O₃ nanorod (700 nm) using Fe-(C₃H₇O₂)₃ and its deposition on silicon substrate by chemical vapour deposition method have been reported by Wu et al. [3]. Almeida et al. reported the hydrothermal synthesis of lenticular nanorod and pseudocubes of α -Fe₂O₃ using FeCl₃ and NH₄H₂PO₄ [4]. Surface directing agents such as NaH₂PO₄, NH₄H₂PO₄ have been used for the synthesis of different shape of α -Fe₂O₃ [2].

Iron oxide has been extensively investigated because of their applications such as catalysis, sensors, pigments, magnetic resonance imaging (MRI), drug-delivery, photocatalysis and photoelectrochemical cell [5-9]. Hematite could be utilised for various photocatalytic applications in the visible range due to its high absorptive power. The limitations of this oxide for photocatalytic application comprise the low band gap energy (2.2 eV), poor conductivity and high electron-hole (e⁻-h⁺) recombination. Incorporation of heteroatom (e.g., Si, Bi, Pt and Ta), quantum confinement and architectural control

have been taken into consideration for addressing these issues [10-11]. On the other hand, geometrical configuration and elemental composition of 1D system is very useful for different applications. The electrons are channelized on the two dimensional structure and have very good electron transporting ability to retard the e⁻-h⁺ recombination which makes 1D nanostructure photoactive [12-14]. However, a few works have been reported on photocatalytic phenol degradation over different shaped iron oxide [15-16].

In this paper, we have studied the effect of shape and size of α -Fe₂O₃ on the photocatalytic phenol degradation. Herein, α -Fe₂O₃ nanorod, nanosphere and nanohexagon have been synthesised hydrothermal method using (NH₄)₂HPO₄ as the surface directing agent. Further, one dimensional Fe₂O₃ nanorod was modified with RGO to improve the photocatalytic performance. The novelty of synthesis and highly photocatalytic activity of uniform diameter nanorods are explained with the help of various spectroscopic techniques.

2. Materials And Methods

2.1. Materials

All the chemicals and reagents are of analytical grade and used without further purification. Iron (III) chloride hexahydrate, diammonium hydrogen phosphate, sodium dodecyl sulphate (SDS), polyethylene glycol (PEG) and deionised water were used for the sample preparation. Commercial Fe₂O₃ was used for comparison of catalytic activity with that of synthesized materials.

2.2 Preparation of α -Fe₂O₃ nanorod

In a typical experiment, calculated amount of (NH₄)₂HPO₄ was added to an aqueous solution of FeCl₃·6H₂O and stirred vigorously to get a yellow homogeneous solution. The solution was transferred to a Teflon-lined autoclave and kept in an oven at 180 °C for 36 h. The products were collected by centrifugation, filtered, washed several times with deionized water, and dried at 110 °C for overnight. The dried samples were calcined at 400 °C for 3 h and denoted as S1. Samples prepared in presence of PEG and SDS by following the same conditions as that of previously reported method and denoted as S2 and S3, respectively.

2.3 Preparation of α -Fe₂O₃/RGO nanocomposite

Calculated amount of (NH₄)₂HPO₄ was added to FeCl₃·6H₂O aqueous solution and stirred to get a homogeneous solution. Previously synthesized GO was dispersed in deionised water for 1 h in another beaker, then mixed with FeCl₃·6H₂O solutions and transferred to a Teflon-lined autoclave, followed by hydrothermal treatment at 180 °C for 36 h. The products were collected by centrifugation, filtered, washed several times with deionized water, dried at 110 °C for overnight and calcined at 400 °C for 3h. The 5 wt% GO loaded α -Fe₂O₃ is named as S4.

2.4 Characterization

Phase identification was carried out using a PANalytical X-ray diffractometer with Mo K α radiation ($\lambda = 0.70932 \text{ \AA}$) in the 2θ range from 10 to 40°. FTIR spectra was recorded in a Varian FTIR spectrophotometer (FTS-800) in the range of 400–4000 cm⁻¹. The optical absorbance was observed by UV–visible diffuse reflectance spectra (Varian, Cary 100). Morphology of the samples was studied through a transmission electronic microscope (FEI, TECNAI G² 20, TWIN, Philips) and scanning electron microscope (SEM, Hitachi S-3400N) by collecting secondary electron images at 15 kV. The electronic states of Fe were examined by X-ray photoelectron spectroscopy (XPS, Kratos Axis 165 with a dual anode (Mg and Al) apparatus) using the MgK α source. The OH radical formation was studied by replacing phenol with 5×10⁻⁴ M terephthalic acid (TPA) and 2×10⁻³ M NaOH with the same amount of photocatalyst. The PL spectra were measured on Perkin Elemer LS-55 fluorescence spectrometer with an excitation at 315 nm light.

1.3. Photocatalytic reaction

The photocatalytic activity of all the catalysts was evaluated towards the degradation of phenol under visible light irradiation. In a typical experiment, 20 mg

photocatalyst with 20 mL of 10 ppm phenol solution was taken in a 100 mL closed Pyrex flask. The solutions were exposed to visible light irradiation in an irradiation chamber (BS-02, Germany) for 2 h. After irradiation, the suspension was centrifuged and the concentration of the supernatant solution was analyzed quantitatively at 504 nm (λ_{max} for phenol) using a Cary-100 (Varian, Australia) spectrophotometer. All the catalytic results were reproducible with $\pm 2 \%$ variation.

3. Result and discussion

3.1 Formation and characterisation of different shapes of α -Fe₂O₃ and α -Fe₂O₃/RGO nanocomposite

The mechanism of different shape of nanoparticles formation has not been established till date. In the present system, we have proposed a mechanism which is as follows; the decomposition of (NH₄)₂HPO₄ during hydrothermal reaction leads to formation of NH₄⁺, PO₄³⁻ ions which play a pivotal role for the formation of different shape of FeOOH. The released ammonia acting here as a precipitating agent, helps in nucleation and partly in the growth of iron oxide particles. However, growth of nanocrystal was preferentially controlled by the PO₄³⁻ anion. Fig. 1 shows the XRD pattern of sample S1 and S2. It shows that the particles are well crystallized in rhombohedral α -Fe₂O₃ phase (JCPDS 13-534). No significant changes occur in the XRD patterns of other synthesized samples. The phase purity of α -Fe₂O₃ is maintained after the composite formation and also in spherical particle. The XRD peaks in the lower angle region (Fig. 2) at $2\theta \approx 0.43^\circ$ and 0.86° confirms that the material is mesoporous. The crystallite size of all the samples were measured by using

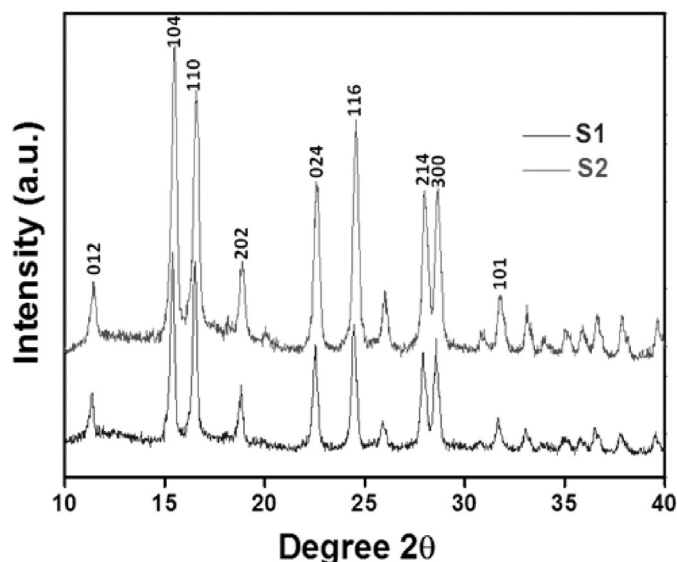


Fig. 1: XRD patterns of sample S1 and S2

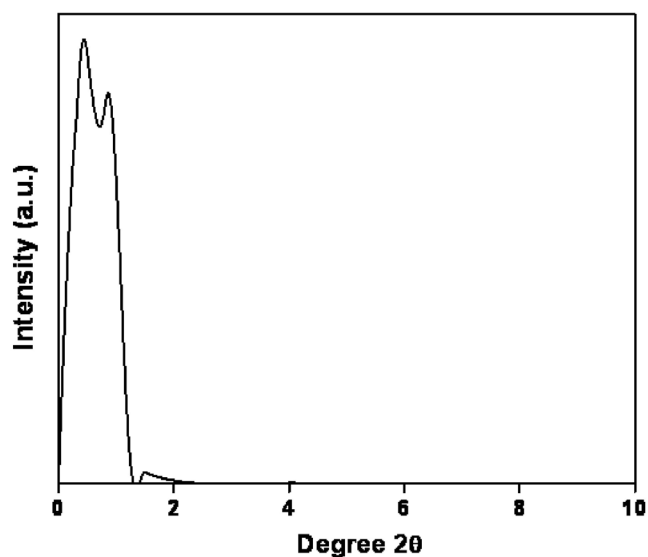


Fig. 2.:LAXRD of sample S1

Scherrer formula. The crystallite sizes of S1, S2, S3 and S4 are 17.48, 18.38, 17.03 and 17.02 nm, respectively. To clarify the crystal structure of particles, the unit cell dimension of the synthesized samples was measured (Table.1). Both the a-edge and c-edge length of the synthesized materials were lower than the reported value [17].

Table 1

Sample name	Crystallite Size (nm)	Aspect ratio	a (nm)	c (nm)	Phenol degradation (%)
Fe ₂ O ₃	-	-	-	-	2 ± 0.5
S1	17.48	2.74	4.89	13.48	25 ± 2
S2	18.38	-	4.75	13.24	5 ± 3
S3	17.03	3.38	4.82	13.37	27 ± 1
S4	17.02	3.32	4.80	13.34	70 ± 2

Fig. 3 represents the TEM microstructure of S1 and S2. S1 possess nanorod shape having average length and diameters of 294 and 107 nm, respectively. The aspect ratio is 2.74. The formation of nanorod might be due to the slow precipitation of iron oxide by NH₃. In S2, the nanostructures are hexagonal/spherical shape, which may be due to the uniform agglomeration of particles in each direction. The diameter of the spherical structures is around 53 nm. The addition of PEG having -OH groups strongly competes with PO₄³⁻ group, act as a destructive reagent and does not help in growing the nanorod shaped structure. This may lead to change the nanorod shaped topography to hexagon/spherical shape. The hydroxyl group dominates over the phosphate group and allows the formation of

hexagon shaped particle after the nucleation. In sample S2, there are two kinds of particle, hexagon shape and another is other than hexagon shape. However, the addition of SDS (Sample S3) doesn't affect the surface structure of the nanorods.

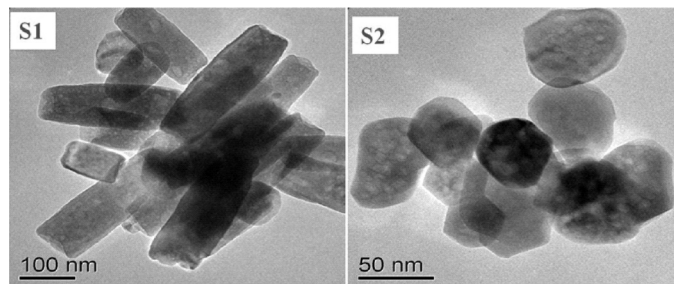


Fig. 3: TEM figure of sample S1 and S2

The reduced structure of GO have flat surface morphology and are sheet structure. The sheets always remain stacked in absence of any foreign material. In the composite case (S4), α-Fe₂O₃ nanorods are well decorated on the surface of the RGO sheets. Here by the introduction of α-Fe₂O₃ nanorods, the sheets are exfoliated and intact with the nanorods providing a composite material.

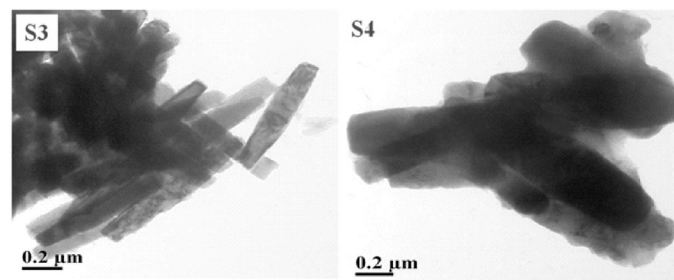


Fig. 4: TEM figure of sample S3 and S4

In UV-Vis DRS spectra, the band edge observed from 530-574 nm. This is in well agreement with the XRD results i.e. all the samples are α-Fe₂O₃. There are five multiplet peaks for Fe 2p observed in the XPS spectra. Peaks corresponding to 708.8 (A) and 720.9 eV (D) are attributed to +2 oxidation states where as 710.8 (B) and 723.6 eV (E) are ascribed to +3 states of iron. Peak with BE of ~ 715.6 eV (C) is identified as the surface peak of α-Fe₂O₃ [18]. In all the samples from S1-S4, the Fe-O vibrational mode absorption band observed in the range 464-468 cm⁻¹ which assures the hematite phase. These results agreed with the XRD, XPS and UV-Vis DRS results. The appearance of a weak peak in the region 1024 cm⁻¹ confirms the presence of some phosphate impurity in all the samples. From the BJH graph, the pore volume and average pore diameter were found to be 0.034 cm³/g and 29 nm, respectively. Although the material is not completely mesoporous like

MCM-41 or SBA-15, but the pore diameter is in the range of mesoporous material. The mesoporous nature of the material is also supported by LAXRD results.

3.2 Photocatalytic reaction

The percentage of phenol degradation was investigated as a function of different catalyst (fig 5 & table 1). Phenol solution with and without catalyst was directly exposed to the visible light for 4 h. It was found that the degradation was negligible in absence of the catalyst. The percentage of photocatalytic degradation in all our catalysts follows the order $\text{Fe}_2\text{O}_3 < \text{S2} < \text{S1} < \text{S3} < \text{S4}$ after 4 h of reaction in visible light. Here, bulk Fe_2O_3 showed lower activity compared to synthesized spherical hematite and 1D nano rod. In addition to morphology, crystallite size is also one of the important factor which has crucial role on the catalytic activity. Here the crystallite size has a trend of $\text{S2} < \text{S1} < \text{S3} < \text{S4}$ and this trend is also maintained in photocatalytic activity. Nanorod shaped catalysts showed high photocatalytic activity. This is because the electron transport in the 1D nanorod is channelized in one direction which lowers the electron-hole ($e^- - h^+$) recombination [19]. Sample S2 shows the lowest degradation as the particles are nanohexagon on which the recombination chances is more as compared to 1D nanostructure. Though both have nanorod morphology, S1 showing less degradation as compared to S3, this can be explained by comparing their aspect ratio. The aspect ratio of S1 is 2.74, less than sample S3 (3.38). The lower aspect ratio might be responsible for the charge carrier recombination and hence decreases the efficiency of photocatalyst. $\alpha\text{-Fe}_2\text{O}_3$ nanorod containing 5 wt% graphene exhibits 70 % of phenol degradation which

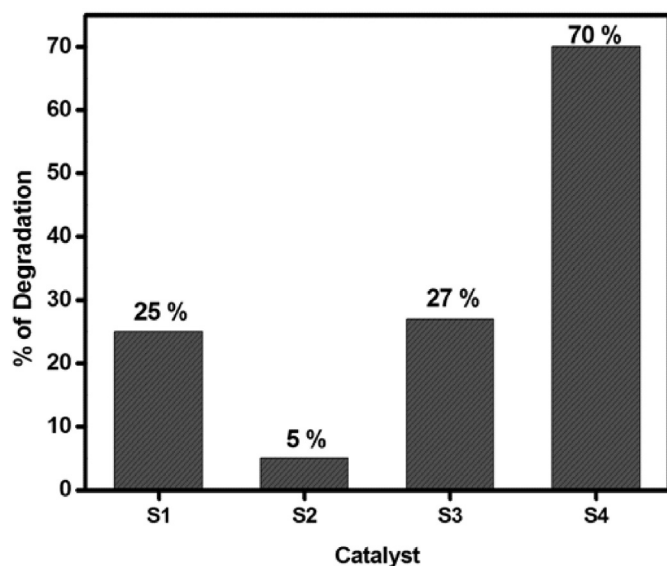


Fig. 5: Photocatalytic degradation studies of phenol over S1, S2, S3 and S4.

is 3 times higher than that of neat $\alpha\text{-Fe}_2\text{O}_3$ nanorod. When $\alpha\text{-Fe}_2\text{O}_3$ nanorod is placed on RGO sheets surface, there is strong interaction and development of synergism between $\alpha\text{-Fe}_2\text{O}_3$ and RGO. This process delays the recombination of excited photoelectrons with holes. RGO acts as electron acceptor centre and also easily channelize them through its flat sp^2 hybridised carbon network. So in composite case ($\alpha\text{-Fe}_2\text{O}_3$ nanorod/RGO), the carrier recombination is delayed, hence percentage of photodegradation enhances. Further, RGO also improves the light harvesting capacity of $\alpha\text{-Fe}_2\text{O}_3$ nanorods and alternately improves the photocatalytic activity. Phenol oxidation and degradation mechanism was well studied by many researchers. Phenol was oxidized to hydroxyl phenols by the oxidising species such as hydroxyl and superoxide radicals formed during the process. Then the hydroxyl phenol compounds break down to corresponding acid and finally converted to CO_2 and water.

3.3 Factors affecting the photocatalytic reaction

Based upon our results and discussion we have arrived at several evidences to establish the superiority of nanorods and composites compared to neat $\alpha\text{-Fe}_2\text{O}_3$ material such as (a) more number of active sites for the accommodation of substrate molecule, (b) lowering of electron-hole recombination, (c) formation of sufficient numbers of hydroxyl radicals.

3.3 (a) More number of active sites for the accommodation of substrate molecules

Surface area has significant role in catalysis and also in photocatalytic activity. Higher surface area has more number of active sites and hence can accommodate more number of substrate molecules. In the present case, there is not much variation in surface area in different shape morphology $\alpha\text{-Fe}_2\text{O}_3$ prepared by hydrothermal method. On the other hand the flat surface of nanorod morphology can accommodate more number of substrate molecules and hence could decompose more number of phenol molecules. Whereas the exposed area is increased by modifying with GO and thus the photocatalytic performance also increases. The $\alpha\text{-Fe}_2\text{O}_3$ nanorod/RGO nanocomposite gives a maximum percentage of phenol decomposition.

3.3 (b) Lowering of electron-hole recombination

Photoluminescence spectra have been used to address the mobility of the charge carriers and the recombination process involved by the electron-hole pairs in semiconductor particles. PL emission results from the radiative recombination of excited electrons and holes. In other words, it is an essential requirement of an effective photocatalyst to have minimum electron-

hole recombination. PL emission intensity is also directly related to the recombination of excited electrons and holes [19]. It is observed that spherical α -Fe₂O₃ with strong PL intensity has high recombination of charge carriers whereas nanorod α -Fe₂O₃ and α -Fe₂O₃ nanorod/RGO showed weak intensity. The weak PL intensity of α -Fe₂O₃ nanorod/RGO may arise due to the well-decorated α -Fe₂O₃ nanorods on the RGO sheet resulting in the decolourisation of photo excited electrons through sp² bonded carbon network. This delays the electrons-holes recombination process and hence is utilized in the redox reaction leading to improved photocatalytic activity.

3.3 (c) Hydroxyl radical formation

Hydroxyl radical performs the key role for the decomposition of the organic pollutants during photocatalytic reactions. The formation of hydroxyl radicals was established using terephthalic acid (TA) as a probe molecule. By reacting with OH radicals, TA transformed directly to 2-hydroxyterephthalic acid (TAOH) which gives a fluorescence signal at 426 nm. [20]. The fluorescent intensity is linearly proportional to the number of hydroxyl radicals formed by the photocatalysts. If generation of hydroxyl radical is more, yield of TAOH will be higher and hence more intense will be the fluorescence peak. Thus, S3 and S4 with highest intensity confirms the generation more number of hydroxyl radicals compared to other photocatalysts. The fluorescence intensity follows the trend, Fe₂O₃ < S2 < S1 < S3 < S4 of photocatalytic performance of all the photocatalyst.

4. Conclusions

We have successfully synthesized α -Fe₂O₃ with different shapes and α -Fe₂O₃ nanorod/RGO composite via hydrothermal precipitation technique in presence and absence of surfactant using (NH₄)₂HPO₄ as the structure directing agent. Degradation of phenol was performed by the irradiation of solar light using catalyst of different morphology and also in α -Fe₂O₃ nanorod/RGO composite. Our synthesized catalysts have better activity compared to bulk Fe₂O₃. Among various morphological samples, nanorod shape α -Fe₂O₃ shows highest photocatalytic activity for degradation of phenol. Modification with RGO further enhances the catalytic activity. So, one dimensional α -Fe₂O₃ nanorods possessing uniform diameter can be processed for the preparation of effective photocatalysts for environment and energy application.

Acknowledgements

The authors are extremely thankful to Prof. B.K. Mishra, Director, IMMT, Bhubaneswar 751013, Orissa, India, for permission to publish the paper. We are highly grateful to Dr. K. S. Ramarao, scientist, IICT, Hyderabad for the LAXRD. The authors are also thankful to CSIR for providing financial assistance.

References

1. H. Deng, X. Li, Q. Peng, X. Wang, J. Chen, Y. Li, *Angew. Chem. Int. Ed.* 44 (2005) 2782
2. X. Li, Xin. Yu, J. He, Z. Xu, *J. Phys. Chem. C* 113(2009) 2837-2845
3. J. J. Wu, Y. L. Lee, H. H. Chiang, D. K. P. Wong, *J. Phys. Chem. B* 110 (2006) 18108
4. T. P. Almeida, M. Fay, Y. Zhu, P. D. Brown, *J. Phys. Chem. C* 113 (2009) 186898
5. Q. Liu, Z. MinCui, Z. Ma, S. W. Bian, W. G. Song, L. Wan, *J. Nanotech.* 18 (2007) 385605
6. G. Wang, X. Gou, J. Horvat, J. Park, *J. Phys. Chem. C* 112 (2008) 15220.
7. F. H. Rhodes, C. R. Burr, P. A. Webster, *Ind. Eng. Chem.* 16 (1924) 960
8. M. V. Yigit, D. Mazumdar, Y. Lu, *Bioconjugate Chem.* 19 (2008) 412
9. M. Mahmoudi, A. Simchi, M. Imani, U. O. Hfeli, *J. Phys. Chem. C* 113(2009) 8124
10. I. Cesar, A. Kay, J. A. G. Martinez, M. Gratzel, *J. Am. Chem. Soc.* 128 (2006) 4582
11. L. Vayssies, C. Sathe, S. M. Butorin, D. K. Shuh, J. Nordgren, *J. Guo Adv. Mater.* 17 (2005) 2320
12. S. K. Mohapatra, S. E. John, S. Banerjee, M. Misra, *Chem. Mater.* 21(2009) 3048
13. Z. Liu, V. Subramaniam, M. Misra, *J. Phys. Chem. C* 113 (2009) 14028
14. G. K. Pradhan and K. M. Parida, *ACS Appl. Mater. Interfaces* 3 (2011) 317-323
15. X. Huang, Z. Yin, S. Wu, X. Qi, Q. He, Q. Zhang, Q. Yan, F. Boey, H. Zhang, *Small*, 7 (2011) 1876-1902
16. R. R. Nair, P. Blake, A. N. Grigorenko, K. S. Novoselov, T. J. Booth, T. Stauber, N. M. R. Peres, A. K. Geim, *Science*, 320 (2008) 1308
17. R. M. Cornell and U. Schwertmann, "The iron oxide: Structure, Properties, Reactions, Occurrences and Uses", Second Edition, 2003, 147.
18. A. P. Grosvenor, B. A. Kobe, M. C. Biesinger and N. S. McIntyre, *Surf. Interface. Anal.*, 36 (2004) 1564.
19. G. Liu, P. Niu, L. Yin and H. M. Cheng, *J. Am. Chem. Soc.*, 134 (2012) 9070.
20. T. Hirakawa and Y. Nosaka, *Langmuir*, 18 (2002) 3247.



Gajendra Kumar Pradhan earned his master degree from Sambalpur University in the year 2005. He completed his Ph. D degree from Utkal University in the year 2013 under the supervision Dr. K. M. Parida. Now he is working as Post-Doctoral Fellow at Seoul National University, South Korea. His research interest includes the fabrication of nanostructures for energy-based applications.



Dr. K. M. Parida did his Ph.D from Utkal University in the year 1981 and obtained his D. Sc degree from the same University in 2001. Dr Parida is working as a Chief Scientist in the Colloids and Materials Chemistry Department at CSIR-Institute of Minerals and Materials Technology, Bhubaneswar, Odisha, India and as Professor at the Academy of Scientific and Innovative Research (AcSIR), New Delhi, India. He is the author of more than 270 international journals and filed 18 national and international patents. His research interest focuses on the design and development of materials comprising a wide cross section such as metal oxides, metal phosphates, metal sulfates, cationic and anionic clays, perovskites, zeolites and nanometal/metal oxide/complex promoted mesoporous materials and their application towards various heterogeneous catalytic reactions.

Effect of Different Phases of Mg-Al Hydrotalcites, Formed by Calcination, on the Knoevenagel Reaction of Benzaldehydes and Malononitrile.

Rohit Gupta^b, Siddheshwar Kshirsagar^a, Savita Ladage^b and Shriniwas D. Samant^{a*}

^aDepartment of Chemistry, Institute of Chemical Technology, N. M. Parekh Road, Matunga, Mumbai-400 019, India

^bHomi Bhabha Centre for Science Education, V.N. Purav Road, Mumbai, Mumbai-400 088, India

Email: samantsd@yahoo.com

Abstract

The objective of the work is to identify the most effective phase of Mg-Al hydrotalcite in the Knoevenagel reaction of benzaldehyde and malononitrile as a *test reaction*. Mg-Al hydrotalcites (HTs) (Mg/Al = 2, 3) were prepared and calcined for different periods of time at different temperatures in the range of 473K to 1273K. The as-synthesized (uncalcined) and the calcined materials were characterized by powder XRD and FT-IR. Knoevenagel reaction of benzaldehyde with malononitrile, as a *test reaction*, was carried out at room temperature in ethanol in the presence of the calcined HTs. The HT with Mg/Al ratio 3 calcined at 773K for 6h was found to be the best catalyst. The activity of the catalysts was related to the actual phase of the catalyst. Mg-Al mixed oxide *periclase* like phase formed by the calcination at 773K was found to be the most effective phase. The Mg-Al HT functions as the appropriate precursor for the formation of this active species. This catalyst was used to carry out the reaction of substituted benzaldehydes with malononitrile.

Keywords: Mg-Al Hydrotalcite, Base catalysis, Knoevenagel condensation

1. Introduction

The area of solid acids and bases has gained immense importance due to increased awareness of environmental concerns. In this area solid bases have been given much less attention than solid acids due to the reasons like deactivation of catalyst, weaker bonding of the base on the support surface leading to leaching of the base, poor stability of support material under harsh reaction conditions. Mg-Al Hydrotalcites (Mg-Al HTs) are solid bases which can be prepared very easily and can be modified[1]. They have been used for various base catalyzed organic reactions[2], such as aldol[3], Michael[4], Claisen-Schmidt[4] and cyanoethylation[5] reaction. Calcination of HTs changes the active species through dehydration, dehydroxylation, and decarbonation. Survey of the literature shows that calcined Mg-Al HTs have been used for such reactions; however, correlation of the activity with the actual phase obtained on calcination is often lacking.

Knoevenagel reaction is simple base catalyzed reaction of benzaldehyde and malonitrile and it has been reported using solid bases. Traditionally the reaction is catalyzed by an alkali or a mild organic base like piperidine. Due to specific advantages of heterogeneous catalysts; environmental benignness being the most important one, in recent years various heterogeneous basic catalysts like basic alumina[6], KF-alumina[7], ZrPON[8], NH₄OAc-

alumina[9], Flurapatite[10], xonotlite/potassium tert-butoxide[11], rare earth cation exchanged NaY[12], and AlPO₄-Al₂O₃[13] have been employed to catalyze Knoevenagel reaction.

The Knoevenagel reaction catalyzed by Mg-Al HT is also known[13,14]. In these studies, Mg-Al HT incorporating t-BuOK[15], calcined Mg-Al HT supported isopropyl amide[16], and hydroxide modified Mg-Al HT[17] have also been used. However, a study of the activity of different phases of Mg-Al HT in this reaction has not been done. Mg-Al HTs calcined at temperatures greater than 700K have also been used for some reactions and the reactions have been labeled as catalyzed by the HT; though Mg-Al HT gives a Mg-Al mixed oxide phase when heated above 500°C[18-20]. On this background, we undertook a study of the Knoevenagel reaction of benzaldehydes and malonitrile in the presence of Mg-Al HT (Mg/Al = 2 and 3) calcined at different temperatures as a *test reaction* to correlate the activity of the catalysts with the phase of Mg-Al HT. The HTs with Mg/Al ratio 2 and 3 were selected for the study.

2. Experimental

Mg-Al HTs (Mg/Al = 2, 3) were prepared by the reported method²¹. The HTs were calcined at 473K, 573K, 673K, 723K, 873K, 1073K and 1273K. The calcination time at each temperature varied from 5-12 h. The powder XRD analysis of the Mg-Al HTs was done on a Siemens Xpert

pro X-ray diffractometer using Cu K α radiation (0.154178 nm). The FT-IR spectra were recorded on a NICOLET IR 200 spectrometer.

The calcined HTs were used as catalysts for the reaction benzaldehydes and malononitrile under solvent free conditions.

2.1 General procedure of the Knoevenagel reaction:

Benzaldehyde (20 mmol), malononitrile (20 mmol), and Mg-Al HT (0.069 g, ~2 mass % of benzaldehyde) were taken in a beaker (100 mL) and stirred continuously, using a magnetic stirrer, at 298 K for 30 min (TLC). Ethanol (5 mL) was added to the beaker and the solution was heated to dissolve the product. The catalyst was separated by filtration and the product was obtained by evaporation of ethanol.

Each reaction was done three times and the average yield was noted. The variations were found to be within $\pm 3-4\%$.

3. Results and discussion

The powder XRD of the uncalcined HTs with Mg/Al = 2, 3 (Fig. 1) indicate the HT phase[14]. The difference in the pattern of the two samples is due to more crystalline nature of HT with Mg/Al = 3 than Mg/Al = 2 HT. Lattice parameter *c* was calculated from the diffraction peaks due to (003), (006), and (009) planes whereas parameter *a* was

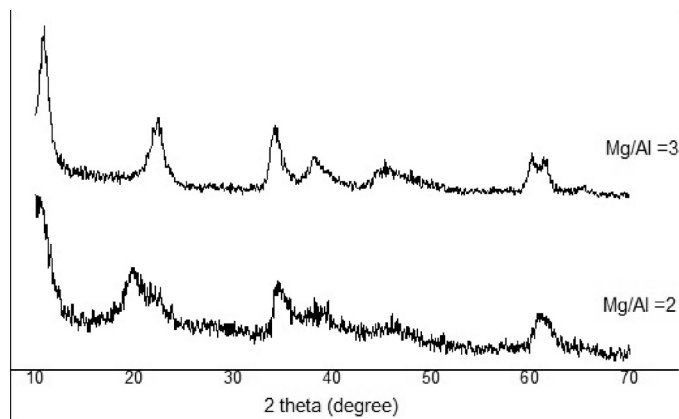


Fig. 1: Powder XRD patterns of uncalcined hydrotalcites with Mg/Al ratio 2 and 3

Table 1: Structural parameters *a* and *c* of Mg-Al HTs

Mg-Al HT	Structural parameter (<i>a</i>) $a = 2d_{110}(\text{\AA})$	Crystalline size(<i>c</i>) $c = 3d_{003}(\text{\AA})$
Mg/Al=2	3.043	22.85
Mg/Al=3	3.064	23.42

calculated from diffraction peak due to (110) plane (Table 1). These parameters are in agreement with the values reported in the literature[14]. The spacing between the neighboring cations in the brucite layer increases with increase in Mg/Al ratio. It is known that the basicity changes depending on the Mg²⁺/Al³⁺ ratio. By increasing the ratio the number of the basic sites increases. Here the Mg/Al HT with Mg/Al= 3 is expected to be more active than Mg/Al HT with Mg/Al =2.

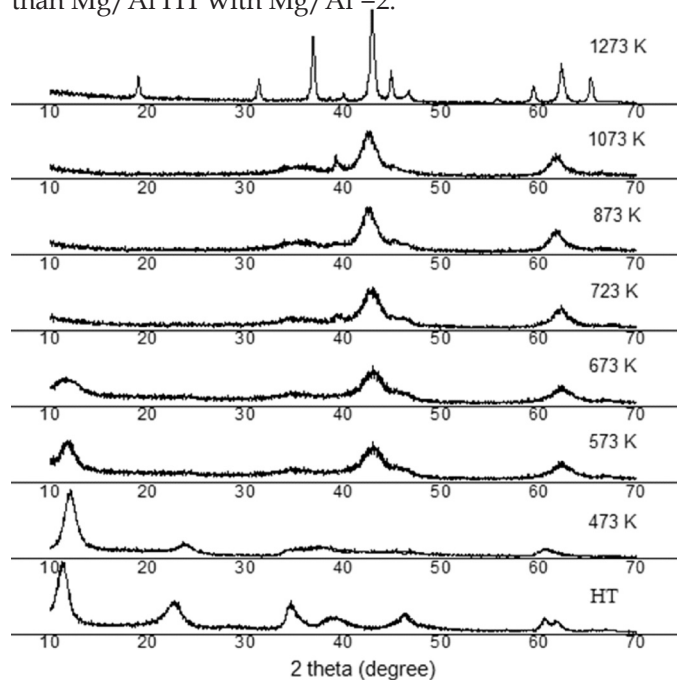


Fig. 2: X-ray diffraction patterns of uncalcined Mg-Al HT (Mg/Al = 3) and Mg-Al HT (Mg/Al = 3) calcined at different temperatures.

The XRD patterns of the HTs (Mg/Al = 3) calcined at different temperatures are shown in Fig. 2. The structure of the HT gradually changed.

The IR spectra of samples of Mg-Al HT (Mg/Al = 3) uncalcined as well as of those calcined at different temperatures are shown in Fig 3. The IR spectrum of the uncalcined HT shows a strong band at around 1360-1380 cm⁻¹, attributed to the bending vibrations of CO₃²⁻ anions²². This peak disappears on calcination as the CO₃²⁻ anions are gradually expelled. A broad band at 3460 cm⁻¹ is due to the OH⁻ ions present in the brucite layer[14]. As the calcination temperature increases there is a decrease in the intensity of the ν_{OH} peak, indicating the dehydroxylation. The intensity of the band close to 1630 cm⁻¹, related to the bending vibrations of H₂O molecules present in the interlayer region, decreases with increase in the calcination temperature.

The reaction of benzaldehyde (1a) and malononitrile (2) was studied in detail. In the calcination of the HTs, the calcination was carried out at a given temperature over

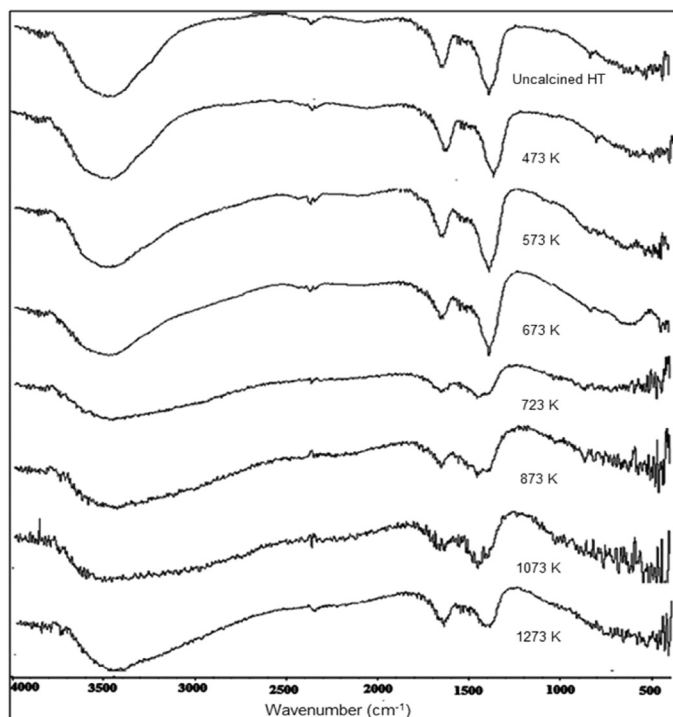


Fig. 3: IR spectra of uncalcined Mg-Al HT (Mg/Al = 3) and Mg-Al HT (Mg/Al = 3) calcined at different temperatures.

different period of time and these samples were used to catalyze the reaction. Each reaction was repeated three times and the average yield is recorded. The reaction is effectively catalyzed by the HTs (Table 2). It was observed that at each calcination temperature, HT with Mg/Al = 3 was superior to HT with Mg/Al = 2. The best result was obtained with HT with Mg/Al = 3 calcined at 773K.

One of the interesting observations was the effect of calcination time on the catalytic activity. At each calcination temperature the activity of the catalyst increased up to 6h of calcination and then decreased. At each calcination temperature the catalyst activated for 12h was substantially less active than that calcined for 6h. This reduction in activity was maximum when the calcination temperature was 873; the catalyst calcined for 12 h was almost 50% less active than the one calcined for 6h. This observation is unusual and to our knowledge is not reported elsewhere.

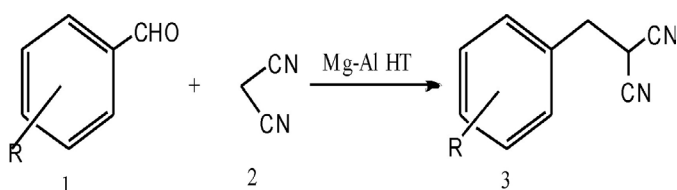


Table 2. The reaction of benzaldehyde (1a) and malononitrile (2) in the presence of Mg-Al HT (Mg/Al = 2, 3) calcined at different temperatures over different periods of time†.

Entry	Mg/Al ratio	Calcination temp (K)	Calcination time (h)	Yield* of(%)
1	2	473	6	32
2	2	573	5	47
3	2	573	6	50
4	2	573	8	49
5	2	573	10	42
6	2	573	12	39
7	3	473	6	39
8	3	573	5	50
9	3	573	6	54
10	3	573	8	50
11	3	573	10	46
12	3	573	12	44
13	2	723	5	65
14	2	723	6	68
15	2	723	8	67
16	2	723	10	63
17	2	723	12	59
18	3	723	5	73
19	3	723	6	79
20	3	723	8	76
21	3	723	10	68
22	3	723	12	63
23	2	873	5	45
24	2	873	6	49
25	2	873	8	33
26	2	873	10	29
27	2	873	12	26
28	3	873	5	52
29	3	873	6	58
30	3	873	8	38
31	3	873	10	33
32	3	873	12	29
33	2	1073	6	44
34	3	1073	6	50
35	2	1273	6	40
36	3	1273	6	45

Reaction conditions: Benzaldehyde (20 mmol), malononitrile (20 mmol), ethanol (5 mL), Mg-Al HT (Mg/Al = 3) (2 mass % of benzaldehyde), temperature 298 K, Time- 20 min.

† Each reaction was carried out three times and the average is recorded.

* Isolated yields; the yield of the product was calculated based on the benzaldehyde.

It is also seen that in the range of 573K to 873K, as the calcination temperature increased the yield of **3a** increased and was maximum at the calcination temperature of 773K and dropped as the calcination temperature increased further (fig 4). Observing this trend with the catalysts

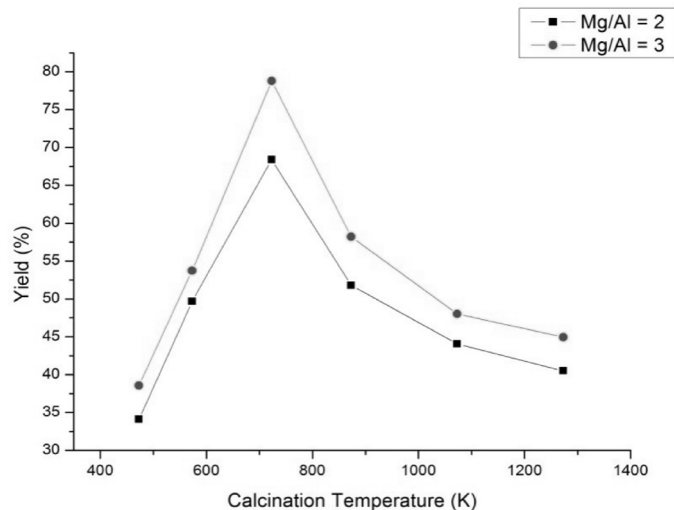


Fig. 4: The effect of calcination temperature on the yield of the product.

calcined between 573K and 873K, the Mg-Al HTs with Mg/Al = 2, 3 were also calcined at 443K, 1073K and 1273K only for 6h. These catalysts were much less active than the corresponding catalysts activated at 773K.

The effect of calcination temperature on the Mg-Al HT has been described in the literature[23-29]. The as-synthesized HT is lamellar and the characteristic peaks of the lamellar phase are at $2\theta = 11.53^\circ$ and 23.30° . With the increase in the temperature of calcination different phases of the HT are formed. At 473K the material is only dehydrated and partially dehydroxylated. The dehydroxylation continues up to 873K and at 873K the crystal structure collapses and a mixed Mg-Al-O called as a HT-P (periclase) is formed. In the XRD of the materials calcined at and above 723K the characteristic HT peaks almost disappear. At around 1000K the phase is composed of MgO and $Mg_2Al_2O_4$ and at 1273K a phase composed of periclase and spinel is formed. Thus in the material calcined above about 723K different phases of Mg and Al oxides are present and the HT structure is totally destroyed. There are references of the use of Mg-Al HT calcined at or above 723K as catalysts in different base catalyst reactions. However, the catalyst species actually present are not HT phases, but mixed oxides.

Our work proves that the best catalyst for the Knoevenagel reaction of benzaldehyde and malononitrile is Mg-Al mixed oxide periclase like phase formed by the

calcination of Mg-Al HT (Mg-Al HT = 3) at 723K for 6h. The Mg-Al HT functions as the appropriate precursor for the formation of this active species.

To generalize the observation, the reaction of various substituted aromatic aldehydes and malononitrile using Mg-Al HT (Mg/Al = 3) calcined at 773K was carried out (Table 3). The aldehydes substituted by electron withdrawing groups gave higher yields as compared to those substituted by electron donating groups.

Table 2: Knoevenagel reaction of substituted benzaldehydes and malononitrile in the presence of Mg-Al HT (Mg/Al = 3) calcined at 773K.

Entry	Benzaldehyde	Yield (%)*
1	C_6H_5CHO	80
2	4-Cl C_6H_5CHO	79
3	4- CH_3 C_6H_5CHO	61
4	4- OCH_3 C_6H_5CHO	43
5	3- NO_2 C_6H_5CHO	65
6	4- NO_2 C_6H_5CHO	82
7	4- $N(CH_3)_2$ C_6H_5CHO	60
8	4- OH C_6H_5CHO	76
9	3,4 (OCH_3) ₂ C_6H_5CHO	49

Reaction conditions: Aromatic aldehyde (20 mmol); malononitrile (20 mmol); ethanol (5 mL); (Mg/Al = 3) HT (2 mass % of aromatic aldehyde and malononitrile); temperature 298 K; Time- 20 min. * Isolated yields; the yield of the product was calculated based on the aldehyde.

4. Conclusion

Knoevenagel reaction of benzaldehyde and malononitrile is catalyzed by Mg-Al HT Mg/Al = 2, 3. The HT with Mg/Al = 3 was more active than the HT with Mg/Al = 2. The calcination temperature as well as calcination time were found to have profound effect on the catalytic activity. The HT (Mg/Al = 3) calcined at 723 K was the most effective, while those calcined at lower or higher temperatures were less effective. The optimum time for calcination was 6h, and decreasing or increasing the calcination time led to decrease in the yield. The active phase catalyzing the reaction was a Mg-Al mixed oxide periclase type phase formed on calcination.





Acknowledgement

This work was conducted as a part of National Initiative on Undergraduate Science (NIUS) Chemistry Programme of Homi Bhabha Centre for Science

Education (HBCSE, TIFR). We are thankful to Dr. A.K.Tyagi (BARC), Mr. Rakesh (BARC), and Mr. Nilesh Kulkarni (TIFR) for powder XRD analysis; and Ms. Swapna Narvekar and Ms. Indrani Sen, HBCSE, for the help extended.

References

1. F. Cavani, F. Trifiro and A. Vaccari, *Catal. Today*, 11 (1991) 173.
2. F.B. Sels, D.E. DeVos and P.A. Jacobs, *Catal. Rev.*, 43 (2001) 443.
3. A. Guida, M.H. Lhouty, D. Tichit, F. Figueras and P. Geneste, *P. Appl. Cat., A*, 164 (1997) 251.
4. (a) H.A. Prescott, Z.J. Li, E. Kemnetz, A. Trunschke, J. Deutsch, H. Lieske and A. Auroux, *J. Cat.*, 2005, 234, 119.
(b) M. Climent, A. Corma, S. Iborra and J. Primo, *J. Cat.*, 151 (1995) 66.
5. P.S. Kumbhar, V. J. Sanchez and F. Figueras, *J. Chem. Soc. Chem. Comm.*, (1998) 109.
6. F. Texier-Boullet and A. Foucaud, *Tet. Lett.*, 23 (1982) 4927.
7. J. T. Li, G. F. Chen, S. X. Wang, L. He and T.S. Li, *Aust. J. Chem.*, 58 (2005) 231.
8. N. Fripiat and P. Grange, *J. Chem. Soc. Chem. Comm.*, (1996) 1409.
9. S. Balalaie and N. Nemati, *Syn. Comm.*, 30 (2000) 869.
10. S. Sebti, R. Nazih, R. Tahir and A. Saber, *Syn. Comm.*, 31 (2001) 993.
11. S. Chalais, P. Laszlo and A. Mathy, *Tet. Lett.*, 26 (1985) 4453.
12. T.I. Reddy and R.S. Varma, *Tet. Lett.*, 38 (1997) 172.
13. J. A. Cabello, J.M. Campelo, A. Garcia, D. Luna and J.M. Marinas, *J. Org. Chem.*, 49 (1984) 5195.
14. A. Corma, V. Fornes, R. M. Martin-A and F.J. Rey, *J. Catal.*, 134 (1992) 58.
15. B. M. Choudary, M. L. Kantam, B. Kavita, B., C. V. Reddy and F. Figueras, *Tetrahedron*, 56 (2000) 9357.
16. M. L. Kantam, A. Ravindra, C. V. Reddy, B. Sreedhar and B. M. Choudary, *Adv. Syn. Catal.*, 348 (2006) 569.
17. K. Ebitani, K. Motokura, K. Mori, T. Mizugaki and K. Kaneda, *J. Org. Chem.*, 71 (2006) 5440.
18. R. J. Chimentao, S. Abello, F. Medina, J. Llorca, J. E. Sueiras, Y. Cesteros and P. Salagra, *J. Cat.*, 252 (2007) 249.
19. F. Li, X. R. Jiang, D.G. Evans and X. Duan, *J. Porous Mater.*, 12 (2005) 55.
20. S. Abello, F. Medina, D. Tichit, J. Perez-R, X. Rodriguez, J. E. Sueiras, P. Salagra, P. and Y. Cesteros, *Appl. Cat. A*, 282 (2005) 191.
21. A. Corma and R. M. Martin-A, *J. Catal.*, 130 (1991) 130.
22. A. Corma, A., V. Fornes, R.M. Martin-A, H. Garcia and J. Primo, *J., Appl. Cat.*, 59 (1990) 237.
23. M. Turco, G. Bagnasco, U. Costantino, F. Marmottini, T. Montanari, G. Ramis and G. Busca, *J. Catal.*, 228 (2004) 43.
24. Y. Liu, E. Lotero, J. G. Goodwin and X. Mo, *Appl. Cat. A*, 331 (2007) 138.
25. P. Kustrowski, D. Sulkowska, Z. Chmielarz, L. A. Rafalska, B. Dudek and R. Dziembaj, *Micropor. Mesopor. Mat.*, 78 (2005) 11.
26. R. J. Chinetao, S. Abello, F. Medina, J. Llorca, J. E. Sueiras, Y. Cesteros and P. Salagre, *J. Cat.*, 252 (2007) 249.
27. C. O. Veloso, C. N. Perez, B. M. deSouza, E. C. Lima, A. G. Dias, J. L. F. Monteiro and C. A. Henriques, *Micropor. Mesopor. Mat.*, 107 (2008) 23.
28. F. Li, X. R. Jiang, D. G. Evans and X. Duan, *J. Porous Mat.*, 12 (2005) 55.
29. M. Diserio, M. Ledda, M. Cozzolino, G. Minutillo, R. Tesser and E. Santacesaria, *Ind. Engg. Chem. Res.*, 45 (2006) 3009.

	<p>Mr. Rohit Gupta has completed his Integrated M.Sc. (Chemistry) from IISER Kolkata. Currently, he is pursuing his Ph.D. in Polymer chemistry at University of Massachusetts, Amherst.</p>
	<p>Dr. Siddheshwar Wasudeo Kshirsagar was born at Buldana, India. He received his Ph.D. degree in Chemistry in 2010 from the Department of Chemistry, Institute of Chemical Technology (Formerly UDCT), Mumbai, India under the supervision of Prof. S. D. Samant. He worked as Research Scientist at Emcure Pharmaceuticals limited Pune, India for 3 years. Currently he is working as a Senior Research Investigator at Syngene International Limited Bangalore India.</p>
	<p>Dr. Savita Ladage is a faculty at Homi Bhabha Centre for Science Education, Tata Institute of Fundamental Research, Mumbai. With masters in analytical chemistry from University of Mumbai, she completed her Ph.D. in the field of Chemistry education from Homi Bhabha Centre for Science Education. Her past work involved studying students' misconceptions in chemistry and currently she is the coordinator for Indian Chemistry Olympiad programme and the National Initiative on Undergraduate Science programme. The former programme leads to selection of Indian teams to participate in the International Chemistry Olympiads whereas the later is aimed at nurturing talent at undergraduate level.</p>
	<p>Professor Shrinivas D. Samant obtained his M.Sc. (Organic Chemistry, 1976) and Ph.D. (Organic Chemistry, 1980) from Ramnarain Ruia College, Mumbai (University of Mumbai). After a short span of lecturership in the same college, he moved to the Institute of Chemical Technology (formerly UDCT, University of Mumbai), Mumbai, as a Reader in Organic Chemistry, in 1982. In 1997, he was promoted to the post of Professor of Organic Chemistry. Research areas of his interests are mechanistic organic chemistry, chemistry of surfactants, organic sonochemistry, catalysis, new methods of organic synthesis. He has guided 48 students for Ph.D. and has published 125 research papers to his credit.</p>

Novel Supported ionic liquid catalysed synthesis of tetraarylporphyrins

Deepali A. Kotadia and Saurabh S. Soni*

Department of Chemistry, Sardar Patel University, Vallabh Vidyanagar 388120, Gujarat, INDIA

*Author to whom all correspondence should be address (email: soni_b21@yahoo.co.in)

Telephone: +91-2692-226857-Ext.216, Tele Fax: +91-2692 236475

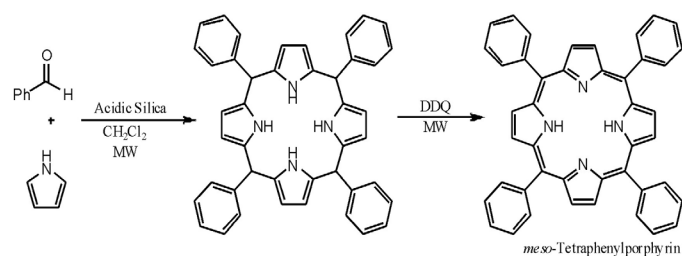
Abstract

Tetraphenylporphyrin, TPP, offers attractive features in a wide variety of model studies. Condensation of benzaldehyde with pyrrole followed by oxidation generally provides TPP in a one flask synthesis. The most commonly used method for synthesis of TPP is Lindsey method in which the halogenated solvent and harmful acids are used. Herein we have synthesized mesoporous acidic silica using sol-gel process with amphiphilic block co-polymer Pluronic P123 ((PPO)₂₀-(PEO)₇₀-(PPO)₂₀) polymer as structure directing agent. The structural and morphological characterization of synthesized catalyst is carried out which confirms its porous structure. This solid acidic catalyst is used very first time for synthesis of TPP by the reaction of pyrrole with benzaldehyde in dichloromethane, forming porphyrins in a comparable yield to the Lindsey method under milder reaction conditions using microwave irradiation. The synthesized catalyst is reusable at least four times with a little loss in its catalytic activity.

1. Introduction

The porphyrins lie at the focal point formed from divergent fields of research, including solar energy conversion, catalysis, spectroscopy, and the development of organic metals [1]. The synthesis of *meso*-substituted porphyrins has traditionally been achieved by Rothenmund method [2], or Adler method [3]. Then after, new method for porphyrin synthesis and various related work have been carried out by Lindsey and group [4-7]. The Adler method is efficient in term of yields and quantities in the case of simple tetraarylporphyrins, while the Lindsey method is widely used for the synthesis of porphyrins bearing sensitive substituents on the phenyl rings. But, in a series of Lindsey methods, the halogenated solvent and harmful acids can be recognized to be prerequisite because of their superior solubility for porphyrins and catalytic activity for the ring condensation, respectively. *meso*-Tetraarylporphyrin can be synthesized by a one-step cyclocondensation of monopyrrole with benzaldehyde, in the presence of a catalyst and an oxidant (Scheme 1). Several catalyst-oxidant systems have been studied after the development of Lindsey's method and the more recent methods introduced oxidizing co-solvents, clays, Ionic liquids, molecular iodine, hydrogen peroxide in acetic acid, mixtures of xylene and chloroacetic acid, transition metal salts or vapor phase synthesis without any solvent or catalyst [8-10]. This shows variety of homogeneous and heterogeneous catalyst systems have been used among which heterogeneous systems are far more superior due to its easy recovery, and reusability. But still it remains a challenge to develop a more energy efficient heterogeneous

catalyst with high stability which proves to be proficient for synthesis of porphyrins giving good yields and recyclability.



Scheme 1 Microwave assisted synthesis of acidic Silica catalyzed *meso*-Tetraarylporphyrin

In parallel, silica based mesoporous nanoparticles are increasingly being employed as heterogeneous catalyst for many reactions. These mesoporous materials have attracted more attention due to tailoring ability of pore structure over a wide range. Since the discovery of mesoporous silicas synthesized using surfactants as templates and strong mineral acid as catalyst, the templating method has been widely applied to prepare mesoporous silica with high surface areas, tuneable pore size, large pore volumes and rich morphology [11,12]. These properties make mesoporous silica as an excellent material for catalyst system. Porous silica with high surface area and unique particle morphology, which can be synthesized through acid catalyzed templating pathways can be an efficient solid acid catalyst in this context as surface Lewis acidity together with high surface area could play crucial role in porphyrin synthesis.

Herein, we first report the use of self assembled mesoporous silica nanoparticles synthesized using templating method where Pluronic P123 polymeric surfactant was used as template and [MMBIM]HSO₄ ionic liquid (synthesized earlier, [13]) as acid source. The synthesized acidic silica is used for efficient synthesis of *meso*-Tetraphenylporphyrins under microwave assisted heating in Dichloromethane solvent giving good yields in very short reaction time.

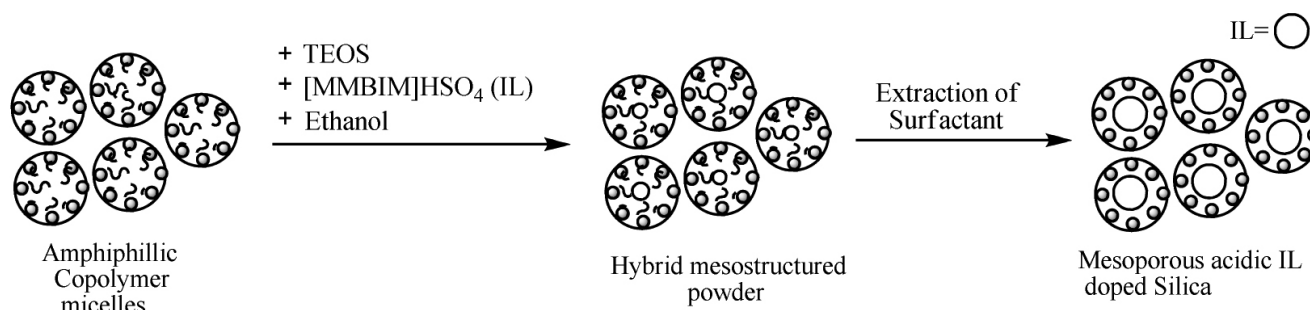
2. Experimental

2.1 Materials and Methods

The block co-polymer surfactant (P123, PEO-PPO-PEO MW-5750 g/mol), Tetraethoxysilane (TEOS), Benzaldehyde and Pyrrole were purchased from Sigma-Aldrich, India. Ethanol used was of Analytical grade laboratory reagent. The IL used was synthesized through process reported earlier by us [13]. The Synthesized mesoporous nanoparticles were characterized for their structure and texture by IR (ABB FTIR, Canada and Perkin-Elmer, Spectrum GX), Brunauer, Emmett and Teller (BET) surface area, BET surface area, average pore volume, and average pore diameter were measured by physisorption of N₂.

2.2 Synthesis of mesoporous silica

Mesoporous silica was synthesized using a prehydrolyzed solution containing TEOS (tetraethoxysilane), ethanol and Ionic liquid [MMBIM]HSO₄ (pH of IL = 2.3) as acid source and stirred for an hour. A second solution prepared by dissolving P123 block co-polymer surfactant ((PPO)₂₀-(PEO)₇₀-(PPO)₂₀) in ethanol under acidic conditions (maintained using [MMBIM]HSO₄), was then added to the former one and allowed to stir for further 3h. The resultant was then kept for ageing for one day under humid atmosphere (RH = ~60%) and then under atmospheric conditions for self evaporation of solvent which was then dried, grounded to form fine white colored free flowing powder. The powdered silica was then rinsed with ethanol for 2h at 80°C to remove surfactant (three times) and then dried under at 80°C for 2h. (Please see Scheme 2)



Scheme 2 Schematic representation of acidic IL supported porous silica

2.3 General process for Tetrarylporphyrin synthesis

Benzaldehyde (10 mmol), pyrrole (10 mmol) and silica catalyst (100mg) were added successively to 10mL CH₂Cl₂, without particular precautions. After the first activation (210W, 40°C, 1 min), TLC showed total conversion of benzaldehyde. DDQ (15 mmol) was then added and a second activation was performed (210 W, 40°C, 1 min). The mixture was filtered to remove catalyst and purified. The catalyst was washed with CH₂Cl₂ and acetone to ensure removal of all porphyrin products from catalyst and then dried under vacuum at 70°C. The remaining solution is evaporated on column silica and purified by Column chromatography using CH₂Cl₂/petroleum ether as eluent. Pure product was obtained as a purple solid. All physicochemical properties coincided with literature data. ¹H NMR (400 MHz, CDCl₃): 8.87 (8H, Singlet, Pyrrole-H), 8.23–8.26 (8H, Multiplet, *ortho*-H-Ph), 7.75–7.81 (12H, Multiplet, *meta*-H-Ph and *para*-H-Ph), 2.97 (2H, pyrrole -NH); ¹³C NMR (400 MHz, CDCl₃): 118.2, 119.8, 126.3, 127.5, 130.8, 134.9, 141.9.

3. Result and Discussion

Mesoporous silica nanoparticles were obtained by washing of nanocomposites with ethanol solvent to assure removal of P123 surfactant. Then the washed silica material was characterized by FTIR spectroscopy in which the adsorption bands characteristic for P123 could not be observed, indicating that P123 could be almost totally removed by extraction of silica with ethanol solvent repeatedly (Figure 1). Moreover two important peaks at 1088 cm⁻¹ and 1165 cm⁻¹ assigned to S=O stretching vibration, which shows that IL does not wash away during this process.

Nitrogen adsorption and desorption isotherms and size distribution plots of mesoporous silica shows a type IV isotherm with a large hysteresis indicating a 3D intersection network of porous structure. As shown in Figure 2, the specific surface area for synthesized silica was calculated according to the BET equation and was 58.63 m²/g and the

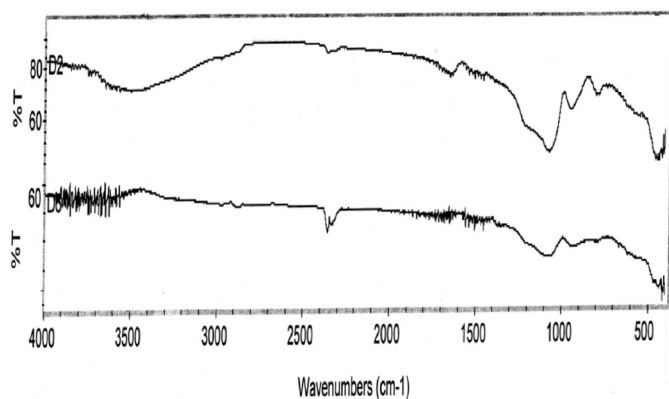


Fig. 1: FTIR plots of mesoporous silica with and without washing with ethanol

total pore volume was $0.07345 \text{ cm}^3/\text{g}$ which corresponds to an average pore diameter ($4V/A$ by BET) of 5.0 nm. The pore size distribution derived from the isotherm data using BJH model was 4.2 nm. This result shows that silica nanoparticles have porosity and large surface area therefore; it can be a good candidate as catalyst.

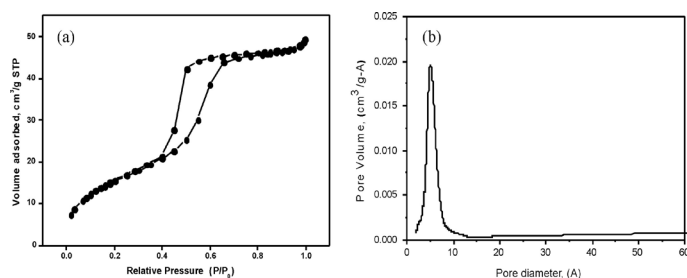


Fig. 2: (a) N_2 gas adsorption-desorption isotherm, (b) pore size distribution plots of mesoporous silica

The catalytic performance of synthesized mesoporous silica was carried out for the synthesis of porphyrins. An initial examination for the reaction pyrrole, benzaldehyde and mesoporous silica as catalyst in dichloromethane solvent has conducted for the formation porphyrinogens which is further oxidized in presence of 2,3-dichloro-5,6-dicyanobenzoquinone (DDQ) [14] to give desired porphyrin in comparative yield. There are few factors

on which yield of porphyrin is dependent which includes choice of oxidant and acid catalyst, duration of condensation period, concentration of acid, pyrrole and benzaldehyde. The mesoporous structure plays an important role in synthesis, as per our hypothesis, if the porphyrinogen formation was carried out in a restricted nano-size shape, the intramolecular cyclization would be more dominant than the cyclization conducted in a homogeneous solution and the longer copolymer formation would be suppressed. This is the primary and foremost reason for selecting and synthesizing mesoporous silica and thus is applied as catalyst for porphyrin synthesis. The second most important factor is concentration of pyrrole and benzaldehyde, which we have monitored and optimized (Table 1, Entry 1,2,5). The result shows that use of excess pyrrole for the reaction may to polymerization and formation of major side products. Equivalent amount of pyrrole and benzaldehyde are sufficient to precede the reaction with good efficiency.

As the concentration of acid catalyst has a significant effect on the rate and course of reaction varying amount of acidic silica was used to check for the efficient porphyrin formation (Table 1, Entry 2,3,4). The optimum acidic silica amount of 100 mg was found to be sufficient for catalyzing the reaction. Another most important criteria for porphyrin synthesis is the condensation time (the time given to the starting materials to condense completely). As the reaction is microwave assisted, the reaction was irradiated for few minutes and by varying time, to our surprise the reaction gets completed within 1 min of irradiation which can be seen by the disappearance of benzaldehyde spot in TLC. The reaction time of 1 min was found to be the best possible time for completion of condensation reaction giving porphyrinogen in good amounts.

The reaction was carried out at 210W microwave power level and the maximum temperature attained during course of reaction is 40°C . Next step is the oxidation of porphyrinogen to porphyrin which is performed with DDQ. The addition of DDQ to porphyrinogen gives a

Table 1 Optimization of process for synthesis of *meso*-Tetraphenylporphyrin

Entry	Reagent Concentration (mmol)		Catalyst (mg)	MW power (W)	Isolated Yield (%)	Time (min)
	Pyrrole	Benzaldehyde				
1	15	10	100	210	25	2
2	10	10	100	210	47	2
3	10	10	50	210	29	4
4	10	10	120	210	45	2
5	15	10	120	210	24	2
6	10	10	100	245	42	2
7	10	10	100	180	20	5

nearly instantaneous conversion to porphyrin. The major advantage of this process lies here that no homogeneous acid catalyst is used thus no neutralization step is required to suppress the acid and its side effects unlike other reported processes. After the formation of porphyrin, the synthetic procedure is mild, clean, and convenient. The porphyrin formed upon oxidation was taken up for chromatographic separation, where the tar like polymeric material formed as side-product remains at the top-most part of the column and doesn't drain out while eluting with solvent. The rest column was eluted with CH_2Cl_2 /Pet ether (1:1 to 3:1) to elute several small bands of fast moving pigments followed by CH_2Cl_2 to elute porphyrin. The absorption spectra for each fraction have been recorded for the confirmation of porphyrin. The absorption spectrum of Tetraphenylporphyrin shows a strong absorbance at 420nm along with four weaker absorbances at 510, 550, 590, and 610nm (Figure 3). The pure porphyrin fractions were combined and concentrated to afford a crude product which is recrystallized to give Tetraphenylporphyrin in 47% yield. The product was pure as determined by absorption spectroscopy, TLC and ^1H NMR spectroscopy.

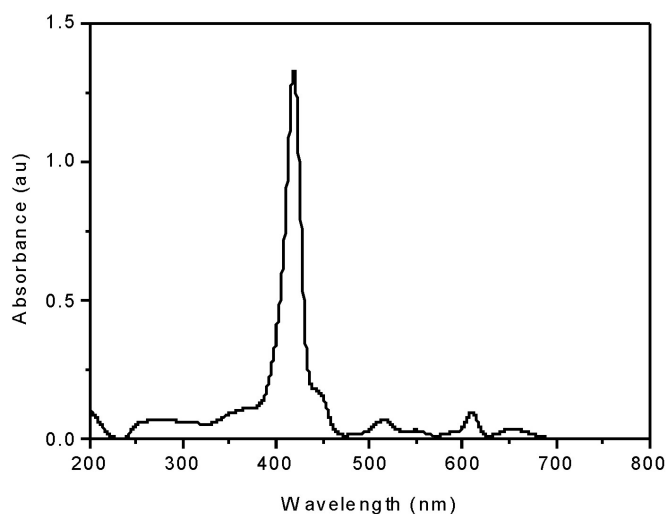


Fig 3: Absorbance Spectrum of meso-Tetraphenylporphyrin

In comparison with other catalyst employed for the synthesis of Tetraphenylporphyrin mesoporous silica showed a much higher activity in terms of short reaction time and mild conditions (Table 2). Other than this, the other catalyst leads to formation of N-confused Tetraphenylporphyrin (NC-TPP) and Tetraphenylsapphyrin (TPS) as by-products which are not obtained in our case. TPP is the sole product obtained without any other side product formed in comparative higher yield and is the same case when MCM-41 was used as catalyst. The reason can be, as explained above due to the mesoporous nature of silica catalyst and ionic liquid that

provides acidic character to the catalyst. The recyclability of catalyst is of prime importance and for the mesoporous silica catalyst, the study shows recyclability up to four times without any significant loss in catalytic activity.

Table 2 Comparison of various catalyst for the porphyrin synthesis

Entry	Catalyst	Yield obtained	Reference
1	BF_3 -etherate/ NaCl	42% TPP, 5.8% NC-TPP	7
2	BF_3 -etherate /TFA	39% TPP, 2.2% NC-TPP, <0.2% TPS	7
3	Iodine	35% TPP	8
4	$[\text{C}_4\text{-SAbim}]$ $[\text{CF}_3\text{SO}_3]\text{IL}$	43% TPP and 10% NC-TPP	9
5	MCM-41	23.5% TPP	10
6	Mesoporous silica	47% TPP	Our work

TPP-Tetraphenylporphyrin, NC-TPP-N-confused
Tetraphenylporphyrin, TPS-Tetraphenylsapphyrin

4. Conclusion

Mesoporous acidic silica catalyst was synthesized using sol-gel templating method where $[\text{MMBIM}]\text{HSO}_4$ ionic liquid was used as acid source. The ionic liquid used impart acidic characteristic to the silica. The silica is mesoporous in nature with 5nm nanoparticles size which can be seen from the BET surface area analysis. This particular characteristic makes it efficient catalyst for Tetraarylporphyrin synthesis. The synthesis of three different substituted porphyrins has been carried out in high purity and good yields which is confirmed by their absorption spectrum and NMR spectroscopy. Thus, the synthesized mesoporous acidic silica proved to be efficient catalyst for porphyrin synthesis.

References

1. K. M. Kadish, K. M. Smith and R. Guilard (Eds.), *The Porphyrin Handbook*, Vol.6, Academic press, San Diego, CA, 2000.
2. P. Rothmund, *J. Am. Chem. Soc.*, 57 (1935) 2010.
3. A. D. Adler, F. R. Longo, J. H. Finarelli, J. Goldmacher, J. Assour and L. Korsakott, *J. Org. Chem.*, 32 (1967) 476.
4. J. S. Lindsey, H. C. Hsu and I. C. Schreimann, *Tetrahedron Lett.*, 27 (1986) 4969.
5. J. S. Lindsey, I. C. Schreimann, H. C. Hsu, P. C. Kearney and A. M. Marguerattaz, *J. Org. Chem.*, 52 (1987) 827.
6. G. R. Geier III, D. M. Haynes and J. S. Lindsey, *Org. Lett.*, 1 (1999) 1455.
7. G. R. Geier III, Y. M. Ciringh, F. Li, D. M. Haynes and J. S. Lindsey, *Org. Lett.*, 2 (2000) 1745.

8. R. Lucas, J. Vergnaud, K. Teste, R. Zerrouki, V. Sol and P. Krausz, *Tetrahedron Lett.* 49 (2008) 5537 and further reference cited therein.
9. S. Kitaoka, K. Nobuoka, Y. Ishikawa, *Chem. Commun.*, (2004) 1902; *Tetrahedron* 61 (2005) 7678.
10. S. J. Kulkarni, K. V. Raghavan, R. K. Motkuri and S. Nagabandi, US Patents, US 6,524,446 B2.
11. C. T. Kresge, M. E. Leonowicz, W. J. Roth, J. C. Vartuli and J. S Beck, *Nature*, 359 (1992) 710.
12. T. Yanagisawa, T. Shimizu, K. Kurodu and C. Kato, *Bull. Chem. Soc. Jpn.*, 63 (1990) 988.
13. D. A. Kotadia and S. S. Soni, *Catal. Sci. Technol.*, 3 (2013) 469.
14. D. Walker and J. H. Hiebert, *Chem. Rev.*, 67 (1967) 153.



Deepali A. Kotadia received her B.Sc. in Chemistry from the N. V. Patel Science College of Pure and Applied sciences (NVPAS), Vidyanagar, Gujarat in 2007. She completed her M.Sc. with specialization in Organic Chemistry from the Department of Chemistry, Sardar Patel University in 2009. She expects to receive her Ph.D. in Chemistry from the Sardar Patel University in the fall of 2014, under the supervision of Dr. Saurabh S. Soni (Assistant Professor). Her research studies have been centered on the synthesis of homogeneous and heterogeneous catalysts especially bronsted acidic ionic liquids, supported catalysts and metal doped mesoporous materials for cross-coupling, biofuels and other industrially important reactions, with a special focus on green chemistry and environment benign processes. Her thesis studies were supported by UGC funded RFSMS (Research Fellowship in Science for Meritorious Students) Fellowship from 2010 to 2013 and she has been awarded with CSIR-SRF fellowship in 2013.



Dr. Saurabh S. Soni is working as Assistant Professor at Department of Chemistry, Sardar Patel University, Vallabh Vidyanagar. He received his B. Sc., M. Sc. (Physical Chemistry) and Ph. D. from Sardar Patel University. He did post doctorate at Universite Du Maine, France and also received CNRS fellowship during his stay. His areas of research are dye sensitized solar cell, ionic liquids and their applications as catalyst, development of mesoporous materials, and surface activity of block copolymers in aqueous solutions. His research work is funded by various funding agencies like DST, UGC, UGC-DAE etc. Recently, he is awarded with "Young Scientist Award" under DST-Fast Track scheme. He visited countries like France, Australia, Italy for research purpose.

Heterogeneous Photocatalysis: Novel Approach for Carbon-Carbon Bond Forming Reactions

Sudhir S. Arbuj,^{a,*} Bina N. Wani^b and Uttam P. Mulik^a

^aCentre for Materials for Electronics Technology, Panchwati, Pune-411008, India

^bChemistry Division, Bhabha Atomic Research Centre, Mumbai-400085, India

E-mail:sudhir1305@gmail.com

Abstract

The palladium chloride (PdCl₂) and PdCl₂/TiO₂ efficiently catalyzes the Carbon-Carbon bond formation (Heck reaction) between aryl iodides and olefins under photochemical reaction conditions. Both the catalyst provides good conversion under optimized reaction conditions, but in case of bare PdCl₂ recovery of used catalyst was difficult as compared to PdCl₂/TiO₂ catalyst. Use of light reduces the Pd²⁺ to Pd⁰ and enhances the rate of C-C bond forming reaction. After completion of the reaction, Pd²⁺ get reduced to Pd⁰. Further Pd⁰ can be easily converted into Pd²⁺ by heating with ammonium chloride at 400°C for 30 min and the regenerated catalyst could be reused up to third recycle with good catalytic activity. The catalysts (before and after reaction, as well as regenerated) were systematically characterized using Transmission Electron Microscopy, X-ray photoelectron spectroscopy, X-ray diffraction, temperature programmed reduction and DRUV-visible spectroscopy techniques.

Keywords: Photocatalysis, Heck reaction, Carbon-Carbon bond, Heterogeneous

1. Introduction

The process of performing chemical reaction using light in presence of semiconductor oxides/sulphides or other Inorganic materials is termed as photocatalysis [1]. The heterogeneous photocatalysis is an advanced oxidative process and effectively used for various applications mainly environmental and energy related issues [2]. From last 3-4 decades this technique was utilized for degradation of organic contaminants for recovering polluted water and water splitting for generation of Hydrogen as a fuel [3]. Apart from environmental and energy related applications recently this technique can be utilized for carbon-carbon (C-C) bond forming reactions which are important in organic chemistry [4,5]. This coupling reaction provides the simplest and most efficient way to synthesize various compounds useful in the pharmaceutical and agrochemical industries [6]. Among the various carbon-carbon coupling reactions, Heck reaction has received considerable attention as it is an important tool for carbon-carbon bond formation between aryl halides and olefins. The Heck reaction generally performed with 1-5 mol% palladium along with phosphine ligands for stabilization of active palladium intermediates in presence of a suitable base under thermal conditions. Most of the efforts in this field have been directed to enhance the catalytic activity of palladium by using homogeneous as well as heterogeneous reaction conditions [7]. Also various phosphorous, nitrogen, sulfur and carbene based ligands

have been tried successfully [8-11]. However, due to their drawbacks viz. air and moisture sensitive nature, toxicity, expensive, unrecoverable and severe reaction conditions, a ligand free Heck reaction has been developed. Also, the main problem associated with homogeneous reaction medium is the recovery of the precious palladium metal and contamination of the product. To overcome this problem, many researchers have studied the Heck reaction over heterogeneous catalyst mainly palladium supported on various oxides, polymers etc [12-13]. Recently, use of palladium salts such as PdCl₂ or Pd(OAc)₂ without any ligands are increasingly being used for the Heck reaction. In order to increase the effectiveness of catalyst various other methods such as ultrasonication, microwave and electrochemical have been tried [14-16]. Herein, we disclose for the first time, heterogeneous photocatalyzed Heck reaction of various aryl iodides with olefins over PdCl₂ and PdCl₂/TiO₂ as a catalyst at ambient reaction conditions. The systematic study of influence of solvents, different bases, catalyst precursors and regeneration of the catalyst is successfully investigated.

2. Experimental

2.1 Materials and chemicals used

The TiO₂ and PdCl₂ were purchased from Sigma-Aldrich and used without any further purification. All the solvents used are of AR grade and purchased from SRL. The other used iodo compounds and olefins are of Sigma-Aldrich make.

2.2 Preparation of 1 wt. % PdCl₂/TiO₂ catalyst

In 30 ml of distilled water 10 mg of PdCl₂ and 1 gm of TiO₂ were added and stirred 2 hrs at room temperature and then refluxed for 3 hrs. with constant stirring. The excess water was evaporated on water bath and the solid powder was dried in oven at 100°C for two hrs. The dried PdCl₂/TiO₂ powder was mixed in mortar and pestle for 30 min. and used for further reactions.

2.3 General procedure for the photochemical Heck reaction

To a 25 ml round bottom flask 1 mmol of aryl iodide, 3 mmol of olefin, 3 mmol of triethyl amine (TEA) in DMF (5 mL) were mixed, to this mixture 0.5 mol % PdCl₂ or PdCl₂/TiO₂ was added. The resulting reaction mixture was irradiated under 400 Watt mercury vapor lamp with continuous stirring in a closed box. The temperature of the reaction was controlled at 45 ± 3 °C with the help of fans. The mercury vapor lamp was kept vertically in the quartz tube, provided with the water circulation arrangement in order to minimize the heating effect due to IR radiation. The progress of the reaction was monitored by G.C. (HP-5890) equipped with capillary column (HP-5, 30m x 0.32mm x 0.25um). After the completion, the reaction mixture centrifuge at 4000 rpm for 20 min to separate the catalyst. The supernatant solution was diluted with water (10 mL) and the products were extracted using ethyl acetate (3 x 10 mL). Combined organic layer was dried over the anhydrous sodium sulphate and purified by using column chromatography over silica-gel [hexane or hexane/ethyl acetate (9:1)]. The GC-MS spectra's were taken on Shimadzu QP-5050 equipped with TCD and capillary column (DB-5). FTIR spectra's were recorded in Nujol mull and are expressed in cm⁻¹. ¹H (300 MHz) and ¹³C (75 MHz) NMR spectra's were recorded in CDCl₃.

2.4 Characterization of PdCl₂/TiO₂ catalyst

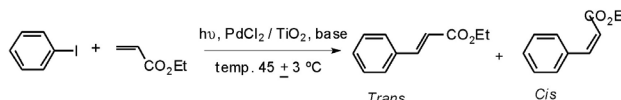
The stability of TiO₂ phases were observed using powder XRD technique (Philips Diffractometer PW 1710, 10 to 70° range, scan rate = 1° min⁻¹) equipped with a monochromator and Ni-filtered Cu Kα radiation. The oxidation state of Palladium was confirmed by using X-ray photoelectron spectroscopy. The UV-visible absorbance characteristics of the catalysts were evaluated in a UV-visible spectrophotometer (Shimadzu 1601, range 200 – 800 nm) in the diffuse reflectance mode. BaSO₄ was used as reference and the band gap values were calculated from the data collected. Temperature programmed reduction (TPR) patterns of the samples were recorded in the temperature range of 27-800°C in a flow of H₂ (5%) in Ar (20 ml min⁻¹) and at a ramp rate of 10°C min⁻¹. The samples

were subjected to a pre-treatment in helium flow at 250°C for 2 h prior to a TPR run.

3. Results and Discussion

3.1 Optimization of reaction parameters

The reaction parameters were systematically optimized using various solvents, organic and inorganic bases and different catalyst concentrations. The reaction between iodobenzene and ethyl acrylate was studied as a model system shown in **Scheme 1**.



Scheme 1. Photochemical Heck reaction between iodobenzene and ethyl acrylate.

In photocatalytic Heck reaction we have observed *trans* and *cis* isomers of corresponding products in the ratio of ~9:1, whereas in thermal reaction conditions only the *trans* product was observed. In order to confirm whether the reaction is photochemical or thermal we carried out the reaction without uv-visible irradiation at 45 °C by keeping all the other parameters same which showed negligible (< 2 % in 5 h) conversion (Table 1; entry 1^b) whereas, under photochemical reaction conditions it gives 97 % conversion (Table 1; entry 1). The same reaction is carried out using PdCl₂ catalyst without use of any support, it showed 99 % conversion with 88 % selectivity for *trans* product. Though its conversion is higher but recovery of the catalyst was not possible using only PdCl₂ catalyst, in order to recover the Pd catalyst we used TiO₂ support as it plays a dual role support as well as light absorbing material. Among the various solvents studied, DMF and DMAc gave excellent conversion and selectivity for the *trans* ethyl cinnamate (Table 1; entries 1-2). NMP shows 74 % conversion (entry 3). The reaction in DMSO and ACN shows poor conversion (entries 4, 5). Formation of soluble palladium complexes [PdCl₂(solvent)₂] might be possible by coordination with polar solvents and this provides the active palladium species. The activity of this species depends on the stability of the respective complexes.

Table 1 Reaction of iodobenzene with ethyl acrylate using different solvents.^[a]

Entry	Solvent	% Conversion	% Selectivity
			Trans
1	DMF	97	89
1 ^b	DMF	2	100
1 ^c	DMF	99	88
2	DMAc	97	86
3	NMP	74	84

Table I contd...

Entry	Solvent	% Conversion	% Selectivity
			Trans
4	DMSO	33	63
5	ACN	10	100
6	DPE	9	85
7	Xylene	1	100
8	THF	4	47
9	Diglyme	4	100
10	1,4-Dioxane	NR	-

^[a]**Reaction conditions:** iodobenzene (1 mmol), ethyl acrylate (3 mmol), triethyl amine (3 mmol), 5 mL solvent, 0.5 mol % PdCl₂/TiO₂ were stirred for 5h under 400W mercury vapor lamp at temperature 45 ± 3 °C. 1^b Reaction carried out without uv-visible irradiation at 45 °C for 5 h. NR- no reaction. 1^c Reaction carried out using only PdCl₂ catalyst

The reaction in ACN shows poor conversion this may be due to formation of stable PdCl₂(ACN)₂ complex, which in turn retards the reaction rate. Arai and coworkers reported the formation of soluble Pd(OAc)₂(NMP)₂ complex through coordination of NMP and TEA with palladium [17].

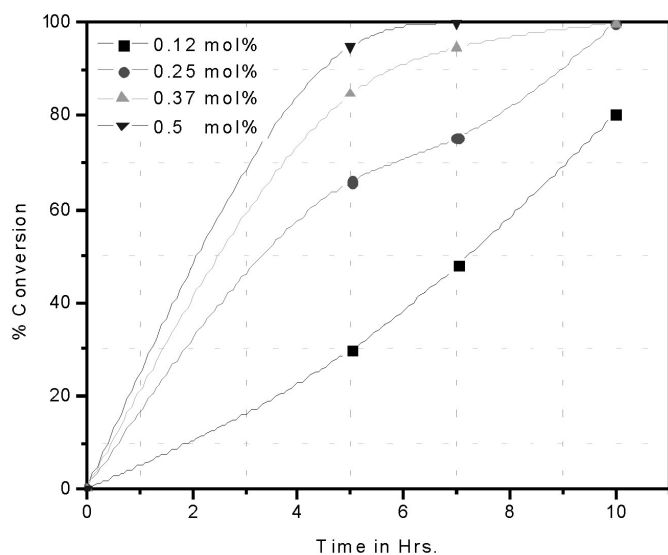


Fig. 1 Graph of % conversion Vs time using different amount of catalyst concentration

Non polar solvents do not show any activity (entry 6). The order of activity is DMF ~ DMAc > NMP > DMSO > ACN > DPE > THF ~ Diglyme > xylene. The catalytic activity of different palladium concentration for the Heck coupling under photocatalytic conditions was studied and results are shown in Fig. 1. It is observed that with increase in palladium concentration the % conversion increases, 0.5 mol % PdCl₂/TiO₂ show 97 % conversion in 5 h.

The lower Pd concentration also gives 100% conversion but it requires higher reaction time. Effect of organic as well as inorganic bases was studied on the reaction between iodobenzene and ethyl acrylate and results are shown in Table 2. TEA and TBA shows higher conversion as compared to other inorganic bases. This is due to the solubility of bases in the solvent which directly affects the conversion of the reaction. The study of different bases depict that TEA is the best base among the studied bases in presence of 0.5 mol% PdCl₂/TiO₂ as a catalyst.

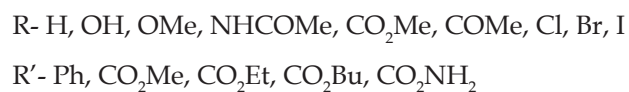
Table 2 Reaction of iodobenzene with ethyl acrylate using different bases^[a]

Entry	Base	% Conversion	% Selectivity
			trans
1	TEA	97	89
2	TBA	93	93
3	NaOAc	12	86
4	K ₂ CO ₃	12	53
5	Cs ₂ CO ₃	NR	-
6	Ca(OH) ₂	NR	-

^[a]**Reaction conditions:** iodobenzene (1 mmol), ethyl acrylate (3 mmol), base (3 mmol), 5ml DMF, 0.5 mol% PdCl₂/TiO₂ were stirred for 5 h under 400W mercury vapor lamp. NR- no reaction.

3.2 Heck reaction between substituted aryl iodides and olefins

Using the optimized reaction conditions, the C-C coupling reaction was studied with various substituted aryl iodides and olefins (Scheme 2) and the results are summarized in Table 3. Reaction of iodobenzene with ethyl, methyl and n-butyl acrylate gave excellent conversion and selectivity (Table 3; entries 1-3).



Scheme 2. Photochemical Heck reaction between substituted aryl halides and olefins.

Styrene, acryl acid and n-butyl methacrylate showed poor reactivity towards Iodobenzene (entries 4-6) and acryl amide and acrylonitrile did not react with iodobenzene under this reaction condition (entry 7, 8). *Ortho*-iodophenol gave 49% conversion with 100% selectivity for *trans* product (entry 9). *Ortho*- and *para*-iodo anisole gave 40 and 85% conversion with 93 and 80% selectivity for corresponding *trans* products, respectively (entries 10, 11). Under

photochemical reaction conditions it is very likely that UV-visible light helps towards the formation of intermediate species between PdCl₂ and substrate, which accelerates the rate of reaction. The formation of this intermediate species depends on the nature nucleofuge and C-I bond strength. The electron withdrawing and electron donating groups directly affect the C-I bond strength which affects the conversion of the reaction. Amino and nitro substituted substrates are not active under photochemical reaction conditions. These functional groups might be retarding conversion of aryl iodides via competing efficiently for optical absorption.

Table 3. Photocatalytic heck coupling of aryl halides and olefins using PdCl₂/TiO₂^[a]

Entry	R	X	R'	Conversion (%)	Selectivity (%) trans
1	H	I	CO ₂ Et	97	89
2	H	I	CO ₂ Me	90	95
3	H	I	CO ₂ ⁿ Bu	94	89
4	H	I	Ph	11	90
5	H	I	COOH	29	100
6	H	I	CH ₃ CO ₂ ⁿ Bu	7 ^b	100
7	H	I	CONH ₂	NR	-
8	H	I	CN	NR	-
9	2-OH	I	CO ₂ Et	49	100
10	2-OMe	I	CO ₂ Et	40	93
11	4-OMe	I	CO ₂ Et	85	80
12	2-NO ₂	I	CO ₂ Et	NR	-
13	4-NO ₂	I	CO ₂ Et	NR	-
14	2-NH ₂	I	CO ₂ Et	NR	-
15	4-NH ₂	I	CO ₂ Et	NR	-
16	2-NHCOMe	I	CO ₂ Et	48	100
17	2-CO ₂ Me	I	CO ₂ Et	72	82
18	3-CO ₂ Me	I	CO ₂ Et	55	93
19	4-CO ₂ Me	I	CO ₂ Et	89	95
20	4-CH ₃	I	CO ₂ Et	94	86
21	4-Cl	I	CO ₂ Et	100	94
22	4-Br	I	CO ₂ Et	100	94
23	3-I	I	CO ₂ Et	99	27, 72 [#]

^[a] **Reaction conditions:** substrate (1 mmol), olefin (3 mmol), triethylamine (3 mmol), 5 ml DMF, 0.5 mol % PdCl₂/TiO₂ were stirred for 5 h under 400W (Hg vapor lamp) UV-visible irradiation at temperature 45 ± 3 °C. ^b reaction time = 7 h [#] di-substituted trans compound.

Under these reaction conditions *ortho*- and *para*-iodoaniline, *ortho*- and *para*-iodonitrobenzene does not show any reaction (entries 12-15). The *ortho*-iodo acetanilide

shows 48 % conversion with 100% selectivity for trans product. The effect of substitution on various positions in an aromatic ring was studied in case of *ortho*-, *meta*- and *para*-iodomethylbenzoate where the activity was in the order *para* > *ortho* > *meta* (entries 17-19). The *para*-iodo toluene gave 94 % conversion with 86 % selectivity for *trans* product (entry 20).

We found that bromo and chloro substituted aryl iodides gave selectively iodo coupled product (entries 21, 22). *Para*-bromo and *para*-chloro iodobenzene gave 100% conversion with 94 % selectivity for *trans* isomer. Di-substituted products were observed for the reaction between 1,3 di-iodobenzene and ethyl acrylate with 100 % conversion showing 72 % selectivity for di-substituted product (entry 23).

The overall photochemical Heck reaction mechanism is believed to involve migratory insertion pathway. Means the photocatalytic mechanism is same as the thermal Heck reaction, Palladium in PdCl₂/TiO₂ catalyst under UV-visible irradiation reduced to Pd(0). The oxidative addition of Pd(0) to the aryl halide (C-X) bonds takes place. The olefin in the Heck reaction coordinates to the palladium, and then undergoes an insertion into the C-C π bond with concurrent migration of the aryl group to the adjacent carbon. The newly coupled aryl-olefin compound is then eliminated via a reductive β-hydride elimination (ethylcinnamate) followed by a base deprotonation of the Pd(II) species and loss of halogen to form a salt.

3.3 XPS analysis

After completion of the reaction the Pd (2+) get reduced to Pd (0) which is not showing any conversion towards Heck reaction under photochemical reaction condition.

The Pd(0) is oxidized to Pd(2+) by heating Pd(0) at 400 °C for 30 min. in presence of ammonium chloride. It gives PdCl₂/TiO₂ catalyst and this regenerated catalyst was used for the recycling study of the catalyst. The activity for the

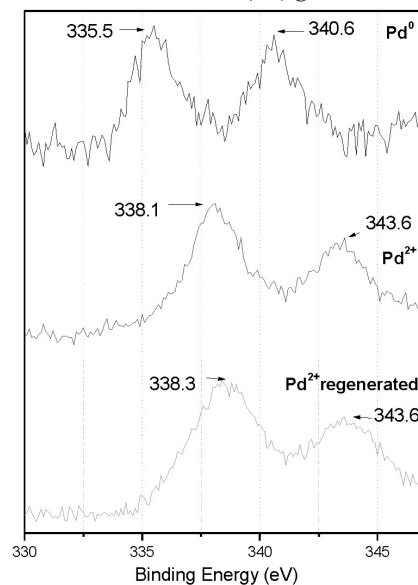


Fig. 2 XPS spectra of used PdCl₂/TiO₂ before and after the reaction and after regenerated

catalyst remains same up to third recycle (shown in Table 4). The formation of Pd(0) and Pd(2+) species were confirmed by X-ray photoelectron spectroscopy. Fig. 2 shows the XPS spectra of as prepared, used and regenerated PdCl₂/TiO₂ catalyst. The binding energy values at 335.3 and 340.7 eV for Pd(3d_{5/2}) and Pd(3d_{3/2}) core levels respectively [18], (Fig. 2) in X-ray photoemission spectra confirms the formation of Pd(0)/TiO₂. The binding energy values at 338.1 and 343.6 eV confirms the formation of Pd(2+) species after heating with ammonium chloride.

3.4 TEM analysis

TEM images of PdCl₂/TiO₂ indicate the palladium particles having size in the range of 5-10 nm are uniformly attached to the TiO₂ surface (Fig. 3a, b). The selected area electron diffraction (SAED) pattern shown in an inset of Fig. 3 'a' and 'c' confirms the crystalline nature of PdCl₂/TiO₂, indexed plane confirms the anatase structure of TiO₂.

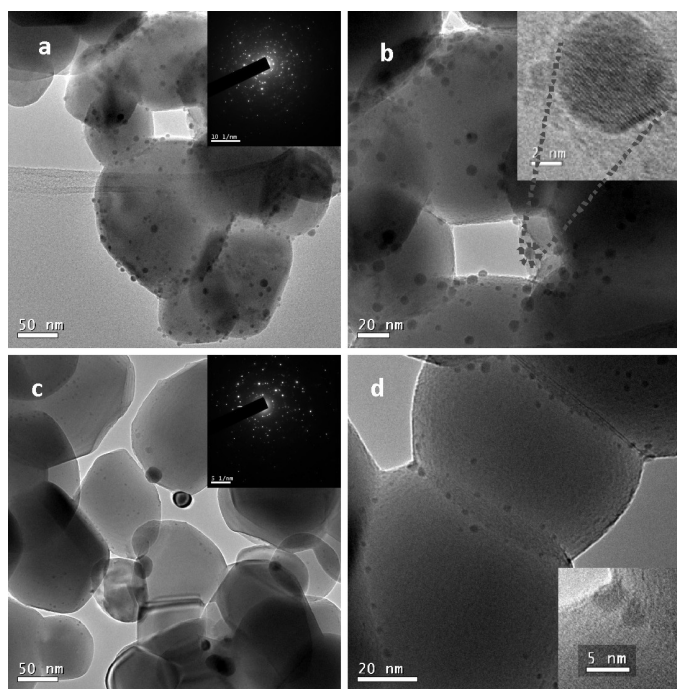


Fig. 3. TEM images of a, b) PdCl₂/TiO₂ before reaction and c, d) regenerated PdCl₂/TiO₂. Inset of Fig. a and c is the SAED pattern of PdCl₂/TiO₂

The inter planar d-spacing (inset of Fig. 3 b) is 0.22 nm support the (111) hkl plane of cubic palladium. The particle size of Pd observed in the range of 3-5 nm in case of regenerated PdCl₂/TiO₂ (Fig.3 c, d), which is much smaller than the original PdCl₂/TiO₂ catalyst. TEM analysis validates the presence of Pd in regenerated PdCl₂/TiO₂ catalyst. After completion of Heck reaction the Pd particles were attached to TiO₂ surface which facilitates the easy

separation of catalyst from reaction mixture giving highly pure products.

Table. 4 Catalyst recycle study for Heck reaction

Entry	Run	% Conversion	% Selectivity
1	First	97	89
2	Second	90	95
3	Third	87	93
4	Fourth	13	99

[a] Reaction conditions: iodobenzene (1 mmol), ethyl acrylate (3 mmol), triethyl amine (3 mmol), 5 mL solvent, 0.5 mol % PdCl₂/TiO₂ were stirred for 5 h under 400W mercury vapor lamp at temperature 45 ± 3 °C.

3.5 XRD analysis

XRD patterns of the catalyst are shown in Fig. 4. The amount of PdCl₂ loaded on anatase TiO₂ is very low (1 wt. %) therefore the palladium peaks were not observed in the XRD patterns. All diffraction peaks are matches with standard anatase TiO₂ pattern indicating the stability of anatase TiO₂. The identical XRD pattern of PdCl₂/TiO₂ before and after regeneration suggests the recyclability of catalyst.

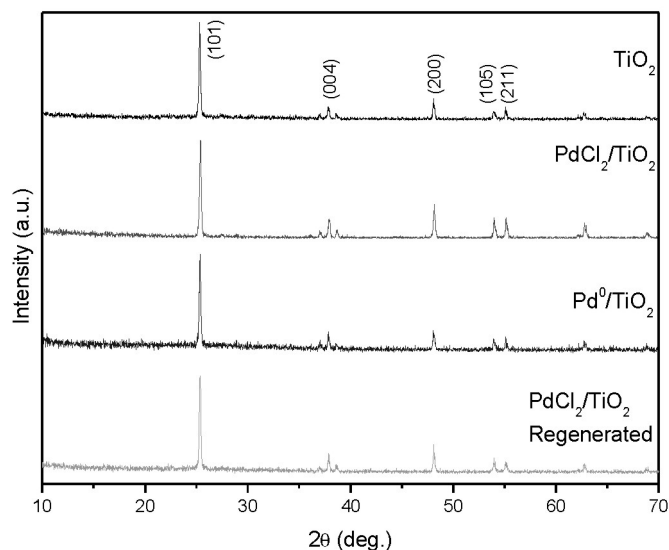


Fig. 4. Xrd pattern of the a) TiO₂, b) PdCl₂/TiO₂, c) used PdCl₂/TiO₂, d) Regenerated

3.6 Diffuse reflectance UV-Visible spectra

Diffuse reflectance UV-visible absorption profile of the PdCl₂/TiO₂ before and after regeneration are same and shown in Fig. 5, indicating the complete regeneration of catalyst. The absorption edge of regenerated PdCl₂/TiO₂ is observed to be around 380 nm corresponds to 3.2 eV and matches with the original PdCl₂/TiO₂ catalyst.

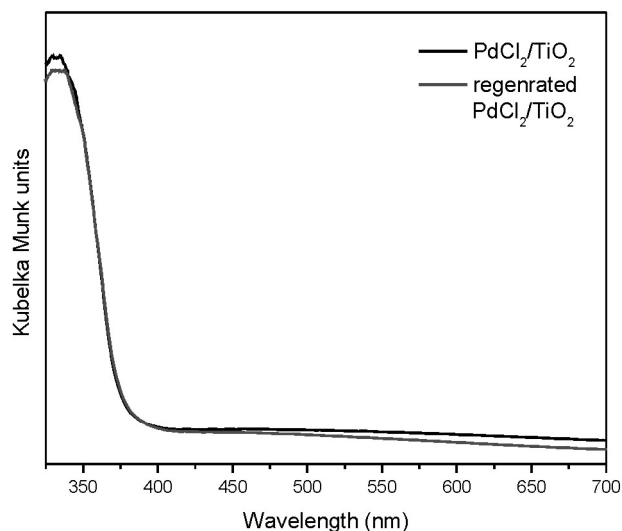


Fig. 5. DRUV-visible absorption profile of $\text{PdCl}_2/\text{TiO}_2$

3.7 Temperature programme reduction

TPR profile of the catalyst were studied and found that the reduction temperature for $\text{PdCl}_2/\text{TiO}_2$ catalyst before reaction is 200°C which is shifted to 235°C for regenerated catalyst (Fig. 6). During the TPR, first the Pd^{2+} get reduced to Pd^0 and then at temp. 365°C it forms palladium hydride. At higher temperature it loses hydrogen resulting negative peak.

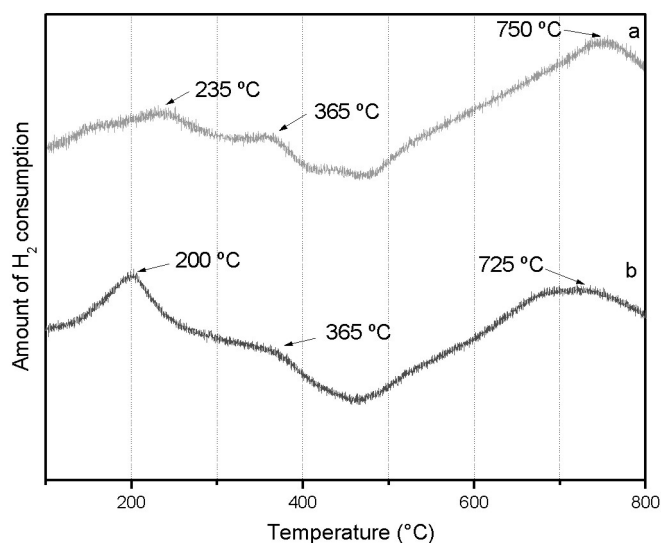





Fig. 6 TPR profile of a) Regenerated $\text{PdCl}_2/\text{TiO}_2$ before reaction and after regeneration and b) $\text{PdCl}_2/\text{TiO}_2$ before reaction.

4. Conclusion

We have developed a simple $\text{PdCl}_2/\text{TiO}_2$ catalyzed photocatalytic C-C coupling reaction for various substituted aryl iodides and olefins which offers good yield for the corresponding coupled products at ambient reaction conditions. The oxidation of $\text{Pd}(0)$ to $\text{Pd}(2+)$ can be achieved by heating the palladium with ammonium chloride at 400°C . The regenerated $\text{PdCl}_2/\text{TiO}_2$ shows better activity up to third recycle. The TEM analysis confirms the formation of Pd particles on the TiO_2 surface.

References:

1. A. Fujishima, T. N. Rao, and D. A. Tryk, *J. Photochem. Photobiol. C: Photochem. Rev.*, 1 (2000) 1.
2. M. R. Hoffmann, S. T. Martin, W. Choi, and D. W. Bahnemann, *Chem. Rev.*, 95 (1995) 69-96.
3. J. M. Herrmann, *Catalysis Today* 53 (1999) 115.
4. M. Fagnoni, D. Dondi, D. Ravelli, and A. Albini, *Chem. Rev.* 107 (2007) 2725.
5. S. B. Waghmode, S. S. Arbut, B.N. Wani, and C.S. Gopinath *Can. J. Chem.* 91 (2013) 348.
6. A. Zapf, M. Beller, *Topics in Catalysis* 19 (2002) 101.
7. N. T. S. Phan, M. V. D. Sluys, C. W. Jones, *Adv. Synth. Catal.* 348 (2006) 609.
8. A. F. Littke, G. C. Fu, *J. Am. Chem. Soc.* 123 (2001), 6989.
9. X. Gai, R. Grigg, M. I. Ramzan, V. Sridharan, S. Collard, and J. E. Muir, *Chem. Commun.* (2000) 2053.
10. M. Dai, B. Liang, C. Wang, J. Chen, and Z. Yang, *Org. Lett.* 6 (2004) 221.
11. J.Y. Lee, P. Y. Cheng, Y. H. Tsai, G. R. Lin, S. P. Liu, M. H. Sie, and H. M. Lee, *Organometallics*, 29 (2010) 3901.
12. L. Djakovitch, and K. Koehler, *J. Am. Chem. Soc.* 123 (2001) 5990.
13. A. Kollhofer, and H. Plenio, *Chem. A Eur. J.* 9 (2003) 1416.
14. L. H. Du, and Y. G. Wang, *Syn. Commun.* 37 (2007) 217.
15. J. Tian, K. D. Moeller, *Org. Lett.* 7 (2005) 5381.
17. M. F. Lengke, M. E. Fleet, G. Southam, *Langmuir*, 23 (2007) 8982.
18. M. Narayana, J. Michalik, S. Contarini, L. Kevan, *J. Phys. Chem.* 89 (1985) 3895.

	<p>Dr. Sudhir S. Arbu is Working as Senior Scientific Assistant at Centre for Materials for Electronics Technology (C-MET), Pune. He completed his Ph. D degree in Photocatalysis from the University of Pune in the year 2012 under the BARC- University of Pune, collaborative research program. His area or research is Nanomaterial synthesis, Photocatalysis, Hybrid solar cells etc. Recently, Dr. Sudhir is involved in the fabrication of Hybrid Solar Cells using synthesized metal sulphide nanostructures and organic conducting polymers. He has published 22 research papers in international journals.</p>
	<p>Dr (Ms) Bina Wani is working as a Scientific Officer at Chemistry Division, Bhabha Atomic Research Center (BARC). She obtained her M. Sc. degree from Bombay University in the year 1982 and awarded Ph. D degree in Chemistry in the year 1986 from the same University. Her research interest lies in the development of various cell components in Solid Oxide Fuel Cell at intermediate temperature (IT-SOFC). Recently she is involved in exploring various materials used in proton conducting SOFCs. She is also involved in developing mixed oxide based catalyst for pollution abatement. She has 66 publications in a various reputed international journals to her credit. She is a recipient of DAE Group Achievement Award 2010.</p>
	<p>Dr. Uttam Mulik received his PhD degree from National Chemical Laboratory (NCL), Pune, (Shivaji University) for Polymer Chemistry in 1982 and joined Centre for Materials for Electronics Technology (C-MET), Pune since 1993. From 1984 to 1993 he worked as an Assistant Manager (R&D) at Goodlass Nerolac Paints Ltd, Mumbai and Incab Industries, Mumbai, respectively. Currently, he is the Director of C-MET, Pune Laboratory. His current research concentrates on the synthesis and fabrication of photosensitive pastes, polymer nano-composites and materials for renewable energy. He has published more than 70 papers in international journals and holds 15 patents. He has received 9 awards in various national and international conferences.</p>

Modeling of Materials for H-Economy using DFT: Implications toward Nano-Catalysis

Chiranjib Majumder*, Seemita Banerjee and Sandeep Nigam

Chemistry Division, Bhabha Atomic Research Centre, Trombay, Mumbai 400 094,

E-mail: chimaju@barc.gov.in

Abstract

The term 'hydrogen economy' is a system of delivering energy using hydrogen. The primary objective behind this concept is to avoid the ill effects of current hydrocarbon economy. In hydrogen economy three steps are involved; (i) production of hydrogen (ii) storage of hydrogen and (iii) transportation of hydrogen. Here we present a brief summary of our recent work on the modeling of a catalyst using density functional theory in combination with molecular dynamics simulation. The primary focus of these studies is to predict advanced nano-catalyst materials for the generation and storage of hydrogen.

1. Introduction

Density functional theory is an extremely successful approach for the description of ground state properties of metals, semiconductors, and insulators [1-4]. The success of density functional theory (DFT) not only encompasses standard bulk materials but also complex materials such as bio-molecules and nano-materials [3-4]. All calculations have been carried out using the plane wave based pseudo-potential approach. While the total energy calculations were carried out under the DFT formalism [5-8], the geometrical search to locate the lowest energy structures has been carried out employing simulation tools [9-10]. The details of the theoretical techniques can be found elsewhere [11-13].

In this article we provide an overview of the key concepts and recent developments in computational modeling of complex materials with a focus on applications in the field of catalytic materials. Catalysts accelerate and boost thousands of different chemical reactions, and thereby form the basis for the multibillion dollar chemical industry worldwide. Research in nanotechnology and nanoscience is expected to have a great impact on the development of new catalysts. Thus, a detailed understanding of chemistry of nanostructures and the ability to control materials on the nanometer scale will ensure a rational and cost-efficient development of new and more capable catalysts for chemical production.

2. Designing of Catalyst for Hydrogen production

Thermochemical cycles have the greatest prospect for hydrogen production from water in the large scale. In this process water is decomposed into hydrogen and oxygen at a much lower temperature in comparison to direct thermal decomposition. Recently, the sulfur-iodine (S-I) thermochemical cycle for water splitting has attracted increasing attention because it can be efficiently used for mass scale production of hydrogen without CO₂ emissions.

The S-I cycle consists of three steps. In the first step H₂O reacts with I₂ and SO₂ to generate H₂SO₄ and HI. In the second step, the H₂SO₄ is thermally decomposed to SO₃ followed by further decomposition of SO₃ into O₂ and SO₂. This SO₂ is recycled back for use in the first step. In the third step H₂ and I₂ are produced through the catalytic decomposition of HI. Among all these reactions the decomposition of H₂SO₄ is the most energy demanding. In particular, the second part of the H₂SO₄ decomposition, where SO₃ is decomposed into SO₂ and O₂ requires very high temperature (between 750 and 900 °C) and does not occur without a catalyst [13-15].

Previously, various oxides of Si, Al, Zn, Cu, Fe, Ni, Co, Mn, Cr, V, and Ti have been employed as catalyst for this purpose [16]. But metal oxide based catalyst have problems of sulfate formation, and surface area modification. In another approach, noble metal particles supported on metal oxide support has been used. Ginosar et al. has reported the stability of various catalysts i.e. Pt/ZrO₂, Pt/Al₂O₃, and Pt/TiO₂ for sulfuric acid decomposition [17]. With a view to design a nanocatalyst for SO₃ decomposition, a comparative study of the SO₃ interaction with three tetramer clusters (Ag₄, Pd₄, and Ag₂Pd₂) deposited on the alumina surface was carried out. Previous studies of Ag₄, Pd₄, and Ag₂Pd₂ clusters deposited on the alumina surface [12] revealed that after deposition all three clusters favor bent rhombus geometry on the alumina surface. The lowest energy structures are presented in Fig.1. It was found that for all deposited clusters the interaction of the SO₃ molecule undergoes via metal-oxygen bond formation. Other configurations with metal-sulfur connections are found to be higher in energy. It may be noted that the situation is different when we consider the interaction of SO₃ molecules with gas phase metal clusters, where Pd₄ and Ag₂Pd₂ clusters bind with SO₃ through metal-sulfur bonds. Moreover, for both deposited and gas phase clusters,

the elongation of the S–O bond is greater for the isomers where the SO_3 molecule is connected to the metal clusters through metal–oxygen bonds. In this context it is worth mentioning that even though Ag_4 , Pd_4 , and Ag_2Pd_2 clusters form similar bent rhombus geometries on the alumina surface and the interface geometry between the SO_3 and the alumina surface is similar in all three cases (via three metal–oxygen bonds), the amount of S–O bond elongation is different. For the interaction of SO_3 with $\text{Ag}_4@Al_2O_3$, $\text{Pd}_4@Al_2O_3$, and $\text{Ag}_2\text{Pd}_2@Al_2O_3$, it was found that the S–O bond elongates up to 1.52, 1.54, and 1.64 Å, respectively. We note that the S–O bond length of 1.64 Å is 14% more than the corresponding gas phase values. Further it is noticed that, for configurations with metal–oxygen bonds, the M–M bond of the M_4 cluster becomes longer or weaker than the situation where the SO_3 molecule connects through a metal–sulfur bond [13].

In Fig. 2 we have presented the isosurface density of the top oxygen layer of the Al_2O_3 surface in different systems. Red represents the maximum electron density, and it systematically decreases as the color changes from red to blue in the spectrum. It is seen that the electron density is symmetrically distributed around O atoms (represented by dark red color) in the case of the clean $Al_2O_3(0001)$ surface. However, after deposition of an M_4 cluster, the charge distribution in the nearby region of some of O atom is different, where the charge density is found to decrease (displaying a brown or yellow color). From Fig. 2 it is clear

that deposition of Pd_4 on the surface leads to maximum removal of charge from the surface. This observation is in line with the results of Bader analysis, which shows a maximum charge on the Pd_4 cluster deposited on alumina. It is also apparent from Figure 2 that interaction of SO_3 with the $M_4@Al_2O_3$ complex leads to further reduction of charge from the alumina surface and the reduction is highest for the $\text{SO}_3\text{-Ag}_2\text{Pd}_2@Al_2O_3$ system. Thus it can be inferred that the alumina surface also transfers finite charge to SO_3 via the M_4 cluster and the amount of charge transfer is maximum for the $\text{Ag}_2\text{Pd}_2@Al_2O_3$ complex.

On the basis of these results it can be inferred that substrate plays a very important role in the elongation of S–O bonds of the SO_3 molecule. Interaction of SO_3 with the $M_4@Al_2O_3$ complex results in removal of charge from the M_4 clusters. As more electropositive nature is generated at the M_4 cluster site, it prompts the tetramer cluster to move toward the oxide surface. Hence, it could extract relatively more charge from the surface and further transfer it to SO_3 and in turn elongate the S–O bond to the maximum extent. In terms of the Pauling electronegativity scale, Pd is more electronegative than Ag. Upon deposition on the Al_2O_3 surface, Pd_4 takes more charge from the surface than Ag_4 . On the other hand, in the gas phase Ag_4 can donate more charge to SO_3 by Ag–O bond formation. As the Ag_2Pd_2 cluster is a bimetallic cluster, the difference in electronegativity of Ag and Pd atoms results in a relatively polar metal–metal bond. Therefore, when bimetallic

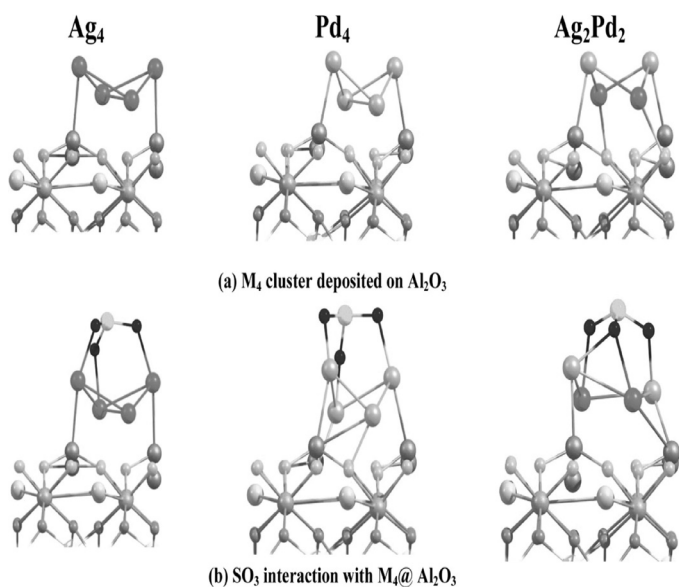


Fig.1 (a) Ground state geometries of M_4 cluster after deposition on Al_2O_3 surface. (b) Lowest energy structures of SO_3 molecule interacting with $M_4@Al_2O_3$ complex.

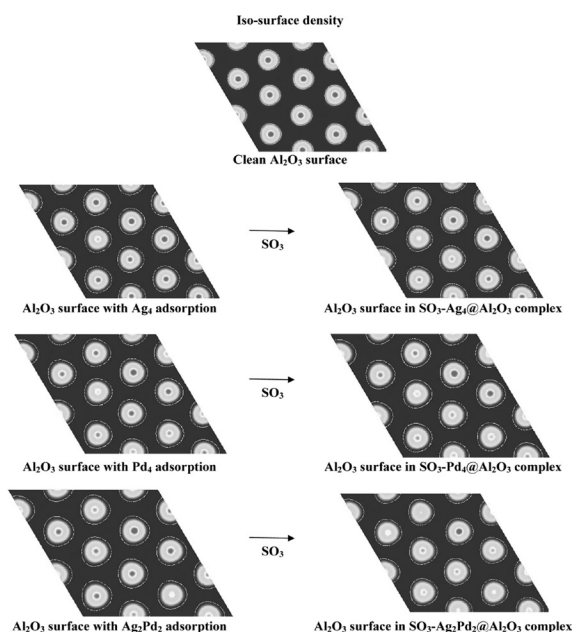


Fig. 2 Iso-surface density of top oxygen layer of Al_2O_3 surface in different systems. The electronic charge increases from blue to red in the spectrum.

Ag_2Pd_2 cluster is deposited on the Al_2O_3 surface, while Pd extracts more charge from the surface, Ag can donate more charge to SO_3 . This combination of efficient acceptor and donor makes $\text{Ag}_2\text{Pd}_2@/\text{Al}_2\text{O}_3$ complex a better catalyst for weakening the S–O bond in the SO_3 molecule.

Significantly, the polarity of the Ag–Pd bond of the $\text{Ag}_2\text{Pd}_2@/\text{Al}_2\text{O}_3$ complex also allows the interaction with S–O bonds in three asymmetrical manners. However, for the homoatomic cluster, the bond elongation is almost symmetric. Especially for the gas phase Ag_4 cluster, the bond elongation of the SO_3 molecule is totally symmetric. Thus maximum and asymmetric charge transfer by the $\text{Ag}_2\text{Pd}_2@/\text{Al}_2\text{O}_3$ complex to SO_3 leads to maximum elongation of one of the S–O bonds to 1.64 Å. As the bond elongation bears the signature of bond weakening, a comparison of the above three results clearly suggests that the dissociation barrier of the S–O bond will be significantly lower on the $\text{Ag}_2\text{Pd}_2@/\text{Al}_2\text{O}_3$ support than that on $\text{Ag}_4@/\text{Al}_2\text{O}_3$ or $\text{Pd}_4@/\text{Al}_2\text{O}_3$. Thus, it is expected that Ag–Pd bimetallic nanoparticles deposited on alumina will reduce the dissociation barrier for SO_3 .

3. Role of Catalyst for Hydrogen Storage

Hydrogen is a clean energy carrier for various applications. However, due to its low energy density, it is difficult to store in a small container leading to additional difficulty in transport. The search of new materials for efficient storage of hydrogen has been the focus of intensive research for the past decade. This poses a serious challenge because a good hydrogen storage materials must meet simultaneously six requirements; (i) high gravimetric (>4.5 wt. %) and volumetric (> 36g H_2/L) densities, (ii) operation temperature approximately in the range 60 – 120°C, (iii) reversibility of the thermal absorption/desorption cycle. (iv) low cost, (v) low-toxicity, (vi) safety requirements, (vii) good cyclic stability. To the best of our knowledge, so far no material has been reported which satisfies all these criteria. There are different candidate materials for solid state hydrogen storage [18-24]. The most conventional and practical one is metal hydride, where different transition metal based and light weight alloys are being considered. Transition metal based alloys are quite promising for their good hydrogen absorption desorption kinetics and favorable thermodynamics whereas light metal alloys shows higher hydrogen absorption capacity but unfavorable kinetics and thermodynamics. Other exclusively studied hydrogen storage materials include metal organic framework, carbon nanostructures etc. Metal organic frameworks (MOF) can absorb hydrogen by physisorption, but it requires operating at cryogenic condition. Carbon nano structures are one of the most

promising solid-state materials for hydrogen storage because of its porosity, high surface area and high gravimetric hydrogen storage properties. Nanotubes, nano scrolls, nano fibers, fullerenes and graphene sheets are among the different well studied structures. In the following section, an attempt has been made to briefly describe the hydrogen storage behavior in various systems, with special emphasis on Mg and C based systems. Here we will describe the role of catalyst for the improvement of hydrogen storage behavior, ranging from 3D bulk, 2D layered structures, 1D tube and 0D small clusters.

3.1 Hydrogen Storage in Mg based systems

The hydrogen storage in the metallic form is the safest method known today and it poses many advantages also. Light metal hydrides, including Li, Al and Mg, are considered to be potential in the vehicular application due to high gravimetric hydrogen storage capacities. Mg can form MgH_2 with a maximum hydrogen storage capacity of 7.6 wt. %. Furthermore, magnesium is cheap and its ore is abundantly available. However, the high thermal stability of magnesium hydride and slow kinetics for hydrogen absorption – desorption are major limitations for its practical application [25-27]. Many experimental and theoretical works have been done to improve the efficiency of Mg metal to meet the stringent criteria for hydrogen storage [28]. One of these attempts is to dope Mg with transition-metal elements. Transition metal atoms act as catalyst on the Mg surface and can greatly reduce the activation barrier for dissociation and diffusion processes of hydrogen. From the first principle calculations, it has been found that dopant atom (M) prefer to substitute

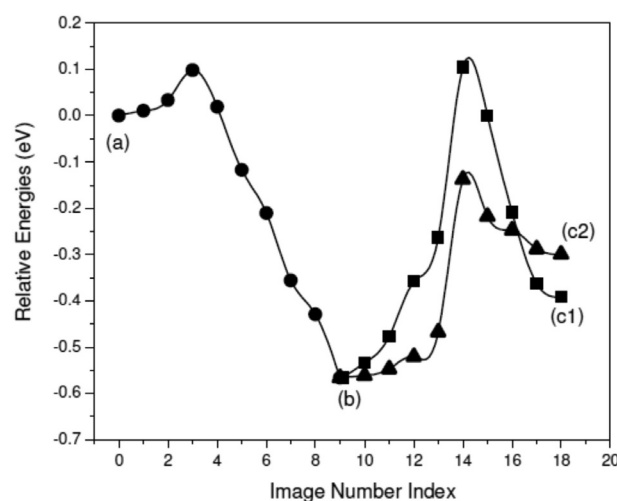


Fig.3 NEB profiles for the dissociation and diffusion of hydrogen on the Mg_{55}VNi surface when Ni atom is at the first layer and V atom is at the second layer. The relative energies of the initial state, after dissociation of hydrogen molecule on the surface, and after diffusion of hydrogen atoms on the surface are marked by (a), (b) and (c), respectively.

one of the Mg atoms from the second layer. In this case the dissociation of the hydrogen molecule is controlled by a high activation barrier. In case two M atoms were doped, the equilibrium geometry shows one M at the top and the other in the subsurface [29]. The most effective hydrogenation behavior was found when both V and Ni were substituted into the Mg surface [Fig. 3]. Another way to improve the efficiency of Mg is to reduce the particle size, where defects, large surface areas, and small diffusion path length help to improve the thermodynamics and kinetics of the sorption processes. To understand the finite size effect, we have also calculated the hydrogen interactions with Mg clusters. Results showed 40 % reduction in the dissociation barrier of hydrogen adsorption on the Ti doped Mg_{55} cluster [30].

3.2 Hydrogen Storage in C based or similar systems

Storage of hydrogen in molecular form is advantageous due to its fast kinetics as well as low binding energy that could lead to the possibility of desorption of hydrogen molecule at low temperature. In the past decades, more and more attention has been focused on the carbon-based nanostructure materials, such as carbon nanotubes (CNTs), fullerenes and graphenes. However, these materials have practical limitations as the desorption temperature of hydrogen is very low and therefore difficult to store hydrogen at ambient conditions. In contrast, the introduction of transition metal (TM) to the pure carbon nanomaterials has been proposed to enhance the hydrogen-uptake capacity and the adsorption energy [31,32]. It was reported that a single Ti atom adsorbed on (8, 0) single-wall carbon nanotube can adsorb up to four hydrogen molecules by formation of Kubas complex, reaching to gravimetric storage capacity of ~8 wt%. Clearly, the hydrogen storage capacity is fundamentally proportional to the specific surface area and the number of dispersed metal atoms. Again the transition metal atoms can act as catalyst for the dissociation of hydrogen molecule towards hydrogen atom thus hydrogen atoms can get chemically adsorbed on carbon the carbon based systems by spillover mechanism. Apart from carbon based materials, several other iso-electronic systems like BN and SiC nanostructures have been explored to understand the hydrogen storage capacity [33-35]. In general, all these dielectric compounds are inert towards hydrogen or interacts very weakly. The primary force of interaction is the electrostatic interaction. The decoration of transition metal atoms on these nanostructures (as shown in Fig. 4) definitely improves the adsorption behavior and storage capacity but due to strong cohesive energy the transition metal atoms prefer to agglomerate on the surface and thereby limits for high

capacity storage material [36].

Unlike transition metal decorated carbon fullerene, which suffers from the metal clustering, metallocarbohedrenes are stable systems with transition metal atoms as part of the carbon nanostructures. The hydrogen storage properties of selected metallo-carbohedrene (M_8C_{12} , $M = Sc, Ti, V$) have been compared. The results revealed that when the $M = Ti$, the cluster can take up total 16 hydrogen

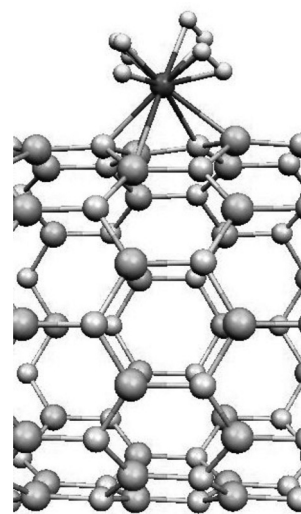


Fig.4 The optimized geometry of Ti doped SiC nanotube when it interacts with four hydrogen molecules.

molecule by physisorption where the hydrogen molecules gets absorbed reversibly on the Ti atoms. Each C atom can bind one hydrogen atom by chemisorption. Though the total hydrogen storage capacity found to be 15.06 wt% but the reversible capacity is 10.96 wt%. In case of Sc_8C_{12} the total hydrogen storage capacity is much higher (20%), as it can adsorb 30 hydrogen molecules by physisorption. The results show that the interaction energy of the hydrogen molecules with cluster is lower compared to the Ti_8C_{12} cluster. For V_8C_{12} the hydrogen storage capacity decreases and the total hydrogen storage capacity found to be 12.33 wt% only [37].

One important factor for a good hydrogen storage material is the desorption profile of the absorbed hydrogen. In fact, to be a good hydrogen storage material, not only desorption kinetics should be fast enough, but also the material should be stable at higher temperature. In this context we have checked the thermal stability and desorption behaviour of Ti_8C_{12} cluster by the *ab-initio* molecular dynamics simulation using Nöse algorithm. To start with, the hydrogenated Ti_8C_{12} cluster ($Ti_8C_{12}, 16H_2$) is heated at different temperatures (100 K, 150 K, 200 K, 300 K and 500 K) followed by equilibration for 7000 steps with 1 fs time scale. The results [Fig. 5] reveal that while at 100 K, and 200 K, one, and three hydrogen molecules are evaporated, respectively, at 300 K four hydrogen molecules are desorbed. Most importantly, above 300 K, the hydrogen molecules tend to dissociate and attach with the nearest C atoms via spillover mechanism. Finally at 400 K, the hydrogen spillover towards the C atom occurs spontaneously which leads to the formation of $Ti_8C_{12}H_{12}$ cluster, where 12 hydrogen atoms are chemisorbed with C atoms. In other words, if we cool the $Ti_8C_{12}H_{12}$ cluster

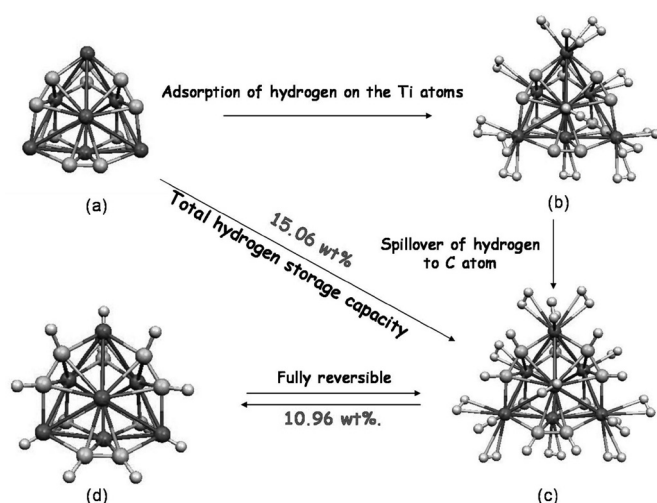


Fig. 5 A schematic representation of the hydrogen adsorption-desorption process in the Ti_8C_{12} cluster.

and keep in hydrogen atmosphere, it can take up 16 H_2 molecules giving rise to $[Ti_8C_{12}H_{12}, 16H_2]$ complex, with total hydrogen storage capacity of 15.06 wt. % for Ti_8C_{12} . However, previous calculations suggest that H atoms are bonded with C atoms via a strong covalent bond. Therefore, desorption of these chemisorbed H atoms are difficult and needs very high temperature. In this situation, the $Ti_8C_{12}H_{12}$ complex can be considered as a host material, which can absorb and desorb 16 molecular hydrogens, leading to 10.96 wt. % of reversible hydrogen storage capacity.

4. Conclusion




In summary, we have attempted to illustrate how density functional theory calculations can be utilized to develop a detailed molecular-level picture of catalytic materials. In particular, we have emphasized the modeling of materials for use in the field of hydrogen economy. Through this brief review we have demonstrated that theoretical modeling provides new insight that can play a significant role in the design of advanced materials. Moreover, DFT opens exciting prospects for the discovery of new catalysts, a learned alternative to blind search. There is a long way to go before we have a general theoretical description of heterogeneous catalysis. Catalysts are complicated, multiphase materials, and there are an enormous number of interesting catalytic processes. We are just at the beginning of an era where DFT calculations contribute a new perspective to the many important experimental tools that have been developed to understand surface reactivity.

References

1. P. Hohenburg and W. Kohn, *Phys. Rev.* **136** B864 (1964)

2. W. Kohn and L. J. Sham, *Phys. Rev.* **140** A1133 (1965).
3. Parr, R. G.; Yang, W. (1989). *Density-Functional Theory of Atoms and Molecules*. New York: Oxford University Press.
4. N. H. March (ed.), *Electron Correlation in the Solid State*, ICP, London, (1999).
5. G. Kresse, J. Furthmuller, *Phys. Rev. B* **54**, 11169 (1996); *Comp. Mater. Sci.* **6**, 15 (1996); D. Vanderbilt, *Phys. Rev. B* **41**, 7892 (1990)
6. P. E. Blochl *Phys. Rev. B* **50** 17953(1994).
7. G. Kresse, D. Joubert *Phys. Rev. B* **59** 1758 (1999)
8. G. Kresse, J. Furthmüller, VASP the Guide. Available from <http://cms.mip.univie.ac.at/VASP>.
9. M.C. Payne, M.P. Teter, D.C. Allan, T.A. Arias, J.D. Joannopoulos *Rev. Modern Phys.*, **64** (1992), pp. 1046-1097.
10. M. P. Allen, D. J. Tildesley *Computer simulation of liquids*. Oxford University Press (1989).
11. S. Nigam, C. Majumder, *Int. J Hydrogen Energy* **37**(4), 3645-3651(2012).
12. S. Nigam, C. Majumder, *Chem. Phys. Lett.*, **537**, 69-74(2012).
13. S. Nigam, C. Majumder, *J. Phys. Chem. C*, **116**, 25594-25601(2012).
14. A. M. Banerjee, M. Pai, K. Bhattacharya, A. K. Tripathi, V. Kamble, S. Bharadwaj, S. K. Kulshreshtha, *Int J Hydrogen Energy*, **33**(1), 319-326(2008).
15. A. M. Banerjee, M. Pai, S. S. Meena, A. K. Tripathi, V. Kamble, S. Bharadwaj, *Int J Hydrogen Energy* **36**(8), 4768-4780(2011)
16. M. Dokiya, T. Kameyama, K. Fukuda, Y. Kotera. *Bull chem soc Jpn* **50**(10), 2657(1977)
17. D. M. Ginosar, R. P. Anderson, A. W. Glenn, AIChE Spring Meeting, Conference Proceedings, Cincinnati, OH, October 30-November 4, (2005).
18. A. Zuttel, P. Sudan, Ph. Mauron, T. Kiyobayashi, Ch. Emmenegger, L. Schlabach. *Int J Hydrogen Energy* **27** 203 (2002).
19. L. Zaluski, A. Zaluska, J. O. Ström-Olsen, *J Alloys Compds.* **253-254** 70 (1997).
20. Asheesh Kumar, K. Shashikala, Seemita Banerjee, J Nuwad, Priyanka Das, C. G. S. Pillai, *Int J Hydrogen Energy*, **37** 3677 (2012).
21. G. Sandrock, K. Gross, G. Thomas, *J Alloys Compds.* **339** 299 (2002).
22. Seemita Basak, K. Shashikala, S.K. Kulshreshtha, *Int J Hydrogen Energy*, **33** 350, (2008).
23. S. J. Yang, J. H. Cho, K. S. Nahm, C. R. Park, *Int J Hydrogen Energy* **35** 13062 (2010).
24. B. Sakintuna, L. D. Farida, H. Michael. *Int J Hydrogen Energy* **32** 1121 (2007).
25. A. Zaluska, L. Zaluski, and J. O. Strob-Olsen, *Appl. Phys. A: Mater. Sci. Process.* **72** 157 (2001).
26. M. Tsuda, W. A. Dinō, H. Nakanishi, and H. Kasai, *J. Phys. Soc. Jpn.* **73** 2628 (2004).
27. Y. Fukai, *The Metal-Hydrogen System: Basic Bulk Properties*

- (Springer- Verlag, Berlin, 1993).
28. Seemita Banerjee, C. G. S. Pillai, and C. Majumder, *Journal of Chemical Physics* **129** 174703 (2008).
 29. Seemita Banerjee, C. G. S. Pillai, and C. Majumder, *Journal of Physical Chemistry C* **113** 10574, (2009).
 30. Seemita Banerjee, C. G. S. Pillai, C. Majumder, *Int J Hydrogen Energy* **35** 2344, (2010).
 31. E. Durgun, S. Ciraci, W. Zhou, and T. Yildirim, *Physical Review Letters*, **97** 226102 (2006).
 32. Y. Yürüm, A. Taralp, T. Nejat Veziroglu, *International Journal of Hydrogen Energy*, **34** 3784 (2009).
 33. S. Banerjee, Sandeep Nigam, C. G. S. Pillai, C. Majumder, *Int J Hydrogen Energy*, **37** 3733, (2012).
 34. Seemita Banerjee, C. G. S. Pillai, C. Majumder, *Int J Hydrogen Energy* **36** 4976, (2011).
 35. S. Bhattacharya, C. Majumder, G. P. Das, *Journal of Physical Chemistry C*, **112**, 17487 (2008).
 36. Q. Sun, Q. Wang, P. Jena, Y. Kawazoe, *Journal of the American Chemical Society*, **127** 14582 (2005).
 37. Seemita Banerjee, C. G. S. Pillai, C. Majumder, *Applied Physics Letters*, **102** 073901 (2013).

	<p>Dr. Chiranjib Majumder joined Chemistry Division, Bhabha Atomic Research Centre as a scientific officer in 1992 after graduating through 35th batch of training school of BARC. He received his Ph.D. degree in 2000. His current research interest is to design novel materials for catalysis by tuning the electronic properties of nano-materials and to underscore the mechanism of cluster-molecule interactions on a support matrix.</p>
	<p>Dr. Seemita Banerjee joined Chemistry Division, Bhabha Atomic Research Centre as a scientific officer in 2005 after graduating through 48th batch of training school of BARC. She has completed her Ph.D in Chemistry from Homi Bhabha National Institute, India in 2013. The contributions of Dr. Banerjee are a combination of applied and fundamental aspects of Hydrogen Storage, Solid state chemistry and Materials science. Her research areas of interest are: Metal hydrides, Mesoporous material, Carbon based materials. Apart from the experiment she is also working on Density Functional Theory for designing advanced materials.</p>
	<p>Dr. Sandeep Nigam joined Bhabha Atomic Research Centre as a scientific officer in 2003 after graduating through 46th batch of training School of BARC. Since then he has been actively involved in the field of cluster science. He was awarded Ph. D. degree from Mumbai University in year 2008 for his theoretical work on pure and mixed clusters. At present he is working on theoretical studies of noble metal cluster deposited on oxide surfaces and their catalytic behavior. He is also contributing in chemical synthesis of mixed oxide nano-particles and their luminescence studies.</p>

Development of Catalysts for Various Applications Related to DAE Programs

Shyamala R. Bharadwaj

Fuel Cell Materials and Catalysis Section, Chemistry Division, BARC, Mumbai.

*Email: shyamala@barc.gov.in

Abstract

Catalytic reactions play a foremost role in majority of industrial chemical processes. As an estimate, about 90% of all chemical reactions in industries rely on catalysts. Fuel Cell Materials and Catalysis Section (FCMCS) of Chemistry Division has made significant contributions in the area of catalysis and developed several catalysts for various applications related to DAE programs. Notable among these are (i) development of catalysts for sulfuric acid decomposition and HI decomposition reactions, and (ii) catalysts for mitigation of hydrogen in nuclear power plants under severe accident conditions. In addition, rich contributions were made to the fundamental research in these areas of technological importance viz. studies on photocatalysts for generation of hydrogen by water splitting and photocatalysts for VOC abatement and pollution control. This article gives a brief overview of the catalysis development program with respect to the above mentioned activities.

1. Introduction

Heterogeneous catalysts are extensively used in chemical industries for reactions such as cracking, dehydrogenation, hydrogenation, oxidation, reduction, decomposition, molecular rearrangement, fermentation etc. The main focus of FCMCS is to develop catalysts for various applications related to the Department of Atomic Energy.

In recent past, studies on Sulfur-Iodine (S-I) cycle for large scale nuclear hydrogen generation have been started at BARC in view of availability of high-grade heat from the proposed Compact High Temperature Reactor (CHTR). FCMCS developed catalysts for the sulfuric acid and hydriodic acid decomposition reactions involved in the Sulfur-Iodine cycle for hydrogen generation.

With regard to safe operation of nuclear plants, hydrogen generated under LOCA conditions poses a major threat. The two major nuclear accidents of Three Miles Island (TMI) and Fukushima incident emphasize the hydrogen risk in nuclear power plants. Use of catalysts has been proposed to be one of the alternatives to mitigate this hydrogen. Hence, extensive studies on development of catalysts for hydrogen mitigation were undertaken.

The conversion of solar energy into hydrogen via semiconductor assisted photocatalytic splitting of water, is one of the most promising technologies for clean and sustainable energy solutions. Members of FCMCS have explored various catalysts for this purpose and also for the utilization of solar energy for environmental remediation like VOC's elimination and dye degradation using suitable semiconductor photocatalysts.

2. Development of catalysts for decomposition of sulfuric acid

With an aim to develop non-noble metal catalysts which are both active and stable, various oxides/mixed oxides and ferrites (MFe_2O_4 ; $M = Co, Ni, Cu$) [1, 2] were prepared via different routes like solid state, precipitation/co-precipitation gel-combustion etc. Their performance as catalysts for the decomposition of sulfuric acid was evaluated and compared with that of commercial Pt/ Al_2O_3 catalyst, in temperature range of 600-850°C. Textural and structural characterization of both synthesized and spent catalysts was carried out employing various techniques such as XRD, IR, SEM/EDX, TEM, XPS, N_2 -BET Surface area, etc. Characterization of fresh and spent catalysts along with thermal decomposition experiments enabled us to propose a plausible mechanism for decomposition of sulfuric acid over these oxides/ferrites which involved the formation and decomposition of metal sulfate, with the metal sulfate decomposition step playing the most crucial role in determining the reaction kinetics. To study the catalytic decomposition of sulphuric acid in temperature range of 600 – 850°C over powder and granular samples, two glass setups were indigenously designed and developed in Chemistry division as shown in Fig. 1.

The performance of Fe_2O_3 , $Fe_{1.8}Cr_{0.2}O_3$ and Pt/ Al_2O_3 catalysts in granular form was evaluated for decomposition of sulfuric acid (98 wt %) as a function of time (100 h at 800°C, acid flux of ~0.6 ml/min), temperature (650-825 °C, acid flux of ~0.6 ml/min) and flux of sulfuric acid (0.2-10 ml/min). The SO_2 yield was found to be ~~remained~~ close to the equilibrium thermodynamic yield value (~ 80 % at

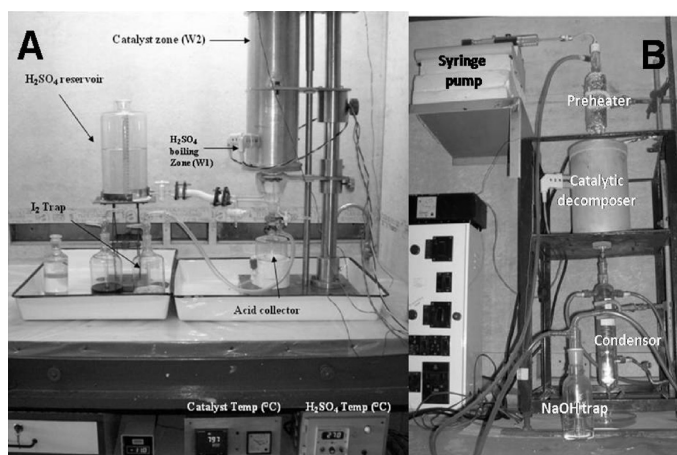


Fig. 1: Experimental set-up in quartz to carry out sulfuric acid decomposition (A) granular catalyst (20 g) and (B) powder catalyst (0.2 g).

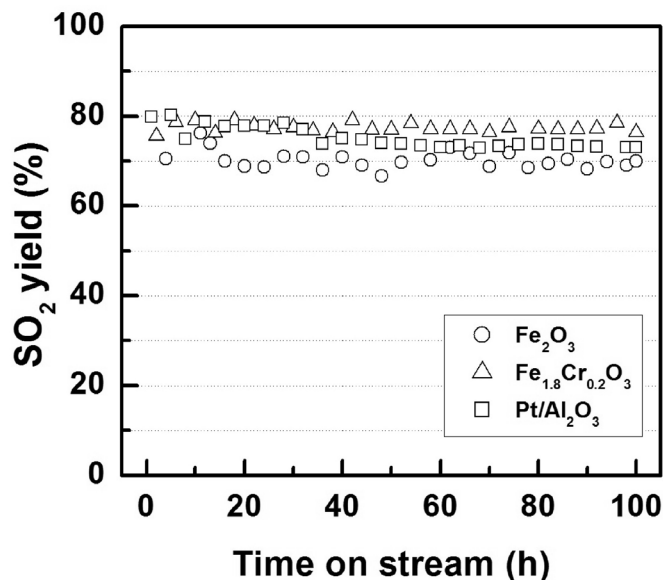


Fig. 2: Prolonged performance of Fe₂O₃, Fe_{1.8}Cr_{0.2}O₃ and Pt/Al₂O₃ catalysts for sulfuric acid (acid flux: ~ 0.6ml min⁻¹) decomposition during 100 h run at 800 °C (20 g granular catalyst in 2.5 cm column; see setup (Fig. 1 A).

800°C). Chromium substituted iron oxide and Pt/Al₂O₃ catalysts exhibited almost similar SO₂ conversions at 800 °C which was slightly higher than the unsubstituted Fe₂O₃. No deterioration in the catalyst performance was observed for the oxide samples during 100 h run, as shown in Fig. 2. Commercially available Pt/Al₂O₃ catalyst works out to be 16 times costlier than iron based catalysts.

On the basis of the overall results obtained from our studies we recommended the Fe_{1.8}Cr_{0.2}O₃ catalyst for use in the laboratory scale Sulfur-Iodine demonstration facility at Chemical Technology Division (ChTD), BARC.

3. Development of porous Pt/Carbon catalyst for HI decomposition

Different Pt-Carbon catalysts based on high surface area carbon supports have been developed using mesoporous and microporous silica templates and have been employed for HI decomposition step of Sulphur - Iodine thermochemical cycle [3]. In this preparation route, carbon precursor like sucrose is impregnated into mesoporous silica template like MCM-41 and SBA-15 and microporous silica template like fumed silica and carbonized by heating at 800 °C, under nitrogen flow. The silica template is removed by hydrofluoric acid to generate porous carbon replica. Platinum has been incorporated in these carbon supports either at initial stage along with sucrose to form a part of carbon framework or by direct impregnation on prepared carbon. Liquid phase HI decomposition at 160 °C has been carried out and conversion upto 17% have been obtained in 2 hrs studies. The effluent analysis depicts insignificant noble metal leaching. The efficiencies of these materials for HI decomposition reaction have been found to be dependent on the structural nature of the porous carbon and their surface morphologies. We have concluded that mesoporous Pt/carbon has higher catalytic activity and stability than microporous Pt/carbon catalysts.

4. Development of catalyst for hydrogen mitigation application

A large amount of hydrogen is generated in nuclear reactor during LOCA conditions. This can be a threat to containment integrity if detonable limit is crossed. Passive autocatalytic recombiner is one of the most feasible remedies for this. New classes of mixed noble metal catalysts, viz Pt + Pd on stainless steel wire gauze have been developed for this purpose [4]. The activity includes development of a novel procedure for preparation of mixed noble metal (platinum-palladium) catalysts by electroless deposition from a single bath containing precursors of both the noble metals and a reducing agent. Evaluation of the deposition steps by SEM-EDAX techniques has clearly indicated that initial nucleation occurs through platinum deposition followed by simultaneous platinum-palladium deposition. These catalysts have been evaluated for their catalytic activity for H₂-O₂ recombination reaction under static air condition, in a 40 litre reactor, in absence and presence of various poisons like carbon dioxide, methane, carbon monoxide and water. The catalytic activity has been found to remain unaffected by the presence of above mentioned poisons. Fig. 3 depicts the change in hydrogen concentration and the catalyst surface temperature with time on these catalysts for H₂+O₂ recombination reaction, for different initial concentration of hydrogen.

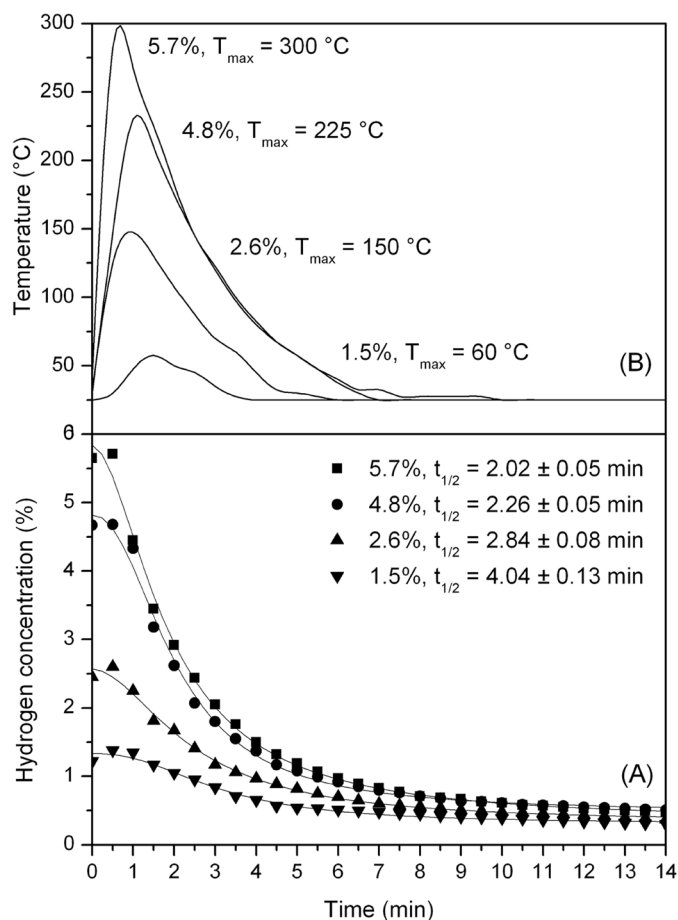


Fig. 3: $t_{1/2}$ and T_{max} for different initial hydrogen concentrations for Pt+Pd on Stainless Steel wire gauze catalyst.

Fig. 4 depicts various forms of supported noble metal based catalysts developed and evaluated for this purpose. Wire gauze supported catalysts have been shortlisted for user evaluation by NPCIL at Hydrogen Recombination Test Facility, Tarapur.

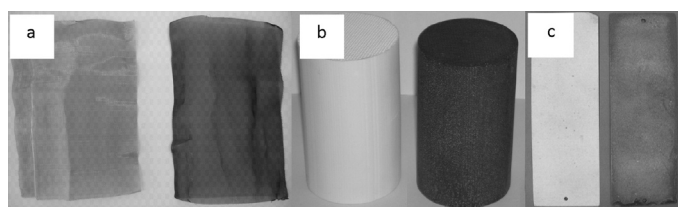


Fig. 4: Various catalysts developed for mitigation of hydrogen (a) noble metal on SS wire gauze, (b) noble metal on cordierite honeycomb and (c) Noble metal on cordierite plate.

5. Photocatalytic hydrogen generation from water using solar radiation

With a view to photocatalytic generation of hydrogen using solar type radiation, our group has focused on the development of suitable photocatalytic materials. A number of novel semiconductors have been developed for

this purpose and tested for their photocatalytic activity. A series of aliovalent and isovalent ions were substituted at A and B site in indium titanates, In_2TiO_5 ($A = Ni^{2+} / Nd^{3+}$; $B = Fe^{3+} / Cr^{3+}$), with an objective to modify their band gap and extend their photo response in visible light. Effect of metal ion substitution [5] and particle size [6] on band gap and photocatalytic activity of indium titanate has also been explored. TiO_2 based photocatalysts like self-doped $(Ti^{3+})TiO_2$ [7], Sn and Eu doped TiO_2 [8], In and N co-doped TiO_2 [9], TiO_2 on various oxides like ZrO_2 , Al_2O_3 , zeolite and CeO_2 [10] were evaluated to obtain catalyst particles with optimum surface area and crystallinity. Among these oxide catalysts, a composite of TiO_2 dispersed on ZrO_2 inert support exhibited the highest photocatalytic activity with a hydrogen generation rate of 1.1 L/h/m²/g using solar type radiation. Indium doped CdS dispersed on ZrO_2 was found to exhibit the better activity than oxide catalysts, with hydrogen generation rate of 3.9 L/h/m²/g.

Photocatalytic activity for hydrogen generation from water using TiO_2 and CdS based photocatalysts were studied. Doping was done to tune the bandgap and composites were made to improve the active surface area and to increase the lifetime of the photogenerated charge carriers. Typical systems studied and the photocatalyst, which showed the highest activity among each system, are shown in Fig. 5. The number given in bracket is the apparent quantum efficiency for that system. It can be seen that among TiO_2 system, TiO_2 - ZrO_2 composite with Pd as cocatalyst showed higher photocatalytic activity and among CdS based systems, CdS- TiO_2 - ZrO_2 composite with Pd co-catalyst showed higher activity. The enhanced activity is attributed to improved visible light absorption and increased lifetime of the photogenerated charge carriers in these systems [11-14].

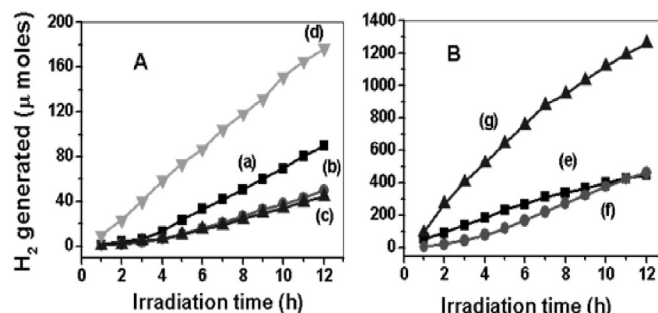


Fig. 5: Photocatalytic activity for hydrogen generation from water for (a) Pd (2%) - TiO_2 , (b) Pd (2%) - TiO_2 (SnO_2 2%), (c) Pd (2%) - $Ti_{0.98}In_{0.02}ON$, (d) Pd (0.15%) - TiO_2 (28 %) - ZrO_2 , (e) & (f) Pd (0.5%) - $Cd_{0.95}In_{0.05}S$ (20%) - ZrO_2 , (g) Pd (0.5%) - CdS (30%) - TiO_2 (30%) - ZrO_2 . Light source: Ordinary day light fluorescent lamps (288 W). Yield is normalized to 50 mg CdS for supported catalysts.

6. Titania based photocatalysts for abatement of air and water pollutants

Heterogeneous photocatalytic degradation of dyes from waste water and volatile organic compounds (VOCs) from polluted air has become a need of times, as the release of these effluents in the ecosystem forms a primary source of pollution affecting all the flora and fauna in its vicinity. Nano titania, doped titania [15-17], alkaline earth titanates [18] and supported titania [19] systems have been evaluated to understand the structure - activity correlation, influence of oxidation states of dopants, particle size, dopant - titania - support interaction and their physiochemical properties and catalytic activity of these materials. Photocatalytic oxidation of model VOCs like ethane, propene and methane in air and dye like methylene blue in water has been studied in detail. In this context, titania based heterogeneous photocatalysts stands-out to be best methodology that can be effectively exploited for the complete mineralization of various dye and VOC pollutants present in natural environment.

Photo-degradation of the dye Rhodamine -B was carried out with Mo-doped TiO₂ photocatalysts and nano TiO₂ samples. These samples were synthesised via sol-gel route and thoroughly characterised using techniques of XRD, TEM, DR-UV, XPS, Raman, FT-IR, EXAFS and XANES. The characterisation results suggest that apart from being Mo-doped TiO₂ anatase phase there is a definite percentage of Mo₂O₃ phase. There is definite red shift in the DR-UV spectra and the band gap study shows that as a function of the Mo-content in the lattice or composite the band gap lowers to the visible absorption. The results showed that under visible light irradiation as a function of Mo-doping the photocatalytic activity of

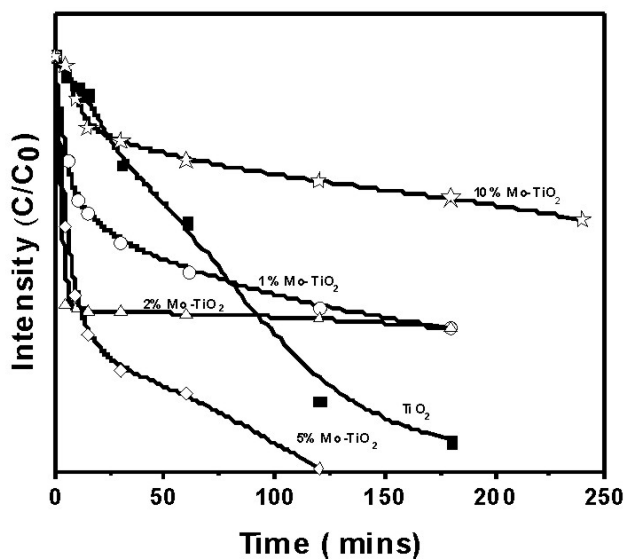


Fig. 6: Rhodamine -B Dye degradation

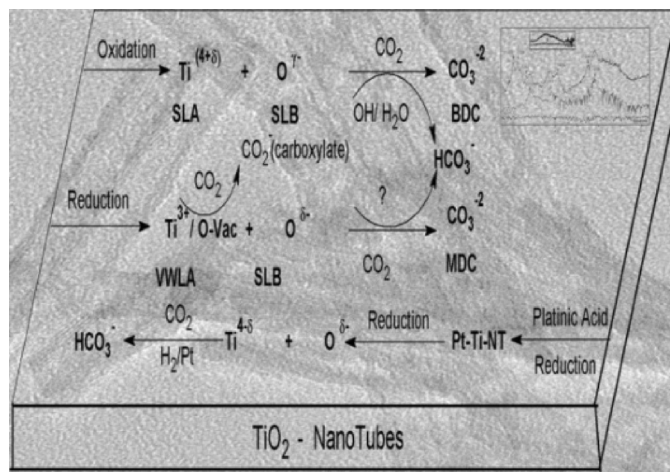


Fig. 7: The Reactive CO₂ adsorption mechanism in TiO₂ -Rates with different photocatalysts nanotubes upon oxidation, reduction of TiO₂ Nanotubes

the samples are as follows 1% <2% <5% > 10%. The Mo-doped TiO₂ samples has better photocatalytic activity as compared to the undoped. UV-vis spectra after different illumination times of a Rhodamine B solution with the nano-TiO₂ particles are shown in Fig. 6. The absence of the hypsochromic shift in the dye degradation profile using nano TiO₂ and doped nano TiO₂ shows the non existence of the de-ethylation channel as a major pathway for the complete degradation of the Rh-B dye. Since there are no additional peaks appearing in the UV-vis spectra in the course of the experiment using titania nano-particles, the dye is completely degraded and not only photobleached.

The reactive adsorption of CO₂ on oxidized, reduced, and platinized TiO₂ nanotubes (Ti-NTs) was studied using infrared spectroscopy. The XPS data demonstrate that upon oxidation, surface O atoms become more electronegative, producing sites that can be characterized as strong Lewis bases, and the corresponding Ti becomes more electropositive producing sites that can be characterized as strong Lewis acids. Reduction of the Ti-NTs produces Ti³⁺ species, a very weak Lewis acid, along with a splitting of the Ti⁴⁺ peak, representing two sites, which correlate with O sites with a corresponding change in oxidation state. Photo-induced reactions of surface species also take place and are remarkably different on the two types of nanotubes. UV illumination of Ti-NT-O₂-H₂ converts bidentate carbonates and bicarbonates to monodentate carbonates and carboxylates. There are less, and different, photo-induced reactions of surface species on Pt-Ti-NT-O₂-H₂: bicarbonates and monodentate carbonates convert to bidentate carbonates on the platinized titania nanotubes, and there is no obvious reaction involving carboxylates and formic acid upon irradiation of the platinized nanotubes.

7. Conclusion

The contributions of the catalysis research group of Chemistry Division, BARC are a combination of applied and fundamental aspects of heterogeneous catalysis. The group has contributed in the area of catalysis and developed several catalysts for various applications related to DAE programs. Notable among them are development of catalysts for (i) sulphuric acid and hydroiodic acid decomposition for Sulphur-Iodine thermochemical cycle, (ii) mitigation of hydrogen in nuclear reactor containment, (iii) production of hydrogen by photocatalytic splitting of water and photocatalytic abatement of volatile organic compounds. Various indigenous equipment's like *in situ* FTIR and EXAFS setups, quartz/glass reactor setups for sulphuric acid and hydroiodic acid decomposition, stainless steel reactor for hydrogen mitigation studies and photocatalytic reactor, have been designed and fabricated for accomplishment of above stated goals. In addition, rich contributions were made to the fundamental research in these areas of technological importance.

Acknowledgements

My colleagues from Fuel Cell Materials & Catalysis Section, A.P. Gaikwad, D. Tyagi, A.M. Banerjee, K. Bhattacharyya, S. Varma, M. R. Pai, R. Sasikala, A. K. Tripathi and Pune University Student Kiran Sanap have contributed immensely to the various activities discussed in this article. I thank all of them and I am confident that they will continue to contribute to the DAE programs in future as well.

References:

- Banerjee A. M., Pai M. R., Bhattacharya K., Tripathi A. K., Kamble V. S., Bharadwaj S. R., Kulshreshtha S. K., International Journal of Hydrogen Energy, 33 (2008) 319.
- Banerjee A. M., Pai M. R., Meena S. S., Tripathi A. K., Bharadwaj S. R., International Journal of Hydrogen Energy, 36 (2011) 4768-4780
- Tyagi D., Scholz K., Varma S., Bhattacharya K., Mali S., Patil P. S., Bharadwaj S. R., International Journal of Hydrogen Energy, 37 (2012) 3602-3611
- Sanap K. K., Varma S., Dalavi D., Patil P. S., Waghmode S. B., Bharadwaj S. R., International Journal of Hydrogen Energy, 36 (2011) 10455.
- Pai M. R., Majeed J., Banerjee A. M., Arya A., Bhattacharya S., Rao R., Bharadwaj S. R., Journal of Physical Chemistry C, 116 (2012) 1458-1471.
- Pai M. R., Singhal A., Banerjee A. M., Tiwari R., Dey G. K., Tyagi A. K., Bharadwaj S. R., Journal of Nanoscience and Nanotechnology 12 (2012) 1957-1966.
- Sasikala R., Sudarsan V., Sudakar C., Naik R., Panicker L., Bharadwaj S. R., International Journal of Hydrogen Energy, 34 (2009) 6105-6113.
- Sasikala R., Sudarsan V., Sudakar C., Naik R., Sakuntala T., Bharadwaj S. R., International Journal of Hydrogen Energy, 33 (2008) 4966-4973.
- Sasikala R., Shirole A.R., Sudarsan V., Jagannath, Sudakar C., R. Naik, Rao R., Bharadwaj S. R., Applied Catalysis A: General, 377 (2010) 47-54.
- Sasikala R., Shirole A. R., Sudarsan V., Kamble V. S., Sudakar C., Naik R., Rao R., Bharadwaj S. R., Applied Catalysis A: General, 390 (2010) 245-252.
- Sasikala R., Shirole A.R., Sudarsan V., Sakuntala T., Sudakar C., Naik R. and Bharadwaj S.R., Int. J. Hydrogen Energy, 34 (2009) 3621.
- Sasikala R., Shirole A.R., Bharadwaj S.R., J. Colloid Interface Sci., 409 (2013) 135-140.
- Sasikala R., Gaikwad A.R., Sudarsan V., Gupta N. and Bharadwaj S.R., Appl. Catal. A: General 464- 465 (2013) 149- 155.
- Sasikala R., Shirole A.R., Sudarsan V., Girija K.G., Rao R. and Bharadwaj S.R., J. Mater. Chem., 21 (2011) 16566 - 16573.
- Bhattacharyya K., Varma S., Tripathi A. K., Bharadwaj S. R. and Tyagi A. K., J. Phys. Chem. C, 112 (2008) 19102 - 19112.
- Bhattacharyya K., Varma S., Tripathi A. K., Tyagi A. K., J. Mat. Res., 25 (2010) 125.
- Bhattacharyya K., Varma S., Tripathi A. K., Bhattacharyya D., Mathon O., Tyagi A. K., J. Appl. Phys.. 106 (2009) 093503.
- Chatterjee S., Bhattacharyya K., Ayyub P. and Tyagi A. K., J. Phys. Chem. C 114 (2010) 9424-9430.
- Hankare P. P., Patil R. P., Jadhav A. V., Garadkar K. M., Sasikala R., Appl. Catal. B: Environmental 107 (2011) 333-339.

List of Life members as on 1st November 2013

Membership Number, Name, Affiliation, E-mail

1. **S. K. Kulshreshtha**, Ex DAE - Mumbai, kulshres@gmail.com
2. **P. R. Vasudeva Rao**, IGCAR - Kalpakkam, prvasudeva.rao@gmail.com
3. **V. Venugopal**, BARC - Mumbai, vvgopal@barc.gov.in
4. **T. Mukherjee**, BARC - Mumbai, mukherji@barc.gov.in
5. **D. Das**, BARC - Mumbai, dasd@barc.gov.in
6. **S.R. Bharadwaj**, BARC - Mumbai, shyamala@barc.gov.in
7. **P.V. Ravindran**, BARC - Mumbai, ravipv@barc.gov.in
8. **C.G.S. Pillai**, BARC - Mumbai, cgspil@barc.gov.in
9. **Avesh Kumar Tyagi**, BARC - Mumbai, aktyagi@barc.gov.in
10. **R. K. Vatsa**, BARC - Mumbai, rkvatsa@yahoo.com
11. **S.K. Mukerjee**, BARC - Mumbai, smukerji@barc.gov.in
12. **A.U. Bhanu**, BARC - Mumbai, aubhanu@barc.gov.in
13. **Anshu Singhal**, BARC - Mumbai, anshus@barc.gov.in
14. **Betty C.A.**, BARC - Mumbai, bettyca@barc.gov.in
15. **S.J. Patwe**, BARC - Mumbai, sjpatwe@barc.gov.in
16. **Sipra Choudhury**, BARC - Mumbai, sipra@barc.gov.in
17. **B.N. Wani**, BARC - Mumbai, bnwani@rediffmail.com
18. **R. Sasikala**, BARC - Mumbai, sasikala@barc.gov.in
19. **Neelam Goyal**, BARC - Mumbai, neelam@barc.gov.in
20. **A. K. Tripathi**, BARC - Mumbai, catal@barc.gov.in
21. **A. Venkataraman**, Gulbarga University, Gulbarga, raman_chem@rediffmail.com
22. **Alexander V. Vaidyan**, St. Stephen's College, Kerala, rrsnc@yahoo.com
23. **Chiranjib Majumder**, BARC - Mumbai, chimaju@barc.gov.in
24. **Gunjan Verma**, BARC - Mumbai, gunjanv@barc.gov.in
25. **Hemlata Bagla**, K.C. College - Mumbai, hemabagla@gmail.com
26. **K. Ananthasivan**, IGCAR, Kalpakkam, asivan@igcar.gov.in
27. **Mainak Roy**, BARC - Mumbai, mainak73@yahoo.com
28. **Manidipa Basu**, BARC - Mumbai, deepa@barc.gov.in
29. **P.A. Hassan**, BARC - Mumbai, hassan@barc.gov.in
30. **Pramod Sharma**, BARC - Mumbai, pramod@barc.gov.in
31. **R. Ganguly**, BARC - Mumbai, rajibg@barc.gov.in
32. **R. Raveendran**, S.N. College, Kollam, Kerala, rrsnc@yahoo.com
33. **R.S. Ningthoujam**, BARC - Mumbai, rsn@barc.gov.in
34. **Rajshree B. Jotania**, Gujrat University-Ahmedabad, rbjotania@gmail.com
35. **Renu Agarwal**, BARC - Mumbai, arenu@barc.gov.in
36. **S. N. Achary**, BARC - Mumbai, sachary@barc.gov.in
37. **Sandeep Nigam**, BARC - Mumbai, snigam@barc.gov.in
38. **Sandip Dey**, BARC - Mumbai, dsandip@barc.gov.in
39. **Shamima Hussain**, Indian School of Mines University - Dhanbad, shamimah1@yahoo.com
40. **Shilpa N. Sawant**, BARC - Mumbai, stawde@barc.gov.in
41. **Shiva Saran Das**, Gorakhpur University, Gorakhpur, ssdas2002@rediffmail.com
42. **Shivram S. Garje**, University of Mumbai, Mumbai, ssgarje@chem.mu.ac.in
43. **Swapan K. Ghosh**, BARC - Mumbai, skghosh@barc.gov.in
44. **V. Ganesan**, IGCAR, Kalpakkam, ganesh@igcar.gov.in
45. **V. Sudarsan**, BARC - Mumbai, vsudar@barc.gov.in
46. **Y. P. Naik**, BARC - Mumbai, yeshnaik@vsnl.com
47. **P. Mandal**, BARC - Mumbai, bpmandal@barc.gov.in
48. **Deepak Sahoo**, BARC - Mumbai, deepak_chembarc@yahoo.co.in
49. **Dheeraj Jain**, BARC - Mumbai, jaind@barc.gov.in
50. **G. Kedarnath**, BARC - Mumbai, gkedarnath@gmail.com
51. **K. Bhattacharya**, BARC - Mumbai, kbarctsv@yahoo.co.in
52. **Manoj Mohapatra**, BARC - Mumbai, manojm@barc.gov.in
53. **P.K. Wattal**, BARC - Mumbai, pk.wattal@gmail.com
54. **R. Manimaran**, BARC - Mumbai, maranswamy@rediffmail.com
55. **R.K. Bajpai**, BARC - Mumbai, rkbajpai1@yahoo.com
56. **S. Vana Varamban**, IGCAR, Kalpakkam, varam@igcar.gov.in
57. **Sathi R. Nair**, ECMS - Navi Mumbai, sathi_61@yahoo.co.in
58. **V.S. Tripathi**, BARC - Mumbai, vst_apcd@barc.gov.in
59. **Thresiamma George**, Nirmala College, Kerala, tresasunny@gmail.com
60. **L.D. Jadhav**, Shivaji University - Kolhapur, ldjadhav.phy@gmail.com
61. **Kitheri Joseph**, IGCAR, Kalpakkam, joskit@igcar.gov.in
62. **R. Raja Madhavan**, IGCAR, Kalpakkam, rajam@igcar.gov.in
63. **Sadhana Suresh Rayalu**, NEERI - Nehru Marg, Nagapur, s_rayalu@neeri.res.in
64. **Dayamoy Banerjee**, BARC - Mumbai, dayabanerjee@gmail.com
65. **Bhaskar Kumar Sen**, BARC - Mumbai, bksen@barc.gov.in
66. **Vrinda Borker**, Dhempe College, Goa, borkarpp@yahoo.com
67. **K.V. R. Murthy**, Phys Dept, Baroda, drmurthykvr@yahoo.com
68. **Raja Kishor Lenka**, BARC - Mumbai, rklenka@barc.gov.in
69. **Vimal Kumar Jain**, BARC - Mumbai, jainvk@barc.gov.in
70. **B. Viswanathan**, IIT, Madras, bviswanathan@hotmail.com
71. **Chetan Prakash Kaushik**, BARC - Mumbai, cpk@barc.gov.in
72. **Sanjay Kumar**, BARC - Mumbai, sanjayk@barc.gov.in
73. **Daisy Joseph**, BARC - Mumbai, djoseph@barc.gov.in
74. **Aparna Banerjee**, BARC - Mumbai, aparnab@barc.gov.in
75. **B. S. Naidu**, BARC - Mumbai, snaidu@barc.gov.in
76. **Srirupa Mukherjee**, Chemistry Division, BARC, srirupam@gmail.com
77. **Rakeshkumar P. Thakkar.**, Reliance Industries, Gujarat, rpt8875@gmail.com
78. **J. Udhayakumar**, BARC, Mumbai, udhayam@barc.gov.in
79. **Jyostna S. Thakur**, C.R. Thakur & C.J. College, New Panvel, thakurjyostna@gmail.com
80. **Tanmay Kumar Ghorai**, Bajkul Milanimahavidyalaya, W.B, tanmay.ghorai66@gmail.com
81. **Rajeev Joshi**, Shivaji University, Kolhapur, rajeev_sj@yahoo.com
82. **Amrut Sadashio Lanje**, Dr. Ambedkar College, Chandrapur, M.S, amrut.lanje@gmail.com
83. **Monica Katiyar**, IIT,Kanpur, mk@utk.ac.in
84. **Sarat Chandra Das**, Salipur College, Orissa, ctkscd@gmail.com
85. **Maibam Aken Singh**, Imphal College, Imphal, aken_maiban@yahoo.com
86. **Nabakumar Pramanic**, IIT, Kharagpur, pramanik_naba@yahoo.co.in
87. **Seema Maheshwari**, MDS Univ., Ajmer, Rajasthan, seemamaheshwari2007@rediffmail.com
88. **Samidha Saxena**, Devi Ahilya University, Indore, samidha.saxena@gmail.com
89. **Hrudananda Jena.**, IGCAR, Kalpakkam, hrje@igcar.gov.in
90. **Sanjiv Kumar**, NCCCM, BARC - Hyderabad, sanjucccm@rediffmail.com
91. **Rajeshkumar M. Patel.**, M.S. University, Baroda, patel.rajeshkumar@rediffmail.com
92. **N. Sivarajasekar**, Kongu Engg. College, Erode, sivarajasekar@gmail.com
93. **K. Nagarajan.**, IGCAR, Kalpakkam, knag@igcar.gov.in
94. **S.K. Sali.**, FCD, BARC, sksali@barc.gov.in
95. **Rajesh V. Pai.**, FCD, BARC, pairajesh007@gmail.com
96. **S.K. Rakshit.**, PDD, BARC, swarup-kr@rediffmail.com
97. **Vivek Kumar Pilonia.**, NIT, Tiruchirappalli, vpilonia2008@gmail.com
98. **A.R. Phani.**, Nano-Ram Technologies, Vijayanagar, arp@nano-ram.org
99. **L.R. Singh**, Imphal College, Imphal, loitung@yahoo.co.in
100. **Shadie Hatamie**, Fergusson College, Pune, HATAMY1335@yahoo.com
101. **Jayshree Ramkumar**, ACD, BARC, jrk@barc.gov.in
102. **S.K. Gupta**, TPPED, BARC, dr Gupta@barc.gov.in
103. **A.P. Mishra**, H.S. Gour University, Sagar, apmishrasagar@gmail.com
104. **G. Panneer Selvam**, IGCAR, Kalpakkam, selvam1988@gmail.com
105. **Prasanta Jana.**, IGCAR, Kalpakkam, prasanta.jana@rediffmail.com
106. **Maitri Mapa.**, NCL, Pune, m.maitri@gmail.com
107. **Sunil Sabharwal**, BARC - Mumbai, sunsab@barc.gov.in
108. **Ratikanta Mishra**, BARC - Mumbai, mishrar@barc.gov.in
109. **Yogesh Kumar Sharma**, University of Delhi, Delhi, yk_sharma2004@yahoo.com
110. **Ziley Singh.**, BARC - Mumbai, zsingh@barc.gov.in
111. **Smruti Dash.**, BARC - Mumbai, smruti@barc.gov.in
112. **Pradeep Samui**, BARC - Mumbai, Praddepsamui@gmail.com
113. **Madhab Chandra Rath**, BARC - Mumbai, madhab@barc.gov.in
114. **R.K. Mishra**, Chemistry Division, BARC, mishrrk@gmail.com
115. **Vivekanand Dubey**, BARC - Mumbai, vdubey@barc.gov.in
116. **P. Bhavani**, Anna University, Chennai, bhavaniPerumal4@gmail.com

117. **Sangeetha.**, Anna University, Chennai, sangeetha@annauniv.edu
 118. **R. Vinodh.**, Anna University, Chennai, vinoth6482@gmail.com
 119. **Bharati Panigrahy**, IIT, Bombay, bharatipanigrahy@iitb.ac.in
 120. **Meera Venkatesh**, BARC - Mumbai, meera@barc.gov.in
 121. **Ashutosh Dash**, BARC - Mumbai, adash@barc.gov.in
 122. **Remani babu Manolkar**, BARC - Mumbai, r-manolkar@rediffmail.com
 123. **Sanjay Kumar Saxena**, BARC - Mumbai, snr1991@yahoo.com.in
 124. **Rubel Chakravarty**, BARC - Mumbai, rubelc@barc.gov.in
 125. **Shyamala S. Gandhi**, BARC - Mumbai, sgandhi@barc.gov.in
 126. **Ramu Ram**, BARC - Mumbai, ramuram.barc.gov.in
 127. **Soumitra Das**, BARC - Mumbai, soumitra@barc.gov.in
 128. **Nital R. Panchal**, Gujarat Univ., Ahmedabad, nital_panchal@yahoo.co.in
 129. **Chetna C. Chauhan.**, Gujarat Univ., Ahmedabad, chetumakwana@gmail.com
 130. **Harjinder Kaur.**, Gujarat Univ., Ahmedabad, hr_ss_in@yahoo.com
 131. **Usha Pal.**, Gujarat Univ., Ahmedabad, ushapal@rediffmail.com
 132. **Shobhana K. menon.**, Gujarat Univ., Ahmedabad, shobhanamenon07@gmail.com
 133. **Gaurang M. Patel.**, Gujarat Univ., Ahmedabad, baps.gaurang@gmail.com
 134. **Meitram Niraj Luwang**, Manipur Univ., Imphal, nirajmeitram@gmail.com
 135. **Dinesh K. Patel**, Chemistry Division, BARC, dineshpatel25@gmail.com
 136. **Satish J. Sharma**, Dept. of Elec., RTM, Nagpur, sjsharma@rediffmail.com
 137. **Suresh S. Umare**, Dept. of Chem., VNIT, Nagpur, ssumare@rediffmail.com
 138. **Ashok Arya**, BARC - Mumbai, ashokarya@gmail.com
 139. **Nitin Labhsetwar**, NEERI - Nehru Marg, Nagapur, nk_labhsetwar@neeri.res.in
 140. **Shashwati Sen**, BARC - Mumbai, shash@barc.gov.in
 141. **Shovit Bhattacharya**, BARC - Mumbai, shovitb@rediffmail.com
 142. **Manmeet Kaur**, BARC - Mumbai, manmeet@barc.gov.in
 143. **Raman Kumar Mishra**, BARC - Mumbai, mishrark@barc.gov.in
 144. **Virendra Kumar**, BARC - Mumbai, vkumar@barc.gov.in
 145. **S.P. Ramnani**, BARC - Mumbai, ramnani@barc.gov.in
 146. **K.A. Dubey**, BARC - Mumbai, dubeyabhinav@rediffmail.com
 147. **Jayashree Biswal**, BARC - Mumbai, jbiswal@barc.gov.in
 148. **Vishwabharati Vilas Malkar**, BARC - Mumbai, 13vishu@gmail.com
 149. **Nalawade Pradnya Parshuram**, BARC - Mumbai, 14pradnya@gmail.com
 150. **Jasmine Annajothi Jacob**, BARC - Mumbai, jasminebarc@gmail.com
 151. **Jayita Bhattacharjee**, BARC - Mumbai, jayita@barc.gov.in
 152. **Sanjay C. Gadkari**, BARC - Mumbai, gadkari@barc.gov.in
 153. **Devidas B. Naik**, BARC - Mumbai, dbnaik@barc.gov.in
 154. **S. Chandramouleeswaran**, BARC - Mumbai, chandru@barc.gov.in
 155. **Ajay Kumar Patra**, BARC - Mumbai, apatra@barc.gov.in
 156. **Sanu S. Raj**, BARC - Mumbai, sanusraj@yahoo.com
 157. **Smt. Sanjukta A. Kumar**, BARC - Mumbai, sanjukta@barc.gov.in
 158. **Jitendra Nuwad**, BARC - Mumbai, nuwad@barc.gov.in
 159. **Sangeeta J. Keny**, BARC - Mumbai, sankenya@barc.gov.in
 160. **Rakesh R. Shukla**, BARC - Mumbai, rakesh@barc.gov.in
 161. **Vinila V. Bedekar**, BARC - Mumbai, vinila3@rediffmail.com
 162. **Sayed Farheen Nasir Hussain**, BARC - Mumbai, farheen_sayed7@yahoo.com
 163. **Pooja P Sawant**, BARC - Mumbai, ppsawant@barc.gov.in
 164. **Sandeep Chavan**, Aditya Birla Science & Technology Centre, Mumbai, sandeep.chavan@adityabirla.com
 165. **Ravi Joshi**, BARC - Mumbai, ravij@barc.gov.in
 166. **Mrinal R. Pai**, BARC - Mumbai, mrinalr@barc.gov.in
 167. **Poulomi Mukherjee**, BARC - Mumbai, poulomi81@gmail.com
 168. **Deepak Tyagi**, BARC - Mumbai, dtyagi@barc.gov.in
 169. **Ananya Verma**, VSB, HWB, Anushakti Nagar, ananya_bar@rediffmail.com
 170. **Sriparna Chatterjee**, TIFR - Mumbai, sriparna251@gmail.com
 171. **Mohit Tyagi**, BARC - Mumbai, tyagi@barc.gov.in
 172. **Prasuna Koshy**, BARC - Mumbai, pkoshy@barc.gov.in
 173. **D.G. Desai**, BARC - Mumbai, dgdesai@barc.gov.in
 174. **S.D. Samant**, Institute of Chemical Technology - Mumbai, samantsd@yahoo.com
 175. **K.M. Garodkar**, Shivaji University - Kolhapur, kmg-chem@unishivaji.ac.in
 176. **S.R. Patil**, Shivaji University - Kolhapur, srp_fsl@rediffmail.com
 177. **Bhattar Swaminatha Laxman**, Shivaji University - Kolhapur, slbhattar@gmail.com
 178. **Srimanth Kagne**, NEERI - Nehru Marg, Nagapur, skagne82@yahoo.com
 179. **Keka R. Chakraborty**, VECC - Kolkata, kekarc@veccal.ernet.in
 180. **B.H. Mehta**, University of Mumbai, Mumbai, b1p1n_281050@yahoo.com
 181. **N.L. Sonar**, BARC - Tarapur, aakash3010@rediffmail.com
 182. **V.K. Yadav**, BARC - Tarapur, vkyadav.1841@rediffmail.com
 183. **Vaishali De**, BARC - Tarapur, vaishali_1074@yahoo.com
 184. **Amreesh Chandra**, IIT - Kharagpur, achandra@phy.iitkgp.ernet.in
 185. **Shiv Govind Singh**, BARC - Mumbai, shivgovind_singh143@yahoo.com
 186. **Manoj Kumar**, BARC - Mumbai, mkjangir@barc.gov.in
 187. **Dimple P. Dutta**, BARC - Mumbai, dimpled@barc.gov.in
 188. **N. L. Singh**, University of Baroda, Vadodara, singhnl_msu@yahoo.com
 189. **Dinesh K. Kanchan**, University of Baroda, Vadodara, d_k_kanchan@yahoo.com
 190. **Prashant K. Mehta**, University of Baroda, Vadodara, pkmehta_phy@yahoo.co.in
 191. **Ranjan Mittal**, BARC - Mumbai, rmittal@barc.gov.in
 192. **M.S. Kulkarni**, BARC - Mumbai, kmukund@barc.gov.in
 193. **D.R. Mishra**, BARC - Mumbai, devesh22@yahoo.com
 194. **N.S. Rawat**, BARC - Mumbai, naru@barc.gov.in
 195. **P. Pramanik**, IIT - Kharagpur, pramanik1946@gmail.com
 196. **Ramanani Venugopalan**, BARC - Mumbai, rvg@barc.gov.in
 197. **Jyoti Prakash**, BARC - Mumbai, jprakash@barc.gov.in
 198. **Jagannath**, BARC - Mumbai, ssai@barc.gov.in
 199. **Rajendra Kumar Sharma**, BARC - Mumbai, rajendra@barc.gov.in
 200. **Nishant N. Patel**, BARC - Mumbai, nnpatel@barc.gov.in
 201. **Siddhartha Kolay**, BARC - Mumbai, siddharthakolay@yahoo.co.in
 202. **Yamini Sharma**, Feroze Gandhi College, Raibareilly, yamini_2001@rediffmail.com
 203. **Chetan J. Panchal**, University of Baroda, Vadodara, cjpanchal_msu@yahoo.com
 204. **Sisir Kumar Sarkar**, BARC-Mumbai, sarkarsk@barc.gov.in
 205. **Charu Dwivedi**, BARC-Mumbai, cdwivedi@barc.gov.in
 206. **Chetan P. Shah**, BARC-Mumbai, chetanshah9@rediffmail.com
 207. **Pallavi S. Page**, BARC-Mumbai, pallavipage@gmail.com
 208. **Bhupesh B. Kalekar**, BARC-Mumbai, bhupkal@barc.gov.in
 209. **Naina Rajee**, BARC-Mumbai, nraje@barc.gov.in
 210. **Darshana A. Acharekar**, BARC-Mumbai, darshanaacharekar@yahoo.com
 211. **Patil Vishwanath Dhamba**, C.K. Thakur A.C.S. College, Panvel, vishvanathpatil@yahoo.com
 212. **M.R. Gonal**, BARC-Mumbai, mrgonal@barc.gov.in
 213. **Debasis Sen**, BARC-Mumbai, debasis@barc.gov.in
 214. **Jitendra Bahadur**, BARC-Mumbai, jbahadur@barc.gov.in
 215. **Ashok K. Ganguli**, IIT, Delhi, ashok@chemistry.iitd.ernet.in
 216. **Sharif Ahmad**, Jamia Millia Islamia, New Delhi, sharifahmad_jmi@yahoo.co.in
 217. **Tokeer Ahmad**, Jamia Millia Islamia, New Delhi, tokeer.ch@jmi.ac.in
 218. **Hindendra Nath Ghosh**, BARC-Mumbai, hnhghosh@barc.gov.in
 219. **S.V.G.V.A. Prasad**, A.J. Kalasala, Andhra Pradesh, dr.svgvprasad@gmail.com
 220. **S. Khare**, Devi Ahilya University, Indore, kharesavita@rediffmail.com
 221. **Rajendra Chokhare**, Devi Ahilya University, Indore, rchowkhare@yahoo.co.in
 222. **Tenson Antony**, Devi Ahilya University, Indore, tensonantony@rediffmail.com
 223. **Suresh M. Chopade**, BARC-Mumbai, csuresh@barc.gov.in
 224. **Kamal P. Chaudhari**, BARC-Mumbai, kamalc@barc.gov.in
 225. **Alpa Y. Shah**, BARC-Mumbai, salpa@barc.gov.in
 226. **Manoj Kumar Pal**, BARC-Mumbai, mpal@barc.gov.in
 227. **Nisha Kushwah**, BARC-Mumbai, knisha@barc.gov.in
 228. **Liladhar Kumbhare**, BARC-Mumbai, liladhar@barc.gov.in
 229. **Prasad P. Phadnis**, BARC-Mumbai, phadnisp@barc.gov.in
 230. **Amey Wadawale**, BARC-Mumbai, ameypw@barc.gov.in
 231. **Vinita Grover Gupta**, BARC-Mumbai, vinita@barc.gov.in
 232. **S.Kannan**, BARC-Mumbai, skannan@barc.gov.in
 233. **Gunadhor S. Okram**, UGC-DAE, Indore, okram@csr.ernet.in
 234. **H.D. Juneja**, Nagpur University, Nagpur, hd_juneja@yahoo.com
 235. **Gatiwant Kumar Mallik**, BARC-Mumbai, gatiwant@barc.gov.in
 236. **Arun Pratap**, M.S. University, Baroda, apratapmsu@yahoo.com

237. **P. Sujatha Devi**, CGCRI, Kolkata, psujathadevi@gmail.com
 238. **Sanhita Majumdar**, CGCRI, Kolkata, mailid_sm@yahoo.com
 239. **Venu H Mankad**, Bhavnagar University, Gujarat, venu.mankad@gmail.com
 240. **Sanjeev K. Gupta**, Bhavnagar University, Gujarat, skgupta.physics@gmail.com
 241. **P.K. Jha**, Bhavnagar University, Gujarat, prafullaj@yahoo.com
 242. **G. Buvanewari**, VIT University, Vellore, gopalbhu@yahoo.com
 243. **Madhvesh Pathak**, VIT University, Vellore, mpathak2000@yahoo.com
 244. **A. Anand Prabhu**, VIT University, Vellore, aprabu21@yahoo.com
 245. **Manmohan kumar**, BARC-Mumbai, manmoku@barc.gov.in
 246. **Avinash S. Pente**, BARC-Mumbai, pavinash@barc.gov.in
 247. **Parag Rama Wavale**, BARC-Mumbai, pwavale@barc.gov.in
 248. **Manoranjan Ghosh**, North Bengal Science Centre, Siliguri, mano.snb@gmail.com
 249. **Chinnakonda S. Gopinath**, NCL, Pune, cs.gopinath@ncl.res.in
 250. **K. Sivaranjani**, NCL, Pune, s.kumarsrinivasan@ncl.res.in
 251. **Soumyaditya Mula**, BARC-Mumbai, smula46@yahoo.com
 252. **B.T. Thaker**, VNS Gujarat University, Surat, btthaker1@yahoo.co.in
 253. **Saurabh K. Patel**, VNS Gujarat University, Surat, saurabh.silvinu@gmail.com
 254. **Parameswar K. Iyer**, IIT Guwahati, Guwahati, pki@iitg.ac.in
 255. **Dhanraj Tukdoji Masram**, University of Delhi, Delhi, ghanraj_masram27@rediffmail.com
 256. **Priya Dasan K.**, VIT University, Vellore, kpriyadasan@yahoo.com
 257. **Rakesh Sharma**, BARC-Mumbai, rakeshs@barc.gov.in
 258. **Archana Sharma**, BARC-Mumbai, arsharma@barc.gov.in
 259. **Hirakendu Basu**, BARC-Mumbai, hirak@barc.gov.in
 260. **R.K. Singhal**, BARC-Mumbai, rsinghal@barc.gov.in
 261. **S.S. Bhoga**, RTM Nagpur University, Nagpur, msr11@hotmail.com
 262. **Anushree P. Khandale**, RTM Nagpur University, Nagpur, anushri.khandale@gmail.com
 263. **Kalpna Ramdas Nagde**, RTM Nagpur University, Nagpur, kalpana.nagde@gmail.com
 264. **Ananda Shamrao Hodage**, BARC-Mumbai, sanjananand2007@gmail.com
 265. **S.M.Yusuf**, BARC-Mumbai, smysnt@barc.gov.in
 266. **Shanker Ram**, IIT, Kharagpur, sram@matsc.iitkgp.ernet.in
 267. **Ajit Dattatray Phule**, IIT, Kharagpur, phule.ajit@gmail.com
 268. **B. Susrutha**, IIT, Kharagpur, susrutha.ma@gmail.com
 269. **Manoranjan Behera**, IIT, Kharagpur, mano.silicon@gmail.com
 270. **Prasanna A.A.**, IIT, Kharagpur, aap13_athma@rediffmail.com
 271. **Trisha Karan**, IIT, Kharagpur, karantrisha@gmail.com
 272. **Arundhati Sengupta**, IIT, Kharagpur, arundhati176@gmail.com
 273. **Akhtar Jahan Siddiqi**, IIT, Kharagpur, akhtar.mtech@gmail.com
 274. **Susmita Misra**, IIT, Kharagpur, misra.susmita@gmail.com
 275. **Akshay Jayant Chinchalikar**, BARC - Mumbai, akshay.chinchalikar@gmail.com
 276. **Debes Ray**, BARC-Mumbai, debes_ray@rediffmail.com
 277. **V.K. Aswal**, BARC-Mumbai, vkaswal@barc.gov.in
 278. **N.B Patel**, V.N.S.G. University, Surat, drnavin@satyam.net.in
 279. **K. Sivasankar**, VIT University - Vellore, cuttisiva@gmail.com
 280. **Jitendra Shankerlal Parekh**, Shree Jayendrapuri Arts & Science College-Gujrat, -
 281. **Pratesh.J. Shah**, Shri J.P. Arts & Science College. Bharuch, acticarbad1@sancharnet.in
 282. **Nitinkumar Bhailalbhai Patel**, Shri J.P. Arts & Science College. Bharuch,
 283. **N.C. Desai**, Bhavnagar University, Gujarat, dnisheeth@rediffmail.com
 284. **J.P. Mehta**, Bhavnagar University, Gujarat, jpm1569@yahoo.co.in
 285. **D.R. Godhani**, Bhavnagar University, Gujarat, drgodhani@yahoo.com
 286. **Chetankumar K. Modi**, Bhavnagar University, Gujarat, chetank.modi1@gmail.com
 287. **Tejas P. Joshi**, Bhavnagar University, Gujarat, tejas2709@gmail.com
 288. **N. Kumar**, BARC-Mumbai, nkumar_bar@yahoo.com
 289. **M.V. Suryanarayana**, CCCM, Hyderabad, suryaccm@rediffmail.com
 290. **O.D. Jayakumar**, BARC-Mumbai, odjaya@barc.gov.in
 291. **Manoj Nalliath**, BARC-Mumbai, nmanoj@barc.gov.in
 292. **Atindra Mohan Banerjee**, BARC-Mumbai, atinmb@barc.gov.in
 293. **Seemita Banerjee**, BARC-Mumbai, seemira@barc.gov.in
 294. **Palash Kumar Manna**, BARC-Mumbai, pkmanna@barc.gov.in
 295. **G. P. Das**, IACS, Kolkata, gourpdas@gmail.com
 296. **Sudha**, Delhi College of Engineering , Delhi, sudha1320@gmail.com
 297. **R. Nagarajan**, University of Delhi, Delhi, rnagarajan@chemistry.du.ac.in
 298. **Sitharaman Uma**, University of Delhi, Delhi, suma@chemistry.du.ac.in
 299. **Nobel Tomar**, University of Delhi, Delhi, nobeltomar@gmail.com
 300. **Vaishali Thakral**, University of Delhi, Delhi, thakral.vaishali@gmail.com
 301. **Epsita Ghanti**, University of Delhi, Delhi, epsitaghati@gmail.com
 302. **Mamta Kharkwal**, University of Delhi, Delhi, mamtachem@yahoo.co.in
 303. **Vinod Kumar**, University of Delhi, Delhi, vinod7674@gmail.com
 304. **Jyoti Singh**, University of Delhi, Delhi, jsingh@chemistry.du.ac.in
 305. **A.G. Kumbhar**, BARC-Mumbai, agk@barc.gov.in
 306. **Sindhunil Barman Roy**, Raja Ramanna Centre - Indore, sbroy@rrcat.gov.in
 307. **Maulindu Kumar Chattopadhyay**, Raja Ramanna Centre - Indore, maulindu@rrcat.gov.in
 308. **Kirankumar R. Surati**, S.P. University - Gujrat, kiransurati@yahoo.co.in
 309. **Saurabh S. Soni**, S.P. University - Gujrat, soni-b21@yahoo.co.in
 310. **Kartik N. Shinde**, RTM Nagpur University - Nagpur, kartik_shinde@rediffmail.com
 311. **Pankaj Poddar**, National Chemical Laboratory, Pune, p.poddar@ncl.res.in
 312. **S.J. Dhole**, RTM Nagpur University - Nagpur, sjdhole@rediffmail.com
 313. **N.S. Dhole**, Sevadal Mahila Mahavidyalaya, Nagpur, nsdhole@rediffmail.com
 314. **Purav M. Badani**, BARC-Mumbai, purab_1986@yahoo.co.in
 315. **Manishkumar P. Patel**, Sardar Patel University - Gujarat, patelmanish1069@yahoo.com
 316. **Raghavendra Yellampalli**, BARC-Mumbai, yraghavendra321@gmail.com
 317. **M.B. Kakade**, BARC-Mumbai, mkakade@barc.gov.in
 318. **S.K. Srivastav**, Manipur University, Imphal, profsrivastava@gmail.com
 319. **S. Dorendrajit Singh**, Manipur University, Imphal, dorendrajit@yahoo.co.in
 320. **M.M. Khandpekar**, Birla College - Kalyan, dr_mmk1968@yahoo.com
 321. **Munish Pandey**, K.M. Agarwal College - Kalyan, drmunishpandey@yahoo.com
 322. **Jyotsana Tiwari**, Hill Spring International School, Kalyan, tyotsana_1979@yahoo.com
 323. **Shirish B. Patel**, K.G. Karjat College of ASC, Karjat, pshirishb1115@gmail.com
 324. **Shailesh S. Dongare**, Birla College - Kalyan, shaileshdongare@yahoo.com
 325. **Smita S. Patil**, Birla College - Kalyan, smita_p6@yahoo.co.in
 326. **S.G. Gourkhede**, Bhavans College - Mumbai, s.gaurkhede@gmail.com
 327. **Kamala Balasubramanian**, G.M. Momin Women's College - Thane, kamala14_in@yahoo.com
 328. **Tarannum Aziz Shaikh**, G.M. Momin Women's College - Thane, -
 329. **Jayashree S. Thakre**, G.M. Momin Women's College - Thane, jaya_thakre@yahoo.co.in
 330. **Jigyasa P. Dave**, Navyug Science College, Surat, -
 331. **Rajendra Thakor Bhai Vashi**, Navyug Science College, Surat, vashirajendra@yahoo.co.in
 332. **Kumar Trupti Ajitsinh**, Navyug Science College, Surat, -
 333. **Patel Pravinkumar Chandulal**, Navyug Science College, Surat, -
 334. **Pragna D. Vashi**, Navyug Science College, Surat, pdvashi@rediffmail.com
 335. **Pushpaben Rameshandra Tandel**, Navyug Science College, Surat, dr.pushpabentandel@yahoo.co.in
 336. **Mallik G. M.**, Navyug Science College, Surat, gmmalik2010@gmail.com
 337. **Contractor K. S.**, Navyug Science College, Surat, drkcontractor@hotmail.com
 338. **Vijay A. Champaneri**, B.K.M. Science College , Gujrat, vijay214219@yahoo.com
 339. **Nongmaithem Mohondas Singh**, Mizoram University - Aizawl, nmdas08@yahoo.com
 340. **Lalrosanga**, Mizoram University - Aizawl, rsanga09@rediffmail.com
 341. **Alka B. Garg**, BARC-Mumbai, alkabgarg@rediffmail.com
 342. **Meenakshi Sunder**, BARC-Mumbai, msunder@barc.gov.in
 343. **Kothari D.C.**, University of Mumbai, kothari.physics@gmail.com
 344. **Deepa Khushalani**, TIFR - Mumbai, khushalani@tifr.res.in
 345. **M. Anitha**, BARC, Mumbai, manitha@barc.gov.in
 346. **P.K. Pujari**, BARC, Mumbai, pujari@barc.gov.in
 347. **Sanap Kiran Khandu**, Pune university, Pune, sanap30@gmail.com
 348. **S.C. Parida**, BARC, Mumbai, sureshp@barc.gov.in
 349. **Rohan. A. Phatak**, BARC, Mumbai, phatakrohan@yahoo.co.in

350. **Debabrata Chattaraj**, BARC, Mumbai, debchem@barc.gov.in
351. **Asok Goswami**, BARC, Mumbai, agoswami@barc.gov.in
352. **Ashok Kumar Pandey**, BARC, Mumbai, ashokk@barc.gov.in
353. **B.S.Tomar**, BARC, Mumbai, bstomar@barc.gov.in
354. **S.Jeyakumar**, BARC, Mumbai, sjkumar@barc.gov.in
355. **Mrinal Kanti Das**, BARC, Mumbai, mrinal83@live.in
356. **Durga Basak**, IACS, Kolkata, sspdb@iacs.res.in
357. **Sourindra Mahanty**, CGCRI, Kokata, mahanty@cgcri.res.in
358. **Rajendra N Basu**, CGCRI, Kolkata, rajenasu54@gmail.com
359. **Mahesh Hiralal Patel**, V.N.S.G. University, Surat, maheshgorani@gmail.com
360. **Patil Rajendra Pandurang**, Shivaji University, Kolhapur, patilraj_2005@rediffmail.com
361. **P.P.Hankare**, Shivaji University, Kolhapur, p_hankarep@rediffmail.com
362. **Anushree Roy**, IIT Kharagpur, anushree@phy.iitkg.ernet.in
363. **Sangita Dhara Lenka**, BARC, Mumbai, sangitadhara@rediffmail.com
364. **Manjulata Sahu**, BARC, Mumbai, manju@barc.gov.in
365. **Santosh Manohar Bhojane**, BARC, Mumbai, santoshm@barc.gov.in
366. **Manoj Kumar Sharma**, BARC, Mumbai, mksaks@yahoo.com
367. **N.L.Misra**, BARC, Mumbai, nlmisra@yahoo.com
368. **Chinagandham Rajesh**, BARC, Mumbai, crajesh@barc.gov.in
369. **Suman Kalyan Sahoo**, Visva-Bharati, Santiniketan, West Bengal, kalyan_apu@yahoo.co.in
370. **A.S.Patel**, Navyug Science College, Surat, aspatel63@yahoo.com
371. **Patel Ketankumar Kantibhat**, Navyug Science College, Surat, ketankpatel14187@gmail.com
372. **Viral Raval**, Valsad , Gujrat, raval-viral-84@yahoo.co.in
373. **Shailesh Khodabhai Zadafiya**, Valsad , Gujrat, shailesh761983@gmail.com
374. **Patil Devidas Ramrao**, R.L.college, Parola, Jalgoan, prof_drpatil@yahoo.co.in
375. **A.V.R.Reddy**, BARC, Mumbai, avreddy@barc.gov.in
376. **G.P.Kothiyal**, BARC, Mumbai, gpkothiyal@yahoo.co.in
377. **K.Indira Priyadarsini**, BARC, Mumbai, kindira@barc.gov.in
378. **R.Vijayalakshmi**, BARC, Mumbai, rvijaya@barc.gov.in
379. **Niharendu Choudhury**, BARC, Mumbai, niharc2002@yahoo.com
380. **Sandip Kumar Dhara**, IGCAR, Kalpakkam, dr.s.dhara@gmail.com
381. **Soumee Chabraborthy**, IGCAR, Kalpakkam, soumee.chakraborty@gmail.com
382. **Ranveer Kumar**, Dr.Hari Singh Gour University, Sagar, ranveerssi@yahoo.com
383. **Jerina Majeed**, BARC, Mumbai, jerinamajid@gmail.com
384. **Suman Rana**, BARC, Mumbai, sumnsana@gmail.com
385. **Shanta S Sharma**, SIES Graduate School of Technology, Nerul, shantashreekumar@gmail.com
386. **Sanjay**, GJU&ST, Hisar, sanjay2000angira@yahoo.co.in
387. **Arpita Pal**, A.C.Patil College, Mumbai, arpitappal@rediffmail.com
388. **Ram Avtar Jat**, BARC, Mumbai, avtar@barc.gov.in
389. **Subrata Chattopadhyay**, BARC, Mumbai, schatt57@gmail.com
390. **Selvakumar Jayaprakasam**, BARC, Vashi, Navi Mumbai, j.maselva@gmail.com
391. **Pintu Kumar Kundu**, BARC, Mumbai, pintukumar2004@yahoo.co.in
392. **Debashree Manna**, BARC, Mumbai, dmanna@barc.gov.in
393. **Tapan K Ghanty**, BARC, Mumbai, tapang@barc.gov.in
394. **Vilas Ramdas Chumbhule**, NCL, Pune, vr.chumbhale@ncl.res.in
395. **Sandesh Vinayakrao Jaybhaye**, Birla college of Arts, Science and Commerce, Kalyan, jaysandesh@gmail.com
396. **Pradnya J Prabhu**, K.J.Somaiya College of Science & Commerce, Mumbai, pjprabhu@rediffmail.com
397. **Sugandha Srikant Shetye**, K.J.Somaiya College of Science & Commerce, Mumbai, drshetye21@rediffmail.com
398. **Rashmi Chauhan**, D.A.V.College, Kanpur, chauhanrasmi@gmail.com
399. **Arvind Tripathi**, Chunniganj, Kanpur, tripathiarvind@yahoo.co.in
400. **Chandra Nath Patra**, BARC, Mumbai, chandra.patra@gmail.com
401. **Brindaban Modak**, BARC, Mumbai, bmmodak@barc.gov.in
402. **Chitra Kamath**, K.J.Somaiya college of science & commerce , vidyavihar, drchitrakamath@gmail.com
403. **Archana Uttamrao Chavan**, Shivaji University - Kolhapur, chavan-au@yahoo.co.in
404. **Bhavana Thakur**, BARC, Mumbai, bhawana_bhanupratap@yahoo.co.in
405. **Sahera S Patel**, Sardar Patel University - Gujarat, swamibhavin@yahoo.com
406. **Prabhakar Shankar Navarkar**, A.D.A, S.V.A.C,M.S.College, Palghar,, -
407. **Suhas Prakash Janwadkar**, A.D.A, S.V.A.C,M.S.College, Palghar,, suhas.janwadkar@gmail.com
408. **Shirish Pitale**, A.D.A, S.V.A.C,M.S.College, Palghar,, shirishpitale@yahoo.com
409. **S.V.Godbole**, BARC, Mumbai, shri_godbole@yahoo.co.in
410. **Nandkumar Dattatrya Dahale**, BARC, Mumbai, nandkumardahale@yahoo.co.in
411. **Dhruva Kumar Singh**, BARC, Mumbai, dksingh@barc.gov.in
412. **M.K.Kotekar**, BARC, Mumbai, mkotekar@gmail.com
413. **Meera S Keskar**, BARC, Mumbai, meerakeskar@yahoo.com
414. **Veena L Khilnani**, K. J. Somaiya college of science & commerce, Mumbai, veenakhilnani@rediffmail.com
415. **Katari Vasundhara**, BARC Mumbai, Vasundharakatari@gmail.com
416. **Priyanka Das**, BARC Mumbai, priyankajuhem@rediffmail.com
417. **Gautham Kumar Dey**, BARC Mumbai, gkdubey@barc.gov.in
418. **Kanhu Charan Barick**, BARC Mumbai, kcbarick@gmail.com
419. **A.C.Sahayam**, ECIL (PO), Hyderabad, sahayamac@hotmail.com
420. **Salil Varma**, BARC Mumbai, salilvarma@redimail.com
421. **Patel Gaurang Kumar Shivabhai**, M S Univ. of Baroda, Vadodara, guru16686@gmail.com
422. **Rakhi Khandelwal**, Govt. Mahila Engineering College, Ajmer, rakhi.gweca@gmail.com
423. **V. Jeseentha Rani**, Loyola College, Chennai, jeseentha@gmail.com
424. **Anup K Ghosh**, BHU, Varanasi, anupkg66@gmail.com
425. **Sanjeev Kumar**, M S Univ. of Baroda, Vadodara, dvksanjeev@gmail.com
426. **Hemant P. Soni**, M S Univ. of Baroda, Vadodara, drhpsoni@yahoo.co.in
427. **Vinayak Kumar Singh**, M S Univ. of Baroda, Vadodara, vks.msu@gmail.com
428. **K.C.Sajjan**, Veerashaiva college, Bellary, kcsajjan23@yahoo.com
429. **Muhammad Faisal**, PES school of Engineering, Bangalore, faismuhammad@gmail.com
430. **G.krishnamoorthy**, Central Leather Research Institute, Chennai, krishnamoorthyganesht@yahoo.com
431. **Rijith.S**, Sree Narayana college, Kannar, Kerala, rijithsreenivas@gmail.com
432. **Asit Parija**, Salipur College, Orissa, asitparija2k8@yahoo.com
433. **Vikas Jivottam Pissurlekar**, PES`s S.R.S.N College of arts & science, Goa, vikjps@rediffmail.com
434. **Kimkholing Lunkim**, Manipur University, Manipur, kim_lunkim@yahoo.com
435. **Naorem Arunkumar Singh**, Manipur University, Manipur, aknaorem@gmail.com
436. **Nityanand chaubey**, University of Allahabad, Allahabad, nchaubey_au@rediffmail.com
437. **Narayana Sharma**, BTM Layout, Bangalore, narayana.sharma@gmail.com
438. **Seram Pramodini Devi**, Manipur University, Manipur, pramodiniseram@rediffmail.com
439. **Prasanna S.Ghalsasi**, M.S. University, Baroda, Vadodara, prasanna.ghalsasi@gmail.com
440. **Chhatrapati Parida**, Orissa University of Agriculture and Technology, Orissa, sivaji_1976@yahoo.co.in
441. **Parthiv Mukundkumar Trivedi**, Ushanagar Soc., Vadodara, parthiv_trivedi2006@yahoo.co.in
442. **V.Jayathirtha Rao**, Indian Institute of Chemical Technology, Hyderabad, jrao@iiet.res.in
443. **Remya Devi P.S**, BARC, Mumbai, remyadevips@yahoo.co.in
444. **Charu Lata Dube**, IIT, Delhi, charu_dubey@rediffmail.com
445. **Sayed Khasim**, PES school of Engineering, Bangalore, syed.physics@gmail.com
446. **Srimaha Vishnu**, IGCAR, Kalpakkam, dsvishnu@igean.gov.in
447. **Nahakpam Santhibala Devi**, Manipur University, Imphal, abenahakpam@rediffmail.com
448. **Nimalini Moirangthem**, Manipur University, Imphal, nima_moirangthem@rediffmail.com
449. **T.H.Goswami**, DMSRDE, Kanpur, thgoswami@yahoo.co.uk
450. **Longjamjaideva Singh**, Manipur University, Imphal, jaideva.longjam@gmail.com

451. **Pranjali Kalita**, IOWA State University, USA, *pkkalita.ncl@gmail.com*
 452. **Vidhyadutta M.S.Verenkar**, Goa University, Goa, *vmsv@rediffmail.com*
 453. **Tanuja P Parulekar**, S.I.W.S., Mumbai, *tanujaparulekar@gmail.com*
 454. **Girdhar Joshi**, Analytical science division, Gujarat, *gdscmcri@gmail.com*
 455. **Varsha P Brahmkhatri**, M.S. University of Baroda, Vadodara, *varshachem@yahoo.co.in*
 456. **Ghanshyam L Jadav**, CSMCRI , Bhavnagar, Gujarat, *jadav.ghanshyam@gmail.com*
 457. **Chirantan Roy Choudhury**, West Bengal State University, W.B, *crchoudhury2000@yahoo.com*
 458. **K.S.Nagaraja**, Loyola College, Madras, *ksnagaraja@gmail.com*
 459. **Amitabha Acharya**, IIT-Bombay, Powai, *amitabhachem@gmail.com*
 460. **Rimpi Dawar**, IGCAR, *rimpi.dawar@gmail.com*
 461. **Ambrose Ashwin Meluin**, TIFR, Mumbai, *ashwinmelvino8@gmail.com*
 462. **Radhe Shyam Ji**, IIT Bombay, Powai, *rsj@iitb.ac.in*
 463. **Balasaheb Bapu Chandanshive**, Tata Institute of Fundamental Research, Colaba, *bchandanshive4@gmail.com*
 464. **Y.Sunitha**, NCCCM, BARC- hyderabad, *sunibarc@gmail.com*
 465. **Raj Kumar Mishra**, Mizoram University - Aizawl, *rkmishramzu@yahoo.com*
 466. **Surjit Konwer**, Tezpur University, Assam, *ksurajit27@gmail.com*
 467. **Ibetombi Soibam**, Manipur University, Imphal, *ibetombi96@gmail.com*
 468. **Santosh Waman Kulkarni**, K.M. Agarwal College - Kalyan, *sudhirkapur@barc.gov.in*
 469. **Sudhir Kapur**, BARC, Mumbai, *sudhir@barc.gov.in*
 470. **Ridhima Chadha**, BARC, Mumbai, *ridhima@barc.gov.in*
 471. **Sandip Kumar Nayak**, BARC, Mumbai, *sknayak@barc.gov.in*
 472. **K.G.Girija**, BARC, Mumbai, *kgirija@barc.gov.in*
 473. **Bedse R.D**, BARC, Mumbai, *bedse@barc.gov.in*
 474. **L. Robindro Singh**, Pachhunga University college, Mizoram University, *robinlaishram@gmail.com*
 475. **Sureeti Pratima Ratilal**, V.N.S.G. University, Surat, *prjriya@rediffmail.com*
 476. **S. Ramanathan**, BARC, Mumbai, *sramanathan1953@gmail.com*
 477. **Kolekar Sanjay Subrao**, Shivaji University - Kolhapur, *kolekarss2003@yahoo.com*
 478. **Jambhale Chitra Laxman**, Sangola College, Sangola, *cljambhale@yahoo.com*
 479. **Sandeep Verma**, IIT, Kanpur, *sverma@iitk.ac.in*
 480. **S.K. Bandyopadhyaya**, VECC-Kolkata, *skband@vecc.gov.in*
 481. **Ajay Kumar Himanshu**, VECC-Kolkata, *himanshu_ak@yahoo.co.in*
 482. **Raghunath Acharya**, BARC,Mumbai, *racharya@barc.gov.in*
 483. **Gaurang Shah**, Cadila pharmaceutical ltd, Ahmedabad, *gshah1975@yahoo.co.in*
 484. **Patel Kalpesh Balvantbhai**, Jogananagar, Surat, *sarvam.polymers@gmail.com*
 485. **Sangita D Kumar**, BARC Mumbai, *sangdk@barc.gov.in*
 486. **Sangeeta N Kale**, Defence Institute of Advanced Technology, Pune, *sangeetakale@diat.ac.in*
 487. **M. C. Chattopadhyaya**, University of Allahabad, Allahabad, *mc46@rediffmail.com*
 488. **Sunaina Devi**, University of Allahabad, Allahabad, *sunaina_ecsl@rediffmail.com*
 489. **Atul Kumar Kushwaha**, University of Allahabad, Allahabad, *atulkk2008@gmail.com*
 490. **Neha Gupta**, University of Allahabad, Allahabad, *neha.evs07@gmail.com*
 491. **Rahul Kumar**, Pratapgarh, U.P, *rahulkumarchem@gmail.com*
 492. **Raj Mani**, University of Allahabad, Allahabad, *rajmanichemistry@gmail.com*
 493. **Sudeep Halder**, Naini, Allahabad, *sudeep1132@gmail.com*
 494. **Vridhhi Nigam**, University of Allahabad, Allahabad, *vridhhi_environment@rediffmail.com*
 495. **Lal Jee Yadhav**, Colonelganj Inter College, Allahabad, *laljee@gmail.com*
 496. **Sharda Sundaram Sanjay**, Christain college, Allahabad, *sharda100@rediffmail.com*
 497. **D.K. Maity**, BARC, Mumbai, *dkmaity@barc.gov.in*
 498. **Devendra Pratap Rao**, D.A.V.College, Kanpur, *dvendraprataprao@yahoo.com*
 499. **P.V.Ananthapadmanabha**, BARC, Mumbai, *pvananth@barc.gov.in*
 500. **Charu R. Vatsa**, Jhunjhunwala College, Mumbai, *rkvatsa@yahoo.com*
 501. **Anuyuna Padhi**, BARC, Mumbai, *padhi532@gmail.com*
 502. **Amlan Kumar Das**, Modi Institute of Technology, Sikar, Rajasthan, *amlan_snigdha@yahoo.com*
 503. **Prathibha Sunil Agrawal**, Hislop college, Nagpur, *prathibha3674@gmail.com*
 504. **Mamta S Wagh**, Kamla Nehru MV, Nagpur, *mamta1852@yahoo.com*
 505. **Sunil.L. Dhaire**, Science college, Maharashtra, *dahire.sunil08@gmail.com*
 506. **N Ramesh Babu**, NIT, Tiruchirapalli, *rameshrohith@gmail.com*
 507. **Balchandra M Bhanage**, ICT, Matunga, Mumbai, *balchandra_bhanage@yahoo.com*
 508. **Kshama Kundu**, BARC, Mumbai, *kshamaroy@yahoo.com*
 509. **Raghvindu Pathak**, Pachhunga University college, Mizoram University, *rppuc31@yahoo.com*
 510. **Anjali patel**, M S Univ. of Baroda, Vadodara, *aupatel_chem@yahoo.com*
 511. **P D Babu**, BARC, Mumbai, *pdbabu1@gmail.com*
 512. **Anjali N Rahatgaonkar**, IOS, Nagpur, *anjali_rahatgaonkar@yahoo.com*
 513. **Raksha P Dhankar**, Sadar Patel Mahavidyalaya, Chandrapur, *rakshadhankar@rediffmail.com*
 514. **Vibha M Nikose**, IOS, Nagpur, *vibha_nikose@yahoo.co.in*
 515. **Kushal R Lanjewar**, IOS, Nagpur, *kusahallanjewar@gmail.com*
 516. **Mahesh Krisnarao Gaidhane**, IOS, Nagpur, *maheshgaidhane83@gmail.com*
 517. **Nitin Kawaduji Longadge**, IOS, Nagpur, *nitinlongadge@gmail.com*
 518. **M.V. Balarama Krishna**, BARC ,Hyderabad, *mvbalaramakrishna@rediffmail.com*
 519. **Mahendra Mohanlal Lakadawala**, NIT, Surat, *auxin_rnd@gmail.com*
 520. **S C Raghavendra**, PES School of Engineering, Bangalore, *sc.raghu@gmail.com*
 521. **Sudhanshu K .Deshpande**, BARC, Mumbai, *skdesh@csr.res.in*
 522. **J. V. Ramana**, BARC, Hyderabad, *jramana1@rediffmail.com*
 523. **Abdul Kareem Parchur**, Banaras Hindu Univ., Varanasi, *kareemskpa@hotmail.com*
 524. **Bhanu Raman**, K. J. Somaiya College of Science & Commerce , Mumbai, *drbhanu.raman@gmail.com*
 525. **Pika Jha**, Solid State Physics Laboratory, Delhi, *pikajha@sspl.drdo.in*
 526. **Neeraj Kumar Gupta**, BARC, Mumbai, *triton2010@gmail.com*
 527. **Athawale Anjali Anand**, Univ. of Pune, Pune, *agbed@chem.unipune.ac.in*
 528. **Vandana Swarnkar**, Jiwaji Univ. Gwalior, *soni.vandana7@gmail.com*
 529. **Ranga Rao**, IIT Madras, Chennai, *grrao@iit.ac.in*
 530. **V. snehalatha**, IGCAR, Kalpakkam, *chem.vsl@gmail.com*
 531. **Santosh Sitarum Bhoir**, BARC, Mumbai, *santoshsbhoir@yahoo.com*
 532. **hemlata Vinod Khadilkar**, BARC, Mumbai, *hemalk@barc.gov.in*
 533. **Jayanthi S Kulkarni**, BARC, Mumbai, *drjayanthi1999@yahoo.com*
 534. **Adish taygi**, BARC, Mumbai, *adishchem@gmail.com*
 535. **Shreekrishna Govind Kulkarni**, BARC, Mumbai, *shreekrishna.g.kulkarni@gmail.com*
 536. **Yogita Subhash Pable**, BARC, Mumbai, *yogip@barc.gov.in*
 537. **Prasanta Kumar Mohapatra**, BARC, Mumbai, *mapatra@barc.gov.in*
 538. **Deepak Rawat**, BARC, Mumbai, *rawatd@barc.gov.in*
 539. **Sangeeta Kishore**, M S Univ. of Baroda, Vadodara, *kishore.sangeeta@gmail.com*
 540. **Surendra Kumar Saini**, Sitapura, Jaipur, Rajasthan, *surendra1feb@gmail.com*
 541. **Rajesh M Kamble**, Mumbai University, Mumbai, *chemrajkam@yahoo.co.in*
 542. **Bhavna A Shah**, VNS Gujarat University, Surat, *bhavna606@gmail.com*
 543. **Sangeeta Adhikari**, NIT, Rourkela, *adhikari.sangeeta8@gmail.com*
 544. **Bharat kumar**, IIT, Delhi, *bharatchaubeydce@gmail.com*
 545. **Gohil S. Thakur**, IIT Delhi, *gohil_thakur08@yahoo.com*
 546. **Chirag B. Mistry**, Narmad south Gujarat univ., Surat, *cbmistry605gmail.com*
 547. **Archana Charanpahari**, NIT, Nagpur, *acharanpahari@gmail.com*
 548. **Ovhal Sheetal Dadasaheb**, Univ. of Pune, Pune, *sheetalovhal@yahoo.com*
 549. **Pragati Thakur**, Univ. of Pune, Pune, *prthakur@chem.unipune.ac.in*
 550. **Bhavana Gupta**, IIT, Bombay, Mumbai, *bgupta1206@gmail.com*
 551. **S. K. Ghosh**, BARC, Mumbai, *sghoshmawab@gmail.com*
 552. **Rajak Syed**, BARC, Mumbai, *rajak@barc.gov.in*
 553. **B J lokhande**, Solapur University, Solapur, *bjlokhandde@yahoo.com*

554. **Ambare revanappa Chandrakan**, Solapur University, Solapur, *revanambare@gmail.com*
555. **Surendra Vithal Khavale**, Solapur University, Solapur, *surendra_khavale@yahoo.com*
556. **G K Nagaraja**, Manglore University, Manglore, *nagarajagk@gmail.com*
557. **T.S.R. Ch. Murthy**, BARC, Mumbai, *murthi321@gmail.com*
558. **R. Srinivasan**, BITS Pilani, Hyderabad Campus, Hyderabad, *rsvasan31@gmail.com*
559. **P. K. Patro**, BARC, Mumbai, *pankajpatro@gmail.com*
560. **T. Mahata**, BARC, Mumbai, *tsmahata@gmail.com*
561. **Chayan Banerjee**, BARC, Mumbai, *chayan@barc.gov.in*
562. **Jasmine Biswal**, Mumbai University, *jasmine.biswal09@gmail.com*
563. **Johar Dey**, North Eastern Hill University, *johar_dey2006@yahoo.com*
564. **Neelam Shivran**, BARC, Mumbai, *neel2k1@gmail.com*
565. **Mohsin Jafar**, BARC, Mumbai, *mohsinj@barc.gov.in*
566. **Bhagyashree K Kharwandikar**, BARC, Mumbai, *kbsshree@barc.gov.in*
567. **Dilip Kumar Mishra**, Sikshya O Anusandhan University, Bhubaneswar, *dilipiuc@gmail.com*
568. **Swaroop Laxmi**, Shri Ramdeobaba Kamala Nehru Coll. of Engg., Nagpur, *swarooplaxmim71@gmail.com*
569. **Archana P. Gaikwad**, BARC, Mumbai, *ashirole@barc.gov.in*
570. **K. Srinivasu**, BARC, Mumbai, *ksvasu@barc.gov.in*
571. **K. C Bairwa**, BARC, Mumbai, *bairwa@barc.gov.in*
572. **Joyeeta Tk. Mukherjee**, BARC, Mumbai, *makhopadhyaya.j@gmail.co.in*
573. **K. P. Muthe**, BARC, Mumbai, *kpmuthe@rediffmail.com*
574. **Amresh I Prasad**, Ramnarain Ruia College, Mumbai, *prasad_amresh@yahoo.com*
575. **Anamika Singh**, Dept. of Life Sciences., University of Mumbai, *anamika.singh5@gmail.com*
576. **K. R. S. Chandrakumar**, BARC, Mumbai, *krsc@barc.gov.in*
577. **P. N. Pathak**, BARC, Mumbai, *ppathak@barc.gov.in*
578. **Harshala J. Parab**, BARC, Mumbai, *harshprb@gmail.com*
579. **Alok Samanta**, BARC, Mumbai, *alokk@barc.gov.in*
580. **Mahesh Sundararajan**, BARC, Mumbai, *maheshsrajan@gmail.com*
581. **Arup Kumar Pathak**, BARC, Mumbai, *akpathak@barc.gov.in*
582. **Kajal Dhole**, BARC, Mumbai, *dhole@barc.gov.in*
583. **Rumu Halder**, BARC, Mumbai, *rumuhalder24feb@gmail.com*
584. **Pranesh Sengupta**, BARC, Mumbai, *praneshsengupta@gmail.com*
585. **Vandana Pulhani**, BARC, Mumbai, *vanpulh@barc.gov.in*
586. **K. V. Vivekananda**, BARC, Mumbai, *kvivek18@gmail.com*
587. **Dilip Kumar Paluru**, BARC, Mumbai, *dilipkumar_paluru@yahoo.co.in*
588. **Champa Lal Prajapat**, BARC, Mumbai, *prajapat@barc.gov.in*
589. **Abhishek Das**, BARC, Mumbai, *abhidas@barc.gov.in*
590. **Kaushik Sanyal**, BARC, Mumbai, *kaushik.sanyal88@gmail.com*
591. **Santosh Kumar Gupta**, BARC, Mumbai, *santoshg@barc.gov.in*
592. **Raghuvveer V Kulkarni**, BARC, Mumbai, *ravik@barc.gov.in*
593. **Juby K. Ajish**, BARC, Mumbai, *jubykuttan@gmail.com*
594. **Krishan Kant Singh**, BARC, Mumbai, *singkrish@gmail.com*
595. **Vishnu R Aijaonkar**, Mumbai University, *vraijaonkar@yahoo.com*
596. **Sabir H Mashraqui**, Mumbai University, *sh_mashraqui@yahoo.com*
597. **Ashwini Kumar Srivastava**, Mumbai University, *akschbu@yahoo.com*
598. **Anil V Karnik**, Mumbai University, *avkarnik@yahoo.com*
599. **Deep Prakash**, BARC, Mumbai, *deep.prakash1970@gmail.com*
600. **Prabhudesai Swapnil Anil**, BARC, Mumbai, *swapnil@barc.gov.in*
601. **R. D. Purohit**, BARC, Mumbai, *rdp.nano@gmail.com*
602. **Smita S. Sheelvantra**, BARC, Mumbai, *aksmita@barc.gov.in*
603. **Apurav Guleria**, BARC, Mumbai, *aguleria@barc.gov.in*
604. **A. K. Tiwari**, BARC, Mumbai, *annukt@barc.gov.in*
605. **Madhusadan K. Bhide**, BARC, Mumbai, *bhidemak@yahoo.com*
606. **Laxmi Narasimha Reddy**, N.C.C./BARC, Hyderabad, *glnr@cccm.gov.in*
607. **Nilesh Laxman Dudwadakar**, BARC, Mumbai, *nileshld@barc.gov.in*
608. **Arijit Sengupta**, BARC, Mumbai, *arijita@barc.gov.in*
609. **Ashish Kumar Singha Deb**, Indira Gandhi Centre for Atomic Research, Kalpakkam, *tuira.lp@gmail.com*
610. **Abhijeet Mishra**, Jamia Millia Islamia, New Delhi, *abhijeetjmi@gmail.com*
611. **G.Muralidharan**, Gandhigram Rural Institute, Gandhigram, *muralg@rediffmail.com*
612. **Y. K. Bhardwaj**, BARC, Mumbai, *ykbhard@barc.gov.in*
613. **Mohd. Ubaidullah**, Jamia Millia Islamia, New Delhi, *mohdubaidullah2007@gmail.com*
614. **P. Pachamuthu**, Anna University, Chennai, *pachachem@gmail.com*
615. **Nandita Maiti**, BARC, Mumbai, *nanbis@gmail.com*
616. **Irfan Hussain Lone**, Jamia Millia Islamia, *irfanchem486@gmail.com*
617. **A. Ajayghosh**, CSIR-NIIST, Trivandrum, *ajayaghosh@niist.res.in*
618. **Tandrima Chaudhuri**, Dr. B. N. Dutta Smriti Mahavidyalaya, *tanchem_bu@yahoo.co.in*
619. **Manjanna**, Kuvempu University, *jmanjanna@rediffmail.com*
620. **V. Balaji**, BARC F, Kalpakkam, *vbalaji1764@gmail.com*
621. **Dipika Sharma**, Dayalbagh Educational Institute, Agra, *dipika.sharma286@gmail.com*
622. **Sumant Upadhyay**, Dayalbagh Educational Institute, Agra, *sumant.upadhyay@gmail.com*
623. **N. Rajmuhon Singh**, Manipur University, *rajmuhon@yahoo.co.in*
624. **Vijay Kumar Netial Chaudhari**, R.T.M., Nagpur University, *vj1784@gmail.com*
625. **Ningthoujam Ghanashyam Singh**, North Eastern Regional Institute of Science and Technology, ITANAGAR, *ghanashyam2@gmail.com*
626. **S. Jayakumar**, Poosaripatti, Pollachi, *sjayakumar.physics@gmail.com*
627. **Jagendrakumar D. Punde**, S. S. Girls College, Gondia, *jagendrapund@gmail.com*
628. **Sudhanshu Sharma**, IIT, Gandhinagar, *ssharma@iitgn.ac.in*
629. **Bhoomika K. Joshi**, KSV University, *bhoomika7884@gmail.com*
630. **M. A. Reddy**, BARC, Hyderabad, *mavreddy@rediffmail.com*
631. **Smita Thosar**, Sandoz Pvt. Ltd., Dighe, Kalwe, *smitathosar@gmail.com*
632. **Priyanka M. Shinde**, Andheri, Mumbai, *bhatpriyanka@rediffmail.com*
633. **Deepak Pathania**, Shoolini University, Solan, *dpathania74@gmail.com*
634. **Bhim Singh Rathore**, Govt. P.G. college, Solan., *brathore66@yahoo.com*
635. **P. N. Bhosale**, Shivaji University, Kolhapur, *p_n_bhosale@rediffmail.com*
636. **Anithakumari Palavalara**, BARC, Mumbai, *anithakumari21_02@yahoo.co.in*
637. **Raza Rasool**, Jamia Millia Islamia, New Delhi, *razarasool@gmail.com*
638. **Sumaiya Hasnain**, Jamia Millia Islamia, New Delhi, *hasnain.sumaiya@gmail.com*
639. **Arun Kumar Upadhay**, Department of Applied science, Teerankar Mahaveer University, Morabad, *up.arun@gmail.com*
640. **Rajan Francis Nicholas Ashok**, Chemistry Department, K. V. College of Engg. Chinnakolam, *ashokfnr@gmail.com*
641. **Arun K Prasad**, SND, MSG, IGCAR, Kalpakam, *akp@igcar.gov.in*
642. **Govind Mughesh**, IPC Department, IISc, Bangalore, *mughesh@ipc.iisc.ernet.in*
643. **Alok Awasthi**, MPD, BARC, *aawasthi@barc.gov.in*
644. **C S Sundar**, MSG, IGCAR, Kalpakam, *css@igcar.gov.in*
645. **Kulamani Parida**, CSIR-IMMT, Bhuwaneshwar, Odisha, *kmparida@immt.res.in*
646. **Daya Shankar Pandey**, Department of Chemistry, BHU, Varanasi, *depbhu@bhu.ac.in*
647. **Rampal Pandey**, Department of Chemistry, BHU, Varanasi, *rpvimesh@gmail.com*
648. **Vinod Kumar Tiwari**, Department of Chemistry, BHU, Varanasi, *tiwari_chem@yahoo.co.in*
649. **Mrigendra Dubey**, Department of Chemistry, BHU, Varanasi, *mrigendradubey@gmail.com*
650. **Anup Paul**, Department of Chemistry, BHU, Varanasi, *kanupaul@gmail.com*
651. **Ashish Kumar Singha Deb**, Department of Chemistry, BHU, Varanasi, *ashish-chem.bhu@gmail.com*
652. **Amit Kumar**, Department of Chemistry, BHU, Varanasi, *aks87bhu@gmail.com*
653. **Sujay Mukhopadhyay**, Department of Chemistry, BHU, Varanasi, *sujay.chemistry07@gmail.com*
654. **Rakesh Kumar Gupta**, Department of Chemistry, BHU, Varanasi, *rakeshbhu.84@gmail.com*
655. **Rajendra Prasad Paitandi**, Department of Chemistry, BHU, Varanasi, *r.paitandi@gmail.com*
656. **Divya Kushwa**, Department of Chemistry, BHU, Varanasi, *divya.kushwa30@gmail.com*
657. **Roop Shibha Singh**, Department of Chemistry, BHU, Varanasi, *roopshibha22singh@gmail.com*
658. **Arnab Biswas**, Department of Chemistry, BHU, Varanasi, *arnabhdhf@gmail.com*
659. **Priyanka Srivastava**, Department of Chemistry, BHU, Varanasi, *priyankasrivastava0028@gmail.com*

660. **Arwind Mishra**, Department of Chemistry, BHU, Varanasi, arvindmishra2003@yahoo.com
661. **Syed Sibtay Razi**, Department of Chemistry, BHU, Varanasi, syedsibtayrazi@gmail.com
662. **Rashid Ali**, Department of Chemistry, BHU, Varanasi, alirashid85@gmail.com
663. **Ramesh Chandra Gupta**, Department of Chemistry, BHU, Varanasi, rameshchembhu@gmail.com
664. **Anshu Dandia**, Dept. Of Chemistry, University of Rajasthan, Jaipur, dranshudandia@yahoo.co.in
665. **Alka Sharma**, Dept. Of Chemistry, University of Rajasthan, Jaipur, sharma_alka21@yahoo.com
666. **Meenakshi Jain**, Dept. Of Chemistry, University of Rajasthan, Jaipur, minimaharani@yahoo.com
667. **Nihat Fahmi**, Dept. Of Chemistry, University of Rajasthan, Jaipur, fahmi@gmail.com
668. **Neelima Gupta**, Dept. Of Chemistry, University of Rajasthan, Jaipur, guptaniilima@gmail.com
669. **Asha Jain**, Dept. Of Chemistry, University of Rajasthan, Jaipur, aashajain27@gmail.com
670. **Sanjiv Saxena**, Dept. Of Chemistry, University of Rajasthan, Jaipur, saxenas348@rediffmail.com
671. **R. V. Singh**, Dept. Of Chemistry, University of Rajasthan, Jaipur, rusjpr@hotmail.com
672. **Abhinav Kumar**, Department of Chemistry, University of Lucknow, abhinavmarshal@gmail.com
673. **Vinita Sharma**, Department of Chemistry, J. N. V. University, Jodhpur, drvsharma29@gmail.com
674. **Pradeep k Sharma**, Department of Chemistry, J. N. V. University, Jodhpur, drpkvs27@yahoo.com
675. **Shobha Sharma**, Department of Chemistry, J. N. V. University, Jodhpur,
676. **Pryanka purohit**, Department of Chemistry, J. N. V. University, Jodhpur, pvkinetics@gmail.com
677. **Sarabjot Singh**, Dept. of Nanotechnology, SGGSW University, Fatehgarh Sahib, isarabjot@gmail.com
678. **Anurag Choudhary**, Department of Chemistry, J. N. V. University, Jodhpur, anurag051981@gmail.com
679. **Amita Dhariwal**, Department of Chemistry, J. N. V. University, Jodhpur, anandamita.amita@gmail.com
680. **Om Prakash**, Department of Chemistry, J. N. V. University, Jodhpur, doctorop29@gmail.com
681. **R. K. London Singh**, Department of Chemistry, D. M. College of Science, Imphal, london_ningthemcha@yahoo.com
682. **Deepak Kumar Padhi**, CMC department, CSIR-IMMT, Bhuwaneshwar, dkpadhi7@gmail.com
683. **Satyabadi Martha**, C&MC Dept. IMMT, Bhuwaneshwar, satyabadi_martha@yahoo.com
684. **Gobinda Chandra Behera**, C&MC Dept. IMMT, Bhuwaneshwar, bcbgobin@gmail.com
685. **Niranjan Biswal**, C&MC Dept. IMMT, Bhuwaneshwar, niranjan8572@gmail.com
686. **Gajendra Kumar Pradhan**, C&MC Dept. IMMT, Bhuwaneshwar, gkpcchem@gmail.com
687. **Surya Kanta Rana**, C&MC Dept. IMMT, Bhuwaneshwar, surjya.nou@gmail.com
688. **Goutam Kumar Naik**, C&MC Dept. IMMT, Bhuwaneshwar, gkn.chem@gmail.com
689. **Hemalata Reddy**, C&MC Dept. IMMT, Bhuwaneshwar, k.hemalatareddy@gmail.com
690. **Gopa Mishra**, C&MC Dept. IMMT, Bhuwaneshwar, gopachemistry@gmail.com
691. **Susanginee Nayak**, C&MC Dept. IMMT, Bhuwaneshwar, susanginee@gmail.com
692. **Amtul Nashim**, C&MC Dept. IMMT, Bhuwaneshwar, amtulnokt@gmail.com
693. **Soumyashree Pany**, C&MC Dept. IMMT, Bhuwaneshwar, pany84@gmail.com
694. **Lagnamayee Mohapatra**, C&MC Dept. IMMT, Bhuwaneshwar, mlagnamayee@gmail.com
695. **G. Bishwa Bidita Varadwaj**, C&MC Dept. IMMT, Bhuwaneshwar, lidita9@gmail.com
696. **Mitarani Sahoo**, C&MC Dept. IMMT, Bhuwaneshwar, mitarani85@gmail.com
697. **Binita Nanda**, ITER, SOA University, binita.driems@gmail.com
698. **Pravat Manjari Mishra**, CSIR-IMMT, Bhuwaneshwar, pravatmarjani@immt.res.in
699. **Anuj k Jain**, IIT Bombay, jain_anij04@yahoo.com
700. **B. N. Jagatap**, Chemistry Group, BARC, bnj@barc.gov.in
701. **Sumit**, SSPD, BARC, sumit.mehan@gmail.com
702. **A. Selvan**, Vel Tech High Tech Engg. College, Avadi, selvanabraham@gmail.com
703. **B. M. Tripathi**, PMD, BARC, biranchitripathi@gmail.com
704. **Trupti Mohanty**, PMD, BARC, Trupti121@gmail.com
705. **Chandrashekar Shankar**, PMD, BARC, kcshankar@gmail.com
706. **Amit Kaushal**, PMD, BARC,
707. **Krishna Ramadurai**, PMD, BARC, krishna.ramadurai@gmail.com
708. **V. Ravi Kanth**, PMD, BARC, kanthkvr@gmail.com
709. **Naraynan Raman**, PMD, BARC, narayanan.iyengar@gmail.com
710. **Rajesh Kumar Kharwar**, BRIT, BARC, rajeshkharwar.ch@gmail.com
711. **Suresh Kumar Kailasa**, S. V. National Institute of Technology, Surat, sureshkumarchem@gmail.com
712. **Vivek Polshettiwar**, TIFR, Mumbai, vivekpol@yahoo.com
713. **B. N. Rajasekhar**, AMPD, RRCAT, Indore, bnrs@rrcat.gov.in
714. **Rashmi Singh**, RRCAT, Indore, rashmi@rrcat.gov.in
715. **Poonam Pahari**, BARC, poonam.pahari@gmail.com
716. **V. G. Subramanian**, University of Hyderabad, gvsp@uohyd.ernet.in
717. **Shyam Kishor**, J. V. College, Barant, U. P., shyam387@gmail.com
718. **Mrs. Jyotirmayee Mohanty**, RPCD, BARC, jyotim@barc.gov.in
719. **Anand S. Burange**, Johanson and Matthey, asgburange@gmail.com
720. **Deepak Satoskar**, Johanson and Matthey, deepak.satoskar@matthey.com
721. **Rajesh Parishwad**, RSC, UK, parishwad@rsc.org
722. **Philip Earis**, RSC, UK, earisp@rsc.org
723. **Sumanta Mukherjee**, PDD, BARC, sumanta.mukherjee20@gmail.com

Printed by:
Ebenezer Printing House
Unit No. 5 & 11, 2nd Floor, Hind Service Industries
Veer Savarkar Marg, Shivaji Park Sea-Face, Dadar (W), Mumbai - 400 028
Tel.: 2446 2632 / 2446 3872 Tel Fax: 2444 9765 E-mail: outworkeph@gmail.com

In this issue

Feature articles	Page No.
1. Designing of Nanoarchitectures for Photo and Electrocatalytic Applications <i>Aparna Ganguly, Oruganti Anjaneyulu, Debashree Das and Ashok K Ganguli</i>	1
2. Photocatalytic Activity of Cellulose Acetate-tin (IV) Molybdate Nanocomposite in Solar Light <i>B.S. Rathore, Gaurav Sharma and Deepak Pathania</i>	11
3. N-Heterocyclic Carbene (NHC) in Organometallic Catalysis –Contributions from IIT Kanpur <i>Sayantani Saha and Jitendra K. Bera</i>	17
4. Anisotropic Effect of Hematite Nanostructure and its Modification for Photocatalytic Application <i>Gajendra Kumar Pradhan and Kulamani Parida</i>	23
5. Effect of Different Phases of Mg-Al Hydrotalcites, Formed by Calcination, on the Knoevenagel Reaction of Benzaldehydes and Malononitrile. <i>Rohit Gupta, Siddheshwar Kshirsagar, Savita Ladage and Shriniwas D. Samant</i>	29
6. Novel Supported ionic liquid catalysed synthesis of tetraarylporphyrins <i>Deepali A. Kotadia and Saurabh S. Soni</i>	35
7. Heterogeneous Photocatalysis: Novel Approach for Carbon-Carbon Bond Forming Reactions <i>Sudhir S. Arbuji, Bina N. Wani and Uttam P. Mulik</i>	40
8. Modeling of materials for H-Economy using DFT: Implications toward nanocatalysis <i>Chiranjib Majumder, Seemita Banerjee and Sandeep Nigam</i>	47
9. Development of Catalysts for Various Applications Related to DAE Programs <i>Shyamala R. Bharadwaj</i>	53

Published by

Society for Materials Chemistry

C/o. Chemistry Division Bhabha Atomic Research Centre, Trombay, Mumbai, 400 085 (India)

E-mail: socmatchem@gmail.com,

Tel: +91-22-25592001